STUDIES OF PROTEIN PRENYLATION IN LIVING SYSTEMS: TOWARD THE BETTER UNDERSTANDING OF DISEASES

A DISSERTATION SUBMITTED TO THE FACULTY OF THE GRADUATE SCHOOL OF THE UNIVERSITY OF MINNESOTA BY

JOSHUA DANIEL OCHOCKI

IN PARTIAL FULFILLMENT OF THE REQUIREMENTS
FOR THE DEGREE OF
DOCTOR OF PHILOSOPHY

ADVISOR: DR. MARK D. DISTEFANO

AUGUST, 2012

Acknowledgements

There are several people in my life who have helped shape the decisions I have made and supported me on my journey thus far. I would like to take a moment to acknowledge those that have been instrumental in my life and career.

Several of my grade school teachers deserve many thanks for making science fun and interesting, and feeding my curiosity with fascinating science demonstrations on simple subjects from electricity and batteries (Mr. Garbe) to baking soda volcanoes (Mr. Wiger). Those teachers are Mr. Garbe, Mr. Wiger, Mrs. Volker, and Mr. Larson. Additionally, my high school teachers were also responsible for molding my curiosity and encouraging my interest in science, especially Mr. Walker, Mrs. Fier-Hansen, and Mrs. Knutson. Two of my undergraduate professors deserve many thanks as well, Professors Lee Sanow and Jay Brown. To Professor Sanow, for guiding me in choosing science as a career and showing me the truly remarkable possibilities it held from an intellectual and career standpoint. To Professor Brown, for being an excellent research mentor, for teaching me the value of accuracy in science, and the importance of knowing when exact precision is or isn't needed.

To my advisor, Mark Distefano, whom I owe a great debt to. You have always been supportive and encouraging, from allowing me to study at a university in Japan for three weeks to helping me get an internship at Genentech for three months, I have always appreciated your support for such endeavors and the flexibility to allow me to do them. You've also taught me about the politics of

science, and the realities a scientist faces in every aspect of their daily life. It seems like every group meeting you always gave some piece of advice, and, in time, I have found nearly all of them to be worthwhile and helpful. You have been the best of mentors and I'm proud to have been able to start my career under your guidance.

To my family: you may not have always understood what I was doing or why I was doing it, but you have always been behind me and I have appreciated it. To my friends: you constantly provided me with much needed distractions and were always a sounding board for my struggles and I will never forget it. I've been constantly motivated by the famous words of Jon Dozier (via Yoda), "do or do not, there is no try." You have all continuously reminded me that it's important to laugh often and not take life too seriously, or you'll never get out alive. I have truly been fortunate throughout my education, and life, to be surrounded by incredibly bright, encouraging, and enthusiastic people. All that you have done for me will never be forgotten.

Abstract

Protein prenylation is a post-translational modification that is present in a large number of proteins; it has been proposed to be responsible for membrane association and protein-protein interactions which contributes to its role in signal transduction pathways. Research has been aimed at inhibiting prenylation with farnesyltransferase inhibitors (FTIs) based on the finding that the farnesylated protein Ras is implicated in 30% of human cancers. Despite numerous studies on the enzymology of prenylation *in vitro*, many questions remain about the process of prenylation as it occurs *in vivo*. This dissertation describes our efforts to better understand the enzymology of protein prenylation in living systems. Initially, we prepared fluorescently labeled farnesylated peptides, based on the C-terminus of the naturally prenylated protein CDC42, to serve as substrates of the prenylation enzymes in living cells. These peptides are cell-permeable, can be imaged with confocal microscopy, quantified in cells with flow cytometry, and be detected by capillary electrophoresis after they have been processed by the cells own machinery. In addition to these peptides, we have also developed unnatural azide and alkyne containing isoprenoid moieties to serve as substrates for the prenyltransferase enzymes. Using the 'click' reaction to a fluorophore we can quantify the levels of prenylated proteins in living systems and we show that this method is applicable to study the connection between protein prenylation and neurodegenerative disorders such as Alzheimer's disease. Taken together, our results highlight the applicability of these peptides and unnatural isoprenoid

analogs as a platform for further study to better understand the enzymology of protein prenylation in living systems and to elucidate its role in certain diseases.

Table of Contents

List of Tables

List of Figures

List of Abbreviations

Ac, Acetyl; Boc, *tert*-butyloxycarbonyl; BOP, (benzotriazol-1-yloxy)tris-(dimethylamino)phosphonium hexafluorophosphate; *t*Bu, *tert*-butyl; capillary electrophoresis with laser induced fluorescence detection, CE-LIF; confocal laser scanning microscopy, CLSM; CPP, cell-penetrating peptide; DIC, *N,N'*-diisopropylcarbdiimide; Dde, 1-(4,4-dimethyl-2,6-dioxacyclohexylidene)ethyl; DIEA, diisopropylethylamine; DMF, *N,N*-dimethylformamide; ESI-MS, electrospray ionization mass spectrometry; 5-Fam, 5-carboxyfluorescein; Fmoc, 9-fluorenylmethyloxycarbonyl; Gg, geranylgeranyl; HCTU, 1H-benzotriazolium-1-[*bis*(dimethylamino)methylene]-5-chlorohexafluorophosphate-(1-),3-oxide; HOBt, 1-hydroxybenzotriazole; micellar electrokinetic chromatography, MEKC; OAc, acetate; Pbf, 2,2,4,6,7-pentamethyldihydrobenzofuran-5-sulfonyl; Pyn, 4-pentynoate; reagent K, TFA-phenol-thioanisole-water-ethanedithiol (82.5:5:5:5:2.5); RP-HPLC, reversed-phase high pressure liquid chromatography; SPPS, solid-phase peptide synthesis; TFA, trifluoroacetic acid; Trt, trityl

Chapter 1: Background

1.1 Post-translational Protein Modification

A post-translational modification (PTM) occurs on a protein after it has been translated from mRNA to protein in the ribosomes of the cell. It has been estimated that more than 5% of the entire proteome (the subset of all proteins) comprises enzymes that perform more than 200 different types of post-translational modifications.[1] These PTMs can be responsible for a protein's activity, localization, turnover, and interactions with other proteins and thus represent an important step in modulating the function of a particular protein.[2] One such modification is called protein prenylation, in which a 15 or 20 carbon isoprenoid moiety is transferred onto the C-terminus of a protein, rendering the protein more hydrophobic so it can associate with the plasma membrane.

1.2 Protein Prenylation

The biological phenomenon of protein prenylation has been extensively studied since the initial discovery of this process on the mammalian protein lamin B in 1989.[3] Following the initial reports of farnesyl protein modification (C_{15} isoprenoid), shortly thereafter proteins modified with a geranylgeranyl group (C_{20} isoprenoid) were discovered in mammalian cells.[4] Together, the post-translational modifications of farnesylation and geranylgeranylation are referred to as prenylation. The process of protein prenylation encompasses three distinct

enzymes: farnesyltransferase (FTase), geranylgeranyltransferase type I (GGTase I), and Rab geranylgeranyltransferase (RabGGTase or GGTase II). Prenylation using FTase and GGTase I involves the addition of either a C_{15} (farnesyl) or C_{20} (geranylgeranyl) isoprenoid moiety onto the C-terminus of a protein that bears a Ca_1a_2X (herein referred to as CAAX) consensus motif (Figure 1.1), where 'C' represents cysteine, 'a_1' and 'a_2' represent an aliphatic amino acid, and 'X' directs whether the protein will be farnesylated or geranylgeranylated. 'X' residues of cysteine, methionine, alanine, serine, or glutamine target farnesylation while leucine, isoleucine, and phenylalanine target the protein to be geranylgeranylated, although there are many exceptions to this rule.[5-7] For instance, the RhoB protein, with a CKVL CAAX box, is found in both farnesylated (30% of total RhoB) and geranylgeranylated (70% of total RhoB) forms in mammalian cells.[8] Additionally, it has been shown that while the 'a_1' CAAX position can allow virtually any amino acid, the 'a_2' residue plays a significant role in determining the type of prenylation.[9-11]

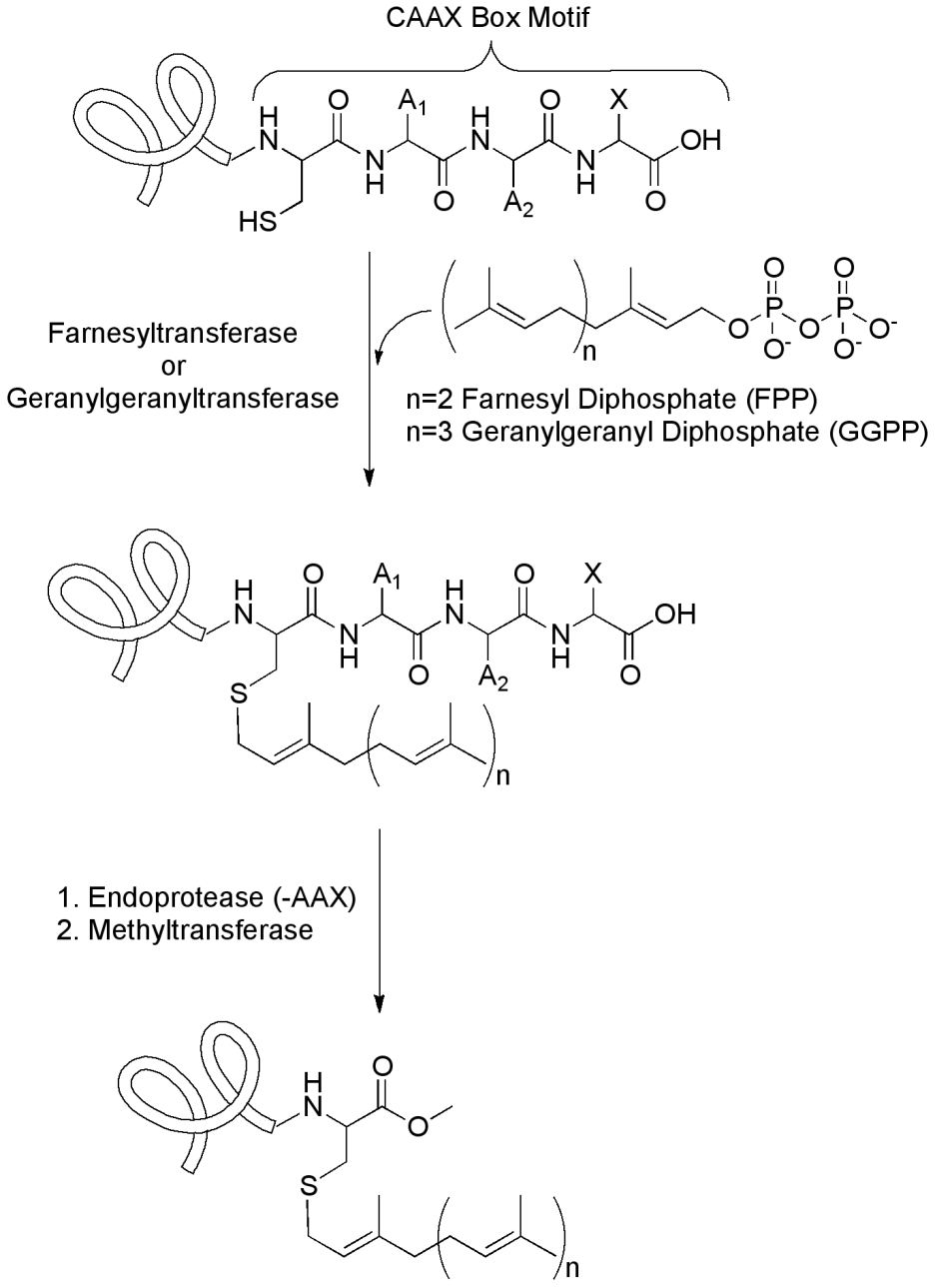

Figure 1.1. Schematic representation of protein prenylation carried out by farnesyltransferase (C15 isoprenoid) or geranylgeranyltransferase type I (C20 isoprenoid).

Another type of prenylation exists that is specifically present on Rab proteins, which are responsible for membrane transport and fusion in the cell.[12] While substrate proteins for FTase and GGTase I have well defined consensus sequences, prenylation by the enzyme Rab geranylgeranyltransferase (RabGGTase or GGTase II) has a less distinct consensus sequence. RabGGTase specifically di-geranylgeranylates Rab proteins that bear two cysteine residues at their C-terminus, with the following possible motifs: CC, CXC, CCX, CCXX, CCXXX, or CXXX); additionally, some Rab proteins can be mono-geranylgeranylated by this same enzyme.[13] Further differentiating this process from prenylation by FTase and GGTase I, Rab geranylgeranylation requires the Rab Escort Protein (REB) for prenylation. The REB binds to Rab proteins and facilitates their formation of a ternary complex with RabGGTase so prenylation can occur (see Figure 1.3).[14] The three prenyltransferase enzymes are all heterodimers, and while FTase and GGTase I share an identical α-subunit, they are only 25% sequence identical in the β-subunit.[15] In contrast, the RabGGTase α-subunit is only 27% identical to FTase, while the β-subunit is 29% identical, despite all three enzymes sharing nearly identical topology (Figure 1.2).[16]

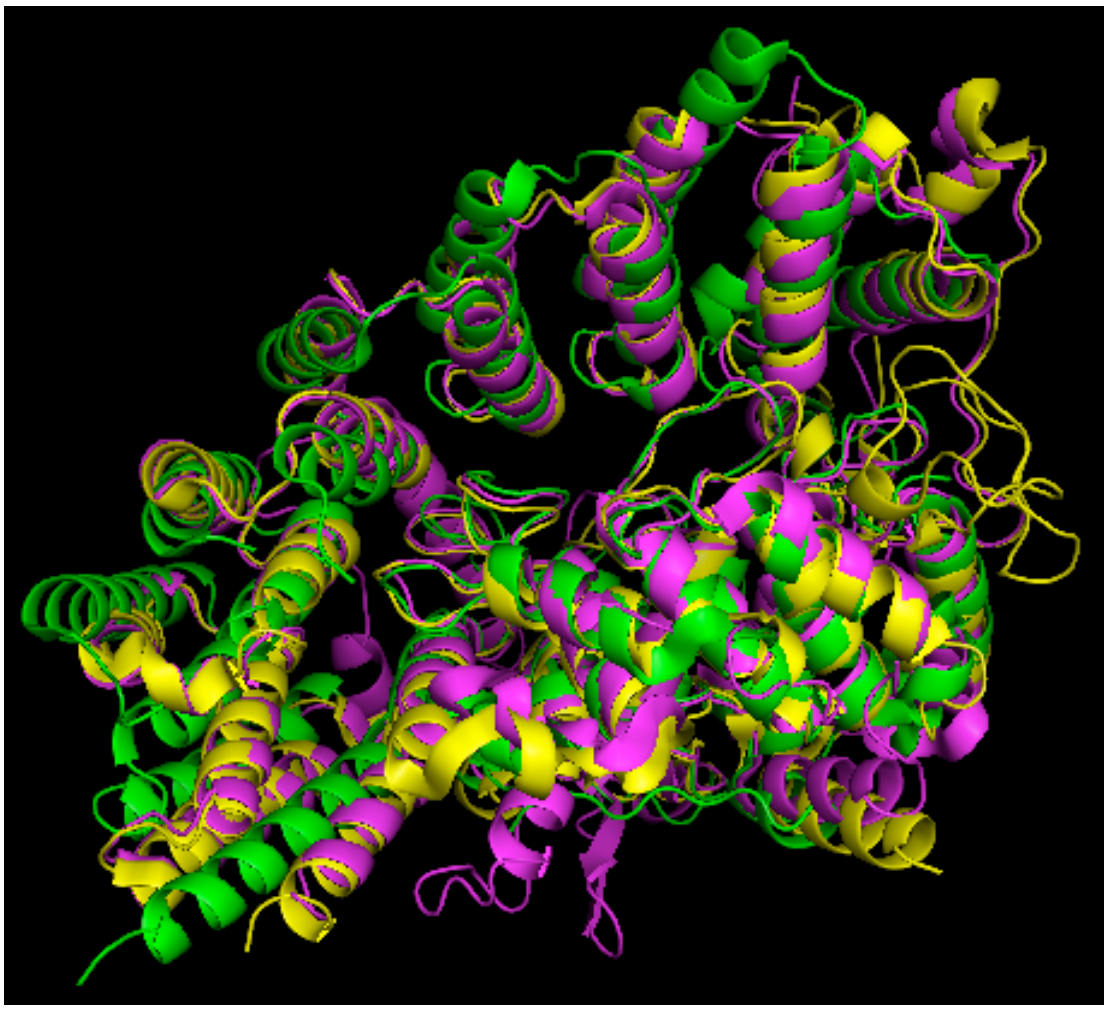

Figure 1.2. Alignment of the crystal structures of all three prenyltransferase enzymes. FTase: yellow, PDB 2BED. GGTase I: green, PDB 1N4P. RabGGTase: magenta, PDB 3C72. Structures were overlaid using the PyMOL program.

Following the prenylation step, further protein processing is required for CAAX bearing proteins. First, the three C-terminal 'AAX' residues are cleaved by the protease Ras-converting enzyme 1 (Rce1). Second, the newly exposed C-terminal carboxylic acid is methylated by isoprenylcysteine carboxylmethyl transferase (ICMT, Figure 1.1). Using an artificial *in vitro* membrane assay, Ghomashchi and coworkers showed that the K-Ras4B peptide has a 70-fold higher affinity for the membrane upon farnesylation, and further proteolysis and C-terminal methylation lead to a 150-fold increase in membrane affinity.[17] It would seem that the main purpose for this modification is to ensure membrane association of many proteins, but prenylation has also been shown to mediate important protein-protein interactions.[18] Approximately 2% of mammalian proteins, an estimated 150 different proteins, receive the prenylation modification.[19,20]

1.3 Biochemistry of Protein Prenylation

Enzymatic farnesylation as well as geranylgeranylation by FTase and GGTase I, respectively, occurs by the same mechanism (Figure 1.3). The prenylation reaction begins when the prenyltransferase enzyme binds the isoprenoid substrate, either the C_{15} farnesyl or the C_{20} geranylgeranyl, and forms a binary enzyme-isoprenoid complex. Following binary complex formation, the CAAX protein substrate binds adjacent to the isoprenoid molecule in the enzyme

active site. As the CAAX protein binds, the cysteine residue coordinates to a Zn^{2+} ion (as a thiolate) in the active site; the Zn^{2+} is necessary for catalysis. This ternary complex is short lived, as the cysteine thiolate reacts at the C-1 position of the isoprenoid, forming a stable, covalent, thioester linkage to the isoprenoid. Upon binding of an additional isoprenoid molecule, the isoprenoid portion of the newly formed prenylated protein moves into an exit groove in the enzyme, and subsequently the prenylated protein product is released from the enzyme; this is the rate-limiting step for the protein prenylation reaction. In addition, FTase needs millimolar levels of the Mg^{2+} ion for catalysis to occur, as this ion stabilizes the diphosphate leaving group of FPP during the reaction. In GGTase I, however, a positively charged lysine residue near the diphosphate stabilizes it and removes the requirement of exogenous Mg^{2+}.

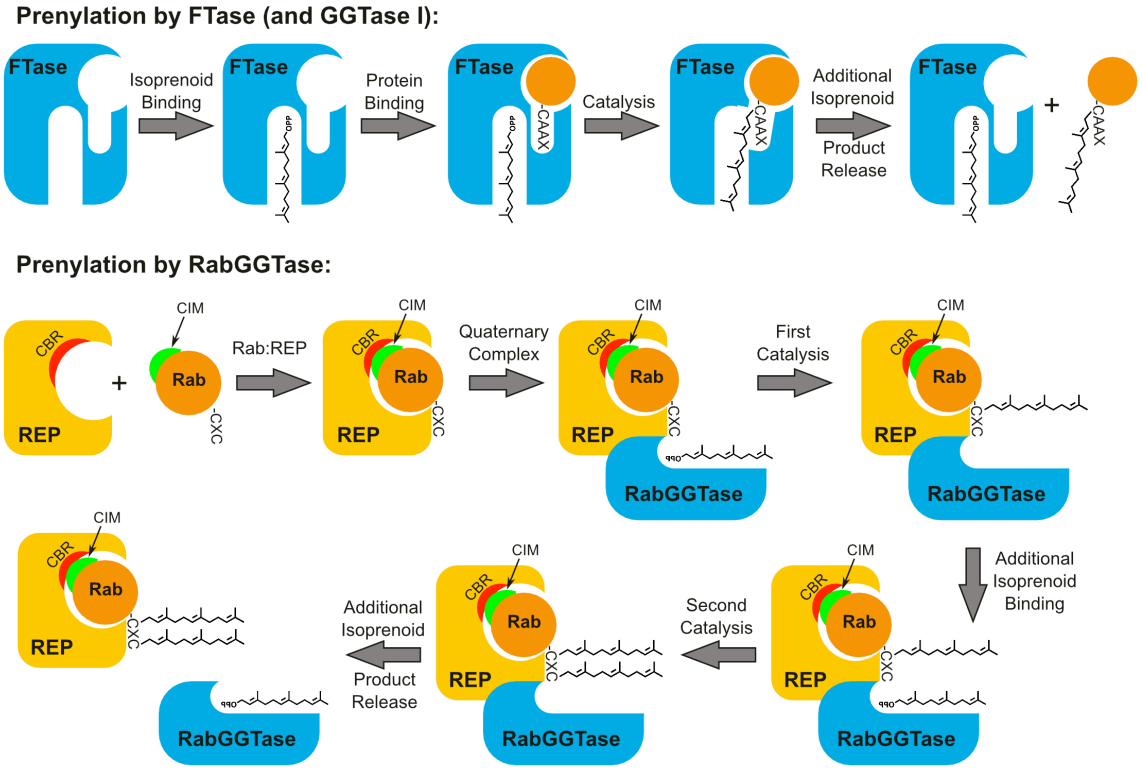

Figure 1.3. Cartoon scheme of the mechanism of prenylation for all three prenyltransferase enzymes.

In contrast, the RabGGTase reaction proceeds with some subtle similarities and some key differences (Figure 1.3). The major difference is that RabGGTase only recognizes a Rab substrate protein when it is bound to a Rab Escort Protein (REP). Similar to FTase and GGTase I, Rab prenylation begins when RabGGTase is loaded with a molecule of GGPP. The next step involves a portion of the REP, the Rab-binding platform (RBP), recognizing a Rab protein substrate and binding to it. This binding is enhanced when the C-terminal binding region (CBR) of the REP interacts with the CBR interacting motif (CIM) on the Rab protein substrate, enhancing the affinity of the REP for the Rab protein substrate (further information on the CBR/CIM interaction can be found in section 1.4). The binary complex now binds with the RabGGTase and GGPP binary complex to form a quaternary complex of REP/Rab/RabGGTase/GGPP, in which the C-terminal cysteine of the Rab substrate binds to the active site Zn^{2+} of RabGGTase as a thiolate. Catalysis now occurs, with the thiolate of the Rab substrate reacting with C-1 of the GGPP isoprenoid to form a covalent thioether linkage. Next, an additional molecule of GGPP binds to the active site of RabGGTase by displacing the previous isoprenoid and the second catalysis occurs. Substrate release occurs analogously to FTase and GGTase I, in which the binding of an additional GGPP molecule forces displacement of the REP/di-prenylated Rab complex from RabGGTase (this is also the rate limiting step in

Rab geranylgeranylation).[14] The REP/di-prenylated Rab complex is now trafficked to a target membrane, by a yet unknown mechanism. The REP protein is not only responsible for Rab protein binding and escort, but also solubilization of the di-prenylated Rab product until its delivery to a membrane.[21]

All three prenyltransferase enzymes have nanomolar affinities (K_M) for their respective isoprenoid substrates. Additionally, the rate-limiting step in the prenylation reaction is the release of product, which relies on the binding of an additional isoprenoid molecule. These two factors combine to give the prenyltransferases relatively slow turnover rates of approximately 3 min^{-1}, depending on the substrate.[20] The rates of the three enzymes themselves span multiple orders of magnitude, with FTase reacting the fastest, followed by GGTase I and lastly RabGGTase (k_{chem} values are 12-17 s^{-1}, 0.5 s^{-1}, and 0.16 s^{-1} for the three enzymes, respectively).[22] Furthermore, RabGGTase catalyzes its first geranylgeranylation four times faster than the second (k_1 = 0.16 s^{-1} and k_2 = 0.04 s^{-1}).[22] This observation is likely due to steric hindrance between the first prenylated cysteine residue and the next, as the two C-terminal cysteine residues are generally adjacent to one another.

1.4 Substrate Specificity of the Prenyltransferase Enzymes

The specificity of the FTase and GGTase I catalyzed reactions arises mainly from the CAAX motif on the substrate protein, although it has been shown recently that analogs of FPP can alter the substrate specificity of the FTase

enzyme.[23] Traditionally, it has been observed that the 'X' residue in the CAAX box is the main determinant in whether the protein will be farnesylated or geranylgeranylated. 'X' residues of cysteine, methionine, alanine, serine, or glutamine target farnesylation while leucine, isoleucine, and phenylalanine target the protein to be geranylgeranylated. More recently, it has been shown that these observations weren't always precise, and that cross prenylation can often occur, albeit at much slower rates than the traditional 'X' residue rates.[10,23-26] Additionally, structural differences in FTase and GGTase I account for the ability of the enzyme to bind either FPP or GGPP. In the isoprenoid binding pocket of FTase (in the β-subunit), there are two residues that limit the length of isoprenoid that can bind: a Trp102 at the end of the binding cavity and a Tyr365 that prevents anything longer than a farnesyl group from rotating to fit (Figure 1.4). In GGTase I, the smaller residues, Thr49 and Phe324, occupy these same positions, respectively. These smaller residues, especially the Thr49, allow the longer GGPP substrate to fit into the active site. This simple 'molecular ruler' controls which isoprenoid can bind to either enzyme.

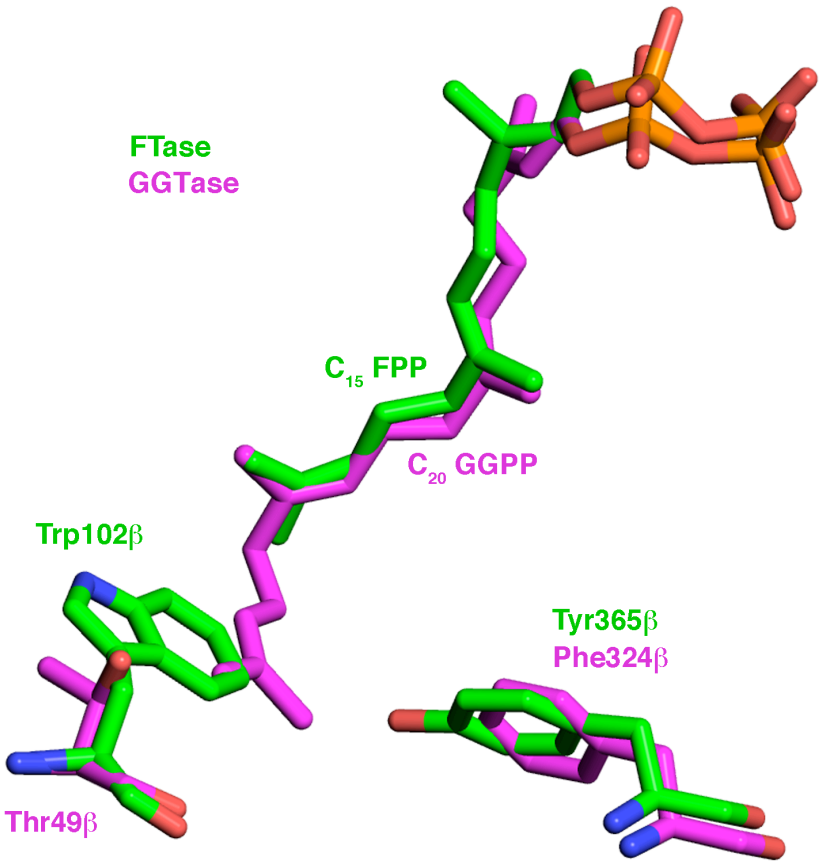

Figure 1.4. Overlay of the crystal structures of FTase and GGTase I showing the active site residues that control isoprenoid binding in the 'molecular ruler' hypothesis. In FTase (green structures), the tryptophan at 102 prevents anything longer than FPP from binding, while in GGTase I (magenta structures) this position is occupied by a threonine, allowing the longer GGPP to fit into the active site. The FTase (green residues, PDB entry 1KZO) and GGTase (magenta residues, PDB entry 1N4P) structures were aligned in PyMOL.

Much less is known about the exact determination of substrate specificity in the Rab GGTase reaction. The first crystal structure of RabGGTase in complex with the REB wasn't solved until 2003.[27] This has hampered detailed mechanistic studies of the RabGGTase reaction and how this enzyme selects its substrates. Recently, Guo and coworkers solved RabGGTase structures complexed with substrates and products which enabled a more complete picture to be revealed.[22] RabGGTase has the broadest lipid substrate specificity among all prenyltransferases.[28] It has been proposed that the interactions between the CIM of the Rab protein and the CBR of the REP are responsible for the substrate specificity of RabGGTase, analogous to the 'AAX' residues in FTase and GGTase I.[22] The REP controls the specificity of RabGGTase by selecting and binding to Rab proteins and facilitating their prenylation. The RabGGTase enzyme itself is highly promiscuous and operates stochastically, geranylgeranylating the protein substrate whenever a cysteine happens be in its active site.[22]

1.5 Biological Significance of Protein Prenylation

Extensive interest in protein prenylation was spurred by the finding that the potentially oncogenic Ras family of proteins were prenylated[29] and that in order to maintain malignant, transforming activity, Ras requires prenylation.[30] Initial therapeutic intervention focused on inhibiting the prenylation of Ras to stop

malignant cell activity by utilizing farnesyltransferase inhibitors (FTIs, see Chapter 2). The success of these compounds in clinical trials has been rather disappointing; however, it has been shown recently that FTIs, and other prenyltransferase inhibitors, may be used as potential therapeutics for several other human afflictions.

Attention has shifted in recent years to studying the involvement of protein prenylation not just in cancer but also in neurodegenerative diseases such as Alzheimer's and Parkinson's disease. For example, the farnesylated protein UCH-L1 is linked to Parkinson's disease and inhibition of the farnesylation of this protein has been suggested as a possible therapy for this disease.[31] In addition, a potential connection to Alzheimer's disease has been revealed based on the finding that the levels of farnesyl diphosphate (FPP) and geranylgeranyl diphosphate (GGPP) are elevated in the brains of Alzheimer's patients.[32-34] Furthermore, evidence for the neuroprotective effect of statins on long term potentiation in neurons has recently been attributed to the reduction of farnesylated proteins and/or FPP.[35] As more evidence of the connection between protein prenylation and aging diseases emerges, it is crucial to develop tools to better understand exactly how prenylation may play a role in neurodegenerative diseases. To this end, this thesis describes work in this area to 1) develop a method to quantify prenylated proteins *in vivo*, so the effects of FTIs and other inhibitors can be quantified and 2) to better understand the enzymology of protein prenylation *in vivo* so more effective inhibitors can be designed.

2. Prenyltransferase Inhibitors for Disease Therapies

2.1 Types of Prenyltransferase Inhibitors

Inhibitors of FTase and GGTase I fall into one of three categories: isoprenoid analog, peptidomimetic (also known as CAAX competitive inhibitors), and bi-substrate inhibitors combining both the isoprenoid analog and peptidomimetic portions (Figure 2.1). Specific inhibitors of RabGGTase include those that are phosphonocarboxylates as well as peptidomimetics (Figure 2.1).

Isoprenoid analog inhibitors of all three prenyltransferases have been the least developed and studied, because of three important reasons:[36] 1) The affinity of the isoprenoids for the prenyltransferases makes it difficult to design inhibitors that can be competitive with the native substrate (for example, the K_D of FPP for FTase is 2 nM[36]). 2) The diphosphate moiety is negatively charged and thus is unable to penetrate the membrane of cells, necessitating a prodrug strategy to mask the negative charges. 3) Several additional enzymes (e.g. squalene synthase, undecaprenyl pyrophosphate synthase, heme O synthase, etc.) utilize isoprenoids as substrates and an isoprenoid analog inhibitor may have significant off-target effects. Additionally, bi-substrate inhibitors that contain both a CAAX competitive portion and an isoprenoid analog portion have not been well developed, as complications in synthesis and water solubility have hampered development. Section 2.2 will focus on those inhibitors that are peptidomimetic as they have been the most studied and developed of all the

classes of prenyltransferase inhibitors.

Structures of FTase and GGTase I Inhibitors:

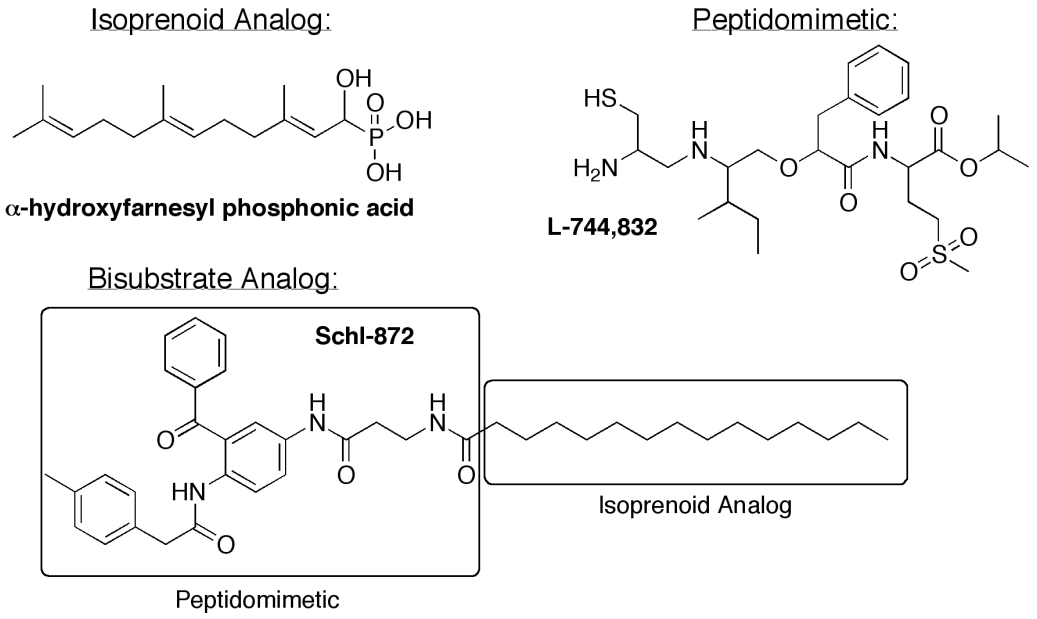

Structures of RabGGTase Inhibitors:

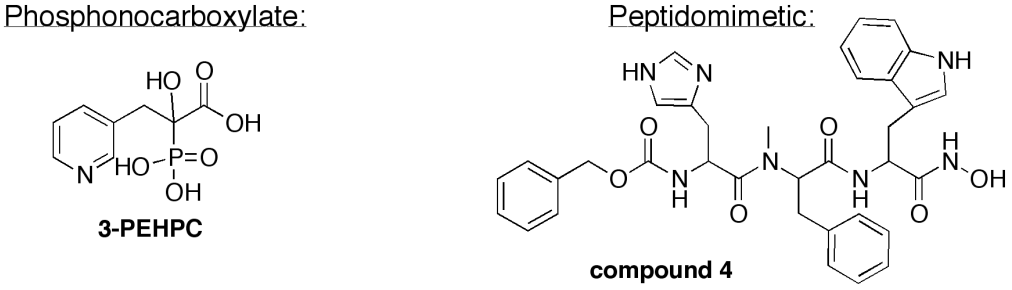

Figure 2.1. Select structures of the various classes of protein prenylation inhibitors. α-hydroxyfarnesyl phosphonic acid and L-744,832 are commercially available, Schl-872 was described by Schlitzer,[37] 3-PEHPC was synthesized by McKenna et al.,[38] and compound 4 was described by Guo et al.[39]

2.2 Evolution of FTIs

The initial development of peptidomimetic FTIs began with the native K-Ras CAAX box CVIM peptide by mutating the A_2 position to a phenylalanine (CVFM), giving an inhibitor with a 25 nM IC_{50} (Figure 2.2).[36] Placing bulky substituents in the A_2 position displaces the peptide in the binding pocket, leading to enzyme inhibition. Other inhibitors of this type have been able to achieve low nanomolar inhibition of FTase (see L-739,750, Figure 2.2),[40] but the peptide based scaffold made them less than ideal for *in vivo* use due to the possibilities of proteolysis. The next generation of FTIs generally contained few amide bonds in the backbone to circumvent this problem. For example, FTI-276 (Figure 2.2) contains a similar scaffold and binds in a similar manner to the FTase active site as L-739,750, achieiving a 0.5 nM IC_{50} (with respect to FTase and 50 nM with respect to GGTase I) without potential degradation issues.[41] Interestingly, changing the C-terminal methionine of FTI-276 to a leucine changes the specificity of inhibition (25 nM for FTase and 5 nM for GGTase I, Figure 2.2).[41]

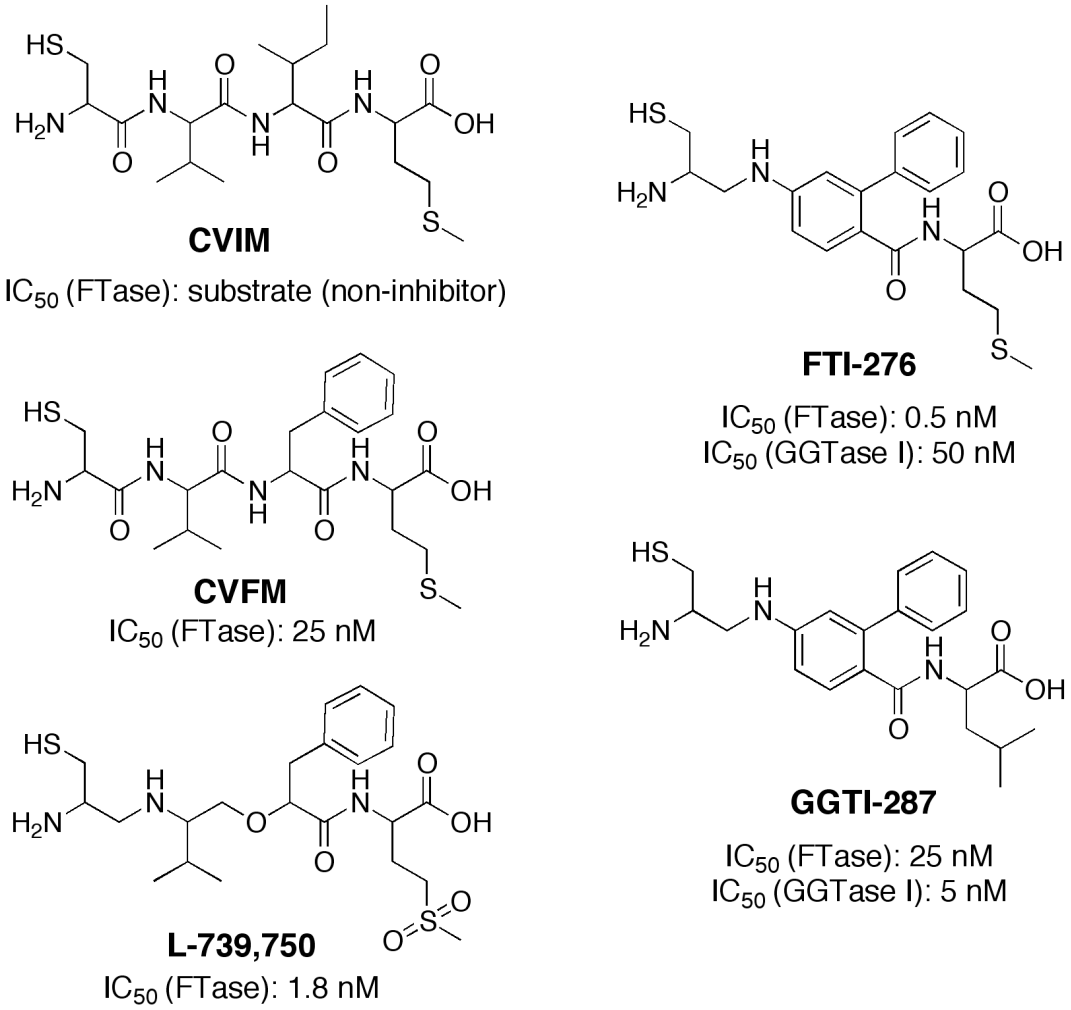

Figure 2.2. Structures of FTIs and a type I GGTI showing the specificity of inhibition by subtle changes in the compound structure. CVIM represents the natural K-Ras substrate peptide, and changing the isoleucine for phenylalanine gives an FTase inhibitor with a 25 nM IC_{50}.[36] L-739,750 represents attempts to remove the amide backbone to improve stability.[40] FTI-276 has a 10-fold selectivity for FTase inhibition over GGTase I[41] but subtly changing the C-terminal methionine to leucine changes the specificity to 5-fold for GGTase I over FTase.[41]

It was presumed in the early development of FTIs that a thiol moiety was necessary in the inhibitor structure to preserve the zinc coordination. Thiols can be oxidized to sulfoxides and sulfones, and the search for thiol replacements to zinc coordination led to the development of FTIs containing phenols, carboxylic acids, and nitrogen heterocycle derivatives. The most potent of these are the pyridine[42] and imidazole[43] based inhibitors (see Figure 2.3) with low nanomolar IC_{50} values. Placing the zinc-coordinating imidazole in a cyclic structure leads to one of the most potent FTIs developed with an IC_{50} of 20 pM (Figure 2.3).[44]

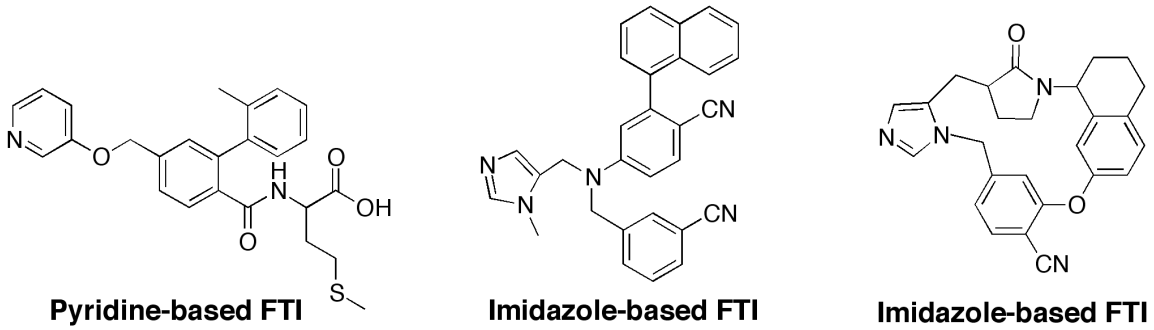

Pyridine-based FTI

IC_{50} (FTase): 0.4 nM

Imidazole-based FTI

IC_{50} (FTase): 0.39 nM

Imidazole-based FTI

IC_{50} (FTase): 20 pM

Figure 2.3. Structures of non-thiol FTIs that still allow for coordination to the active site zinc residue. Pyridine based inhibitors[42] and imidazole based inhibitors[43] have similar, low IC_{50} values as their thiol containing counterparts. A cyclic version of an imidazole based inhibitor has a remarkably low IC_{50} of 20pM.[44] Removing the thiol leads to stabilization from oxidation.

The last evolutionary step for FTIs occurred by attempting to remove the zinc-coordination on the peptidomimetic inhibitor. A class of inhibitors from Schering-Plough, originally based on an anti-histamine scaffold, exemplifies the drawbacks with removing the zinc-coordination (Figure 2.4). SCH 66366 (lonafarnib) lacks any zinc-coordinating moiety but still has an impressive IC_{50} of 1.9 nM.[36] When a similar scaffold is modified slightly to contain an imidazole zinc-coordinating moiety, the IC_{50} is improved nearly 50-fold to 0.04 nM (SCH 211618).[36]

Tuning the FTI to contain various structural elements has given hundreds of FTIs with low nanomolar IC_{50} values. Several of the best FTIs that combine potency, oral-bioavailability, and efficacy in animal models have entered clinical trials for cancer treatment (see Section 2.5). Additionally, a main challenge in the development of FTIs has been providing specificity for FTase over GGTase I, as they share considerable similarity, especially in the active site. Section 2.3 will discuss inhibitors that have been developed specifically to target GGTase I while having minimal impact on FTase.

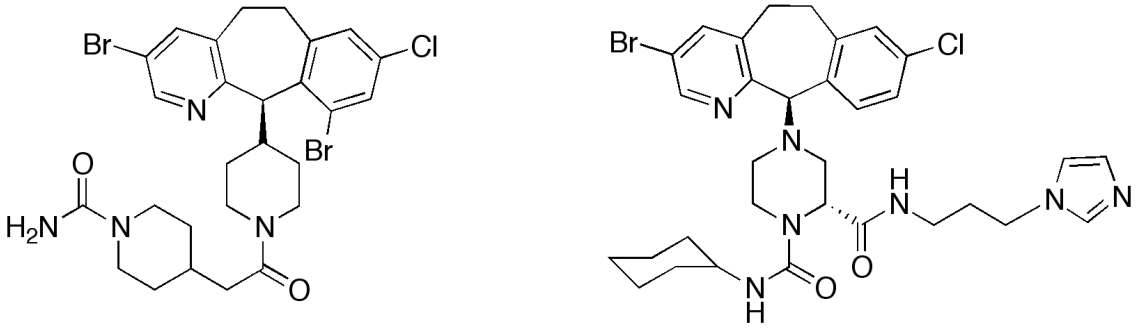

SCH 66336

IC_{50} (FTase): 1.9 nM

SCH 211618

IC_{50} (FTase): 0.4 nM

Figure 2.4. The effects of zinc-coordinating moieties on FTIs. SCH 66336 (lonafarnib) does not contain a zinc moiety but still has an impressive IC_{50} value, while a very close structural analog, SCH 211618, has a zinc coordinating moiety and almost a 50-fold lower IC50.[36]

2.3 Inhibitors for GGTase I

Providing selective GGTase I inhibitors was initially as simple as modifying the peptide backbone residues to contain larger, more hydrophobic elements to better fit in the GGTase I active site and exclude the FTase active site (see Figure 2.2). This strategy has the limitation of only providing approximately 5-fold selectivity for GGTase I over FTase. Structure-activity design efforts to introduce non-oxidizable zinc-coordinating groups, such as an imidazole, into the scaffold from GGTI-287 has led to the development of an inhibitor with greater than 250-fold selectivity for GGTase I over FTase (GGTI-2154, Figure 2.5).[45] Additional tuning and optimization of this C-terminal leucine scaffold led to a dramatic selectivity increase of over 5,000-fold for GGTase I over FTase (GGTI-2418, Figure 2.5).[46] The use of structure-activity relationships has been successful for the development of selective inhibitors of GGTase I; furthermore, the use of library screening has proven immensely beneficial. The inhibitor P5-H6 was developed after screening a 171 compound library for inhibitors of GGTase I (Figure 2.5).[47] This compound exhibits an approximate 100-fold selectivity for GGTase I over FTase. Many potent and selective inhibitors for GGTase I have been developed, however, only one inhibitor, GGTI-2418 (Figure 2.5), has advanced to clinical trials (see Section 2.5).

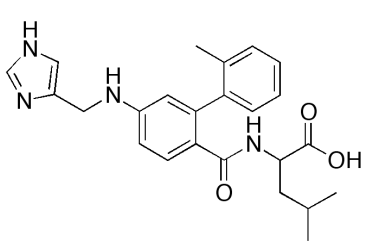

GGTI-2154

IC_{50} (FTase): 5600 nM

IC_{50} (GGTase I): 21 nM

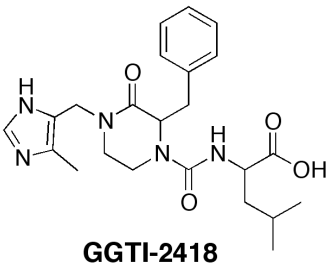

GGTI-2418

IC_{50} (FTase): 53,000 nM

IC_{50} (GGTase I): 9.5 nM

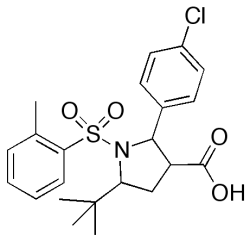

P5-H6

IC_{50} (FTase): >50,000 nM

IC_{50} (GGTase I): 466 nM

Figure 2.5. Inhibitors of GGTase I that are selective for GGTase over FTase. GGTI-2154 exhibits 250-fold selectivity,[45] while GGTI-2418 is 5,000-fold more selective and is the only GGTI to have entered clinical trials.[46] P5-H6 is an example of a selective GGTI that arose from high throughput screening.[47]

2.4 RabGGTase Inhibitor Development

Inhibitors of RabGGTase have been much slower to develop, as the main effort has been placed in pursing FTIs for cancer therapy. Recently, RabGGTase has been shown to be a valid cancer target as the Rab proteins, and RabGGTase itself, are overexpressed in several cancer types, such as ovarian,[48] breast,[48] hepatocellular carcinoma,[49] and thyroid adenomas.[50] The difficulty in the development of RabGGTase inhibitors has been in finding those that are specific only to this enzyme, as there is considerable similarity to the other two prenyltransferases (Figure 1.2). Further, RabGGTase has the largest amount of lipid promiscuity of all three prenyltransferases and doesn't recognize a single, direct substrate, but rather a dimer of Rab and REB, complicating inhibitor development. Nonetheless, progress has been made to identify specific RabGGTase inhibitors with high potency, with the current generation achieving low nanomolar inhibition.

The first generation of RabGGTase inhibitors were based on the scaffold of risedronate, a bisphosphonate drug that is used to strengthen bone and treat osteoporosis through osteoclast inhibition, leading to increased bone mass.[51] Interestingly, the molecular target of risedronate is the farnesyl diphosphate synthase (FPPS) enzyme, which is responsible for the synthesis of farnesyl diphosphate in the cell.[52] Inhibition of FPPS directly decreases the available pool of FPP, in addition to GGPP, which prevents geranylgeranylation of several

proteins and leads to osteoclast inhibition.[53] Inhibition of geranylgeranylated proteins in osteoclasts is crucial for the treatment of osteoporosis, and this drug specifically inhibits the isoprenoid pathway to prevent protein geranylgeranylation, while also inhibiting the RabGGTase enzyme, representing a dual mode of action.[54,55]

Structure-activity relationship studies on risedronate led to the synthesis and evaluation of phosphonocarboxylate derivatives of the bisphosphonates with low micromolar inhibition of RabGGTase (Figure 2.6).[56] The first such compound was 3-PEHPC, which had a modest IC_{50} value for RabGGTase of 24.1 μM.[56] It was believed that the α-hydroxyl in 3-PEHPC was important for bone mineral binding, so a series of halogen substitutions on the α-carbon were synthesized with the goal of improving binding and enhancing RabGGTase inhibition; this, however, only led to minor improvements (Figure 2.6).[56] Substitution of the pyridine ring structure in 3-PEHPC with a imidazo[1,2-a]pyridine cyclic moiety led to the most potent inhibitor of RabGGTase in this compound class, with an IC_{50} value of 1.3 μM, nearly 25-fold better than the initial inhibitor structure.[57] It was recently discovered that this class of inhibitors only inhibits the second geranylgeranylation step of RabGGTase, not the first, and it was suggested that the phosphonocarboxylate inhibitors bind in a site adjacent to the active site, preventing the mono-geranylgeranylated protein from moving to make way for the second prenylation step.[57] Some Rab proteins are only mono-geranylgeranylated and as a consequence are not inhibited by the

phosphonocarboxylates; the development of specific inhibitors of all Rab protein geranylgeranylation has become a top priority.

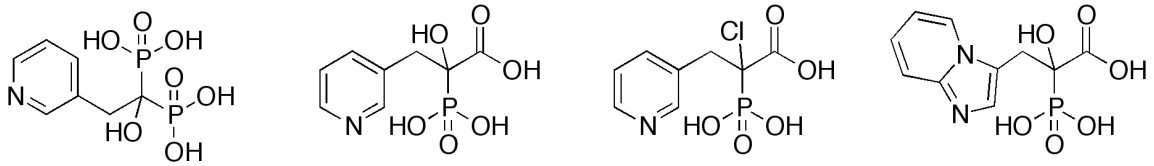

Figure 2.6. Structures and inhibition values of phosphonocarboxylate derivatives of risedronate as inhibitors of RabGGTase. Risedronate, 3-PEHPC, and Cl-3-PEHPC have been described in Marma et al.[56] while 3-IPEHPC was described in Baron et al.[57] Importantly, these compounds were found to only inhibit the second geranylgeranylation step by RabGGTase, and thus are ineffective for mono-geranylgeranylated proteins by RabGGTase.[57]

In addition to the phosphonocarboxylate derivatives, several attempts to make specific peptidomimetic inhibitors for RabGGTase have been attempted, with recent generations performing exceptionally well. In a recent study, Bon and coworkers developed the most selective RabGGTase inhibitors to date by modifying the scaffold of the inhibitor BMS3 (Figure 2.7), which, at the time of their study, was the most potent RabGGTase inhibitor, but that was not selective as it also inhibited FTase.[58] Through structure-activity relationship guided design, their best molecule inhibited RabGGTase with an *in vitro* IC_{50} of 42 nM (Figure 2.7) and displayed high selectivity, as it showed no inhibition of FTase or GGTase I at concentrations up to 9700 nM and 99,500 nM, respectively; the compound also inhibited the proliferation of several cancer cell lines, demonstrating potency in cell-based assays.[58] Continued development of RabGGTase inhibitors in this manner will allow potent inhibitors to be developed with the potential to be used in a clinical setting.

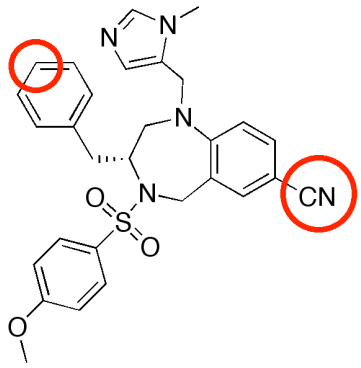

BMS3

IC_{50}: RabGGTase - 724 nM
FTase - 6 nM
GGTase I - >99,500 nM

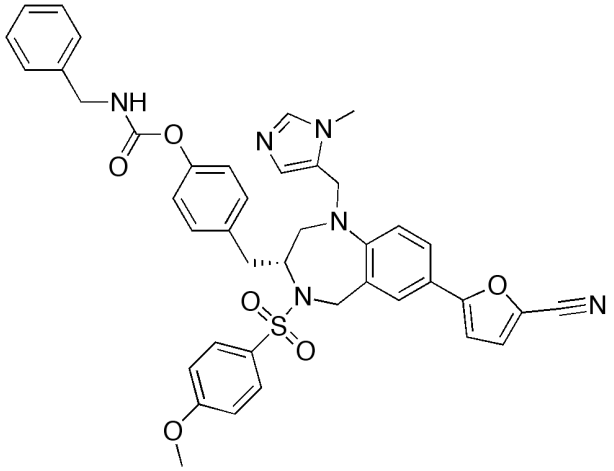

Compound 15

IC_{50}: RabGGTase - 42 nM
FTase - >9700 nM
GGTase I - >99,500 nM

Figure 2.7. Structures of RabGGTase inhibitors used by Bon et al.[58] Starting with the crystal structure of BMS3 bound to RabGGTase, the circled positions in BMS3 were mutated to larger moieties as RabGGTase has room to accommodate the larger substituents but FTase and GGTase I do not. Their best compound displayed remarkable selectivity for RabGGTase with a potent in vitro inhibitory value.

2.5 Prenyltransferase Inhibitors as Cancer Therapeutics

Several inhibitors of FTase and one inhibitor of GGTase have entered clinical trials to test their efficacy in treating various types of cancer in patients. Initial interest in developing farnesyltransferase inhibitors (FTIs) was spurred by the finding that the oncogenic Ras protein is farnesylated[29] and that the farnesyl group is necessary for membrane association and proper function of Ras.[59] Activating mutations in Ras, and specifically K-Ras, are found in more than 30% of all human cancers and have been observed in several tissue specific cancers with alarmingly high frequency, for example greater than 90% of pancreatic cancer and 50% of colorectal cancer harbor K-Ras mutations.[60]

The first report of an inhibitor of FTase was published in 1990[61] and since this time hundreds of different FTIs have been developed, while only four have progressed to clinical trials: tipifarnib, lonafarnib, BMS-214662 and L-778,123 (Figure 2.8).[8] In the 75 different clinical trials using these four compounds alone or in combination with other anti-cancer drugs, a mere 2.3% of all patients treated had an objective response with monotherapy, while only 11.4% had a similar response with combination therapy.[8] The results of these studies have been a tremendous disappointment. The most probable reason for these unanticipated results rests in the fact that the majority of clinical trials enrolled patients harboring mutations in the K-Ras oncogene. It has been shown that the K-Ras protein, as well as N-Ras, can circumvent FTase mediated inhibition by

alternatively prenylating K-Ras with a geranylgeranyl group by GGTase I.[62-65] Patients that had been given an FTI to treat their tumors bearing K-Ras mutations likely suffered from this paradox. Additionally, a majority of the patients enrolled in the 75 clinical trials already had advanced or metastatic disease that may have been too advanced for effective treatment with an FTI. As an example, mice bearing H-Ras mammary tumors showed tumor regression upon daily FTI administration, but when the FTI was withdrawn the tumor reappeared; this may indicate that treating H-Ras bearing tumors early, prior to metastasis, may prove effective.[66] It has been hypothesized that clinical trials utilizing more selective patient enrollments, especially with those patients harboring H-Ras mutations, may have been more effective.

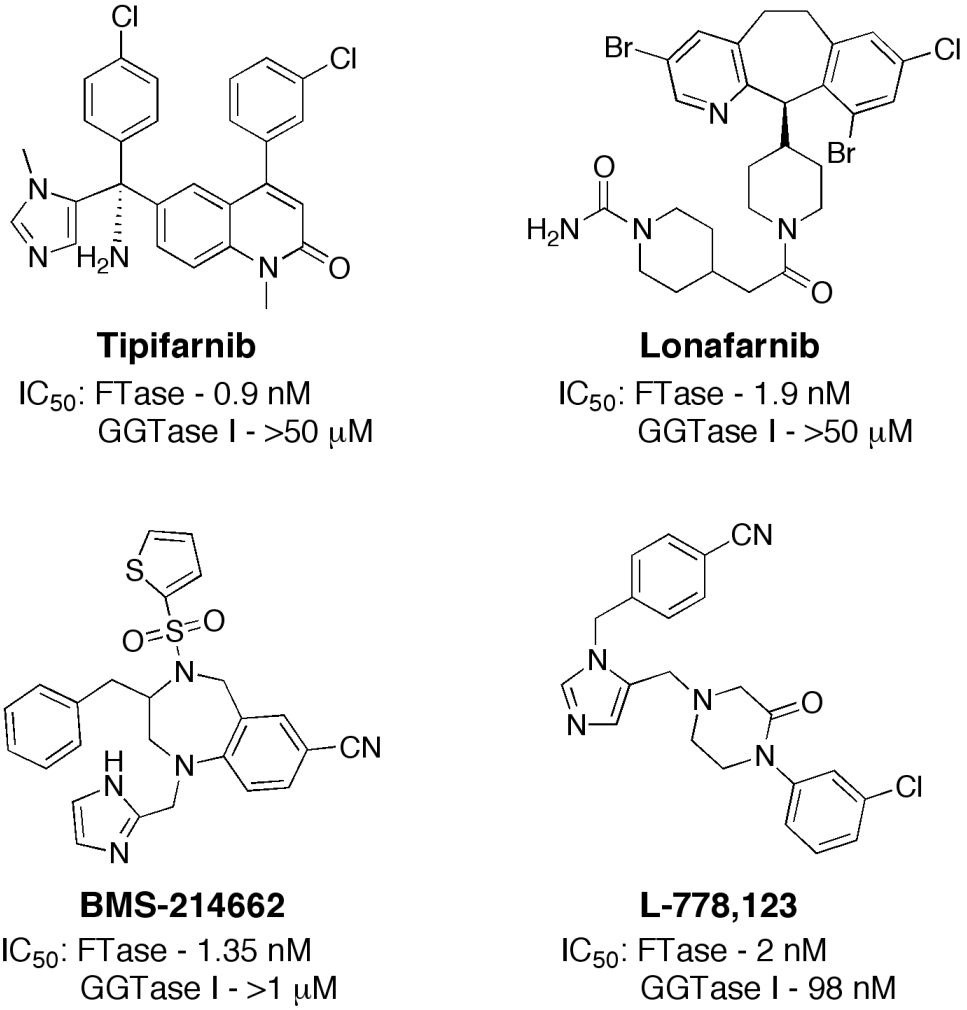

Figure 2.8. Structures of the four FTIs that have been studied in clinical trials for cancer: tipifarnib,[67] lonafarnib,[68] BMS-21466264 and L-778,123.[69]

In early 2009, GGTI-2418 (Figure 2.5) entered Phase I clinical trials investigating tolerability, dosing, and toxicity; patients that had metastatic tumors for which the current therapies were unsuccessful or unavailable were selected for participation. Early results demonstrated that this compound was well-tolerated and had minimal toxicity.[70] However, the Phase I trial of GGTI-2418 has been terminated due to its lack of efficacy in patients (http://kiraxcorp.com/ggti2418.html, personal communication with Kirax Corp. representative). GGTI-2418 was the first GGTase I inhibitor to enter clinical development and, despite its lack of efficacy, it will likely not be the last.

Of the 75 clinical trials involving FTIs for cancer treatment, only two remaining are active, both of which are using tipifarnib. The first is a Phase 2 trial to treat patients with relapsed or refractory lymphoma, while the second is a Phase 3 observational trial to see if tipifarnib or observation alone is better at preventing cancer recurrence in patients with acute myeloid leukemia (www.clinicaltrials.gov).[71] Many of the clinical trials over the last 15 years have been completely unsuccessful, and with the remaining two trials nearing completion, it is likely that clinical trials investigating FTIs in cancer therapy will no longer be a priority.

2.6 FTIs for the Treatment of Progeria

2.6.1 Hutchinson-Gilford Progeria Syndrome

Hutchinson-Gilford Progeria Syndrome (HGPS, progeria) is a rare, autosomal dominant, fatal disorder characterized by early onset aging.[72] Approximately 1 in 4,000,000 children are stricken with this disease and display other phenotypes as a result, such as osteoporosis and alopecia, and those suffering from progeria have a mean survival time of 12.6 years.[73] Remarkably, this disease is the result of a single base pair mutation (C to T) at nucleotide 1824 in the gene coding for the nuclear lamin A protein (LMNA).[74,75] The lamin A protein is initially synthesized as a precursor protein, called prelamin A, that undergoes a series of modifications (Figure 2.9). First, prelamin A is farnesylated, followed by proteolysis of the 'AAX' residues and methylation of the C-terminus. Lastly, an internal cleavage by the enzyme ZMPSTE24 gives rise to non-farnesylated, mature lamin A.[76] In HGPS, the single base pair mutation results in a cryptic mRNA splice site that results in an internal 50 amino acid deletion in prelamin A.[77] Because this form of prelamin A still contains the CAAX box, it is still farnesylated, proteolyzed, and methylated; however, the internal 50 amino acid deletion causes the loss of the ZMPSTE24 internal cleavage site resulting in a permanently farnesylated form of lamin A called progerin (Figure 2.9).[78] Progerin is targeted to the nuclear rim where it interferes with the nuclear lamina, causing mis-shaped nuclei and chromosomal disorganization.[79]

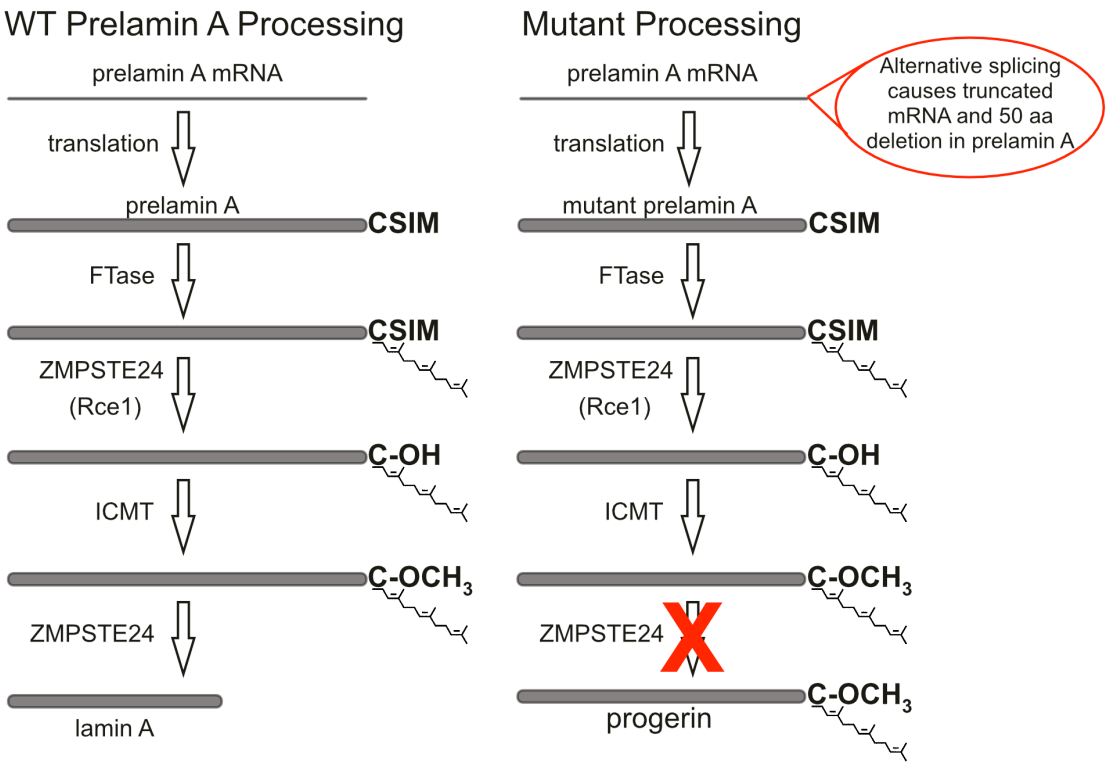

Figure 2.9. Post-translational processing of prelamin A to form mature lamin A. In the left side of the figure the normal processing route from prelamin A to lamin A is shown. In HGPS, a 50 amino acid deletion in prelamin A results from a cryptic splice site in the prelamin pre-mRNA (right side). The consequence of this deletion is the loss of the internal cleavage site for the ZMPSTE24 enzyme, resulting in permanently farnesylated lamin A, called progerin. Because mutant prelamin A still contains the CAAX box, it is still farnesylated.

2.6.2 Treating Progeria with FTIs

The finding that the permanently farnesylated progerin was responsible for the phenotype of progeria led to considerable interest in the use of FTIs in this disease;[80] in theory, if one prevented farnesylation of prelamin A, progerin could not form. Initial studies testing this hypothesis in cell culture were successful, as it was shown that the nuclear blebbing phenotype was lost when fibroblasts from HGPS patients were treated with an FTI.[81] Following these *in vitro* studies a mouse model of HGPS was developed, and it was shown that treatment of these mice with an FTI improved progeria-like disease phenotypes, such as rib fractures and reduced bone density).[80,82,83] Unfortunately, the amelioration of these symptoms was not complete, and eventually all of the mice developed severe disease and died. In addition, it was recently shown that amelioration of the progeria-like symptoms in these mouse models was directly due to blocking the farnesylation of progerin with an FTI.[84]

The prospect of using FTIs as a treatment for progeria in the clinic has been questioned recently due to the finding that progerin can be alternatively geranylgeranylated in the presence of an FTI.[85] Varela and coworkers attempted to use a combination of a statin, to deplete endogenous isoprenoids, and a bisphosphonate, to inhibit the farnesyl diphosphate synthase enzyme. This combination served to reduce the farnesylation of proteins, including lamin A.[85]

These researchers showed that this combination improved progeria-like disease phenotypes in mice. Based on the current evidence, it seems that any therapy targeting protein farnesylation may improve the symptoms of progeria temporarily, but likely will be unable to completely ameliorate the disease in humans.

2.6.3 Clinical Trials with FTIs to Treat Progeria

Prior to assessing the results from a clinical trial to treat progeria, it is necessary to completely establish and characterize all phenotypes, especially those resulting in vascular problems, resulting from this disease. This characterization has been performed,[86,87] and two clinical trials are underway to test the treatment of progeria with FTIs. The first ever clinical trial for the treatment of progeria is a phase 2 trial, started in 2007, that enrolled 29 children with progeria to receive the FTI lonafarnib twice daily for up to two years.[88] The trial ended in early 2010 and the results from the trial should be made available shortly. The second clinical trial is a phase 2 trial that began in 2009 enrolling 45 patients with HGPS to receive a triple combination of zoledronic acid (a bisphosphonate), pravastatin (a statin), and lonafarnib (an FTI).[89] The trial lasted two years and was scheduled for completion in February 2012, with the results of the trial pending. Because no other treatment for progeria currently exists, the results from these trials will be closely scrutinized in the hopes that better therapies can be developed.

2.7 Other Therapies Utilizing Prenyltransferase Inhibitors

2.7.1 FTIs for Parasitic Infections

Several infections caused by parasites have suffered from either resistance to current therapies or a lack of available drugs altogether. Chief among these is malaria, which has seen widespread drug resistance, leading to increased mortality rates, especially in Africa.[90] Several parasitic pathogens contain protein prenylation enzymes, such as *Plasmodium falciparum* (malaria), *Trypanosoma brucei* (African sleeping sickness), *Trypanosoma cruzi* (Chagas disease),[91] *Leishmania major* (leishmaniasis), *Toxoplasma gondii* (toxoplasmosis), *Giardia lamblia* (giardiasis), and *Entamoeba histolytica* (amebiasis).[92-96] The growth of these parasites has been shown to be severely impaired by the inhibition of protein farnesylation with FTIs,[97-100] which suggests that developing inhibitors specific for the parasitic FTase over mammalian FTase may be a viable treatment option to remove the parasitic infection. The structures of the FTase enzymes between parasitic species and metazoans is quite similar, with subtle differences in the substrate specificity and it has been shown that many of the FTIs developed thus far are more potent against cultured parasites than their mammalian counterparts.[101] The reasons for this are unknown, but it may be because the parasites lack GGTase I and thus the protein substrates cannot be alternatively prenylated as they can be in mammalian cells.[101]

Because mammals, like parasites, contain FTase, significant side effects may occur when treating humans with FTIs designed to kill a parasitic infection. For this reason, it is important to develop selective, potent inhibitors of the parasitic FTase while not affecting the mammalian FTase in the host organism (humans). Significant progress has been made in this area, especially while studying *Plasmodium falciparum* FTase (*Pf*FTase). Some initial studies have developed FTIs with approximately 10-fold to 25-fold selectivity for *Pf*FTase over its mammalian counterpart.[102,103] Using structure-activity relationship information based on ethylenediamine analogue scaffolds, Fletcher et al. have developed FTIs that inhibit *Pf*FTase with an IC_{50} of 1 nM that display 136-fold selectivity for *Pf*FTase over mammalian FTase.[104] Development of specific inhibitors for *Pf*FTase has been significantly pursued recently due to the high incidence of drug-resistant malaria, although significant progress on other parasitic diseases has also been made.[91,105,106] With continued development it may be a short matter of time before FTIs to fight parasitic infections appear in the clinic.

2.7.2 Prenyltransferase Inhibitors in Hepatitis Treatment

Hepatitis C virus (HCV) is a persistent infection, often leading to chronic liver inflammation, that affects approximately 200 million people worldwide.[107] The HCV genome encodes for a single protein that is post-translationally processed into at least 10 individual viral proteins.[108] It has been shown that using a GGTase I inhibitor induces dissolution of the HCV replication complex.[109]

This study also demonstrated that because the HCV genome does not encode a geranylgeranylated protein, it may be that a geranylgeranylated host protein is required for viral replication and suggests a GGTase I inhibitor may be a viable therapeutic strategy.[109]

In addition, hepatitis D is caused by the hepatitis D virus (HDV) that requires concomitant infection with the hepatitis B virus and is the most difficult to treat of all the viral hepatitides.[110] It was shown in 1996 that the large antigen of HDV is farnesylated *in vitro* and in animal cells.[111] Since that time, two different FTIs have proven effective at preventing the infection of HDV virions of two different genotypes, including that which is associated with the most severe form of HDV (HDV genotype III virions).[112,113] Both studies concluded that FTIs were a novel class of antivirals with therapeutic potential against these diseases.

2.7.3 Other Therapeutic Uses of FTIs

There are many other potential applications for the therapeutic use of prenyltransferase inhibitors and early evidence indicates that several diseases, such as multiple sclerosis[114] and osteoporosis,[115] could be treated with them. Additionally, fungal pathogens such as *Cryptococcus neoformans* utilize FTase to farnesylate key signal transduction proteins and inhibition of FTase has shown to be a promising treatment for invasive fungal infections.[116,117] Prenyltransferase inhibitors can also be used in non-disease settings, for example in preventing restenosis after balloon angioplasty.[118] Indeed, prenyltransferase inhibitors have

found uses in the treatment of several diseases and afflictions, highlighting the importance of protein prenylation and prenylated proteins in the course of these diseases. However, little is known about the molecular targets of these prenyltransferase inhibitors as well as the enzymology of the prenyltransferases *in vivo*. Chapters 3 and 4 will discuss efforts to elucidate information on the former, while Chapters 5 and 6 will focus on the latter.

3. Unnatural Isoprenoid Analogs to Study Protein Prenylation in Living Cells

Reproduced, in part, with permission from Amanda J. DeGraw, Charuta Palsuledesai, Joshua D. Ochocki, Jonathan K. Dozier, Stepan Lenevich, Mohammad Rashidian, and Mark D. Distefano. Evaluation of Alkyne-Modified Isoprenoids as Chemical Reporters of Protein Prenylation. Chem. Biol. Drug Des. 2010, 76, 460-471. © John Wiley and Sons. Additionally, I would like acknowledge Amanda DeGraw and Charuta Palsuledesai, whom I collaborated with to perform the experiments for some of the data I will show in this chapter and whom prepared the figures.

3.1 Introduction

While decreases in the levels of a number of prenylated proteins have been shown to occur upon treatment with FTIs, direct evidence that these species, and not other undiscovered prenylated proteins, are relevant to the physiological effects of FTIs is severely lacking.[119,120] Determination of the FTase and/or GGTase substrates affected by the inhibition of these enzymes is critical for enhancing our knowledge of the mechanism of action of FTIs and GGTIs. Only a fraction of prenylated proteins have been observed experimentally despite the hundreds predicted by bioinformatics approaches.[121,122] Clearly, comprehensive experimental techniques designed to study the posttranslational modification of proteins with isoprenoids by protein prenyltransferases are

needed. Such techniques would help provide a better understanding of the mechanism of action of FTIs and GGTIs and could assist in the creation of more potent and selective compounds.

3.2 Research Objectives

The goal of the work in this chapter was to develop analogs of isoprenoid compounds that could be used to study the effects of prenyltransferase inhibitors. By using an unnatural analog and allowing cells in culture to metabolically incorporate it, proteins of interest can be tagged through a 'click' reaction and subsequently identified.

3.3 Results and Discussion

3.3.1 Unnatural Isoprenoid Analogs

Our lab has previously reported the synthesis of C15Alk[123] and C10Alk[124] for use in selective protein labeling. The C10Alk is a substrate for farnesyltransferase, while the C15Alk is a dual-substrate for both farnesyl and geranylgeranyltransferase. These compounds were initially used by our lab for *in vitro* labeling experiments, such as immobilizing proteins onto solid substrates.[124] Both substrates are effectively transferred to substrates *in vitro*; however, it has yet to be shown that they can also be utilized by endogenous prenyltransferases in living cells.

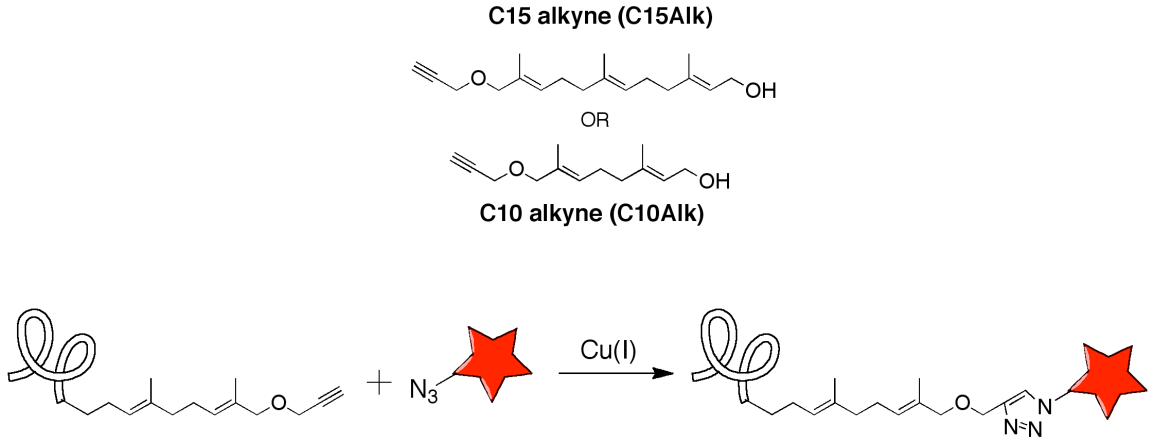

Figure 3.1. Structures of the unnatural isoprenoid analogs used to metabolically label proteins in live cells. Additionally, the scheme for the labeling reaction is shown, in which a protein is modified with the unnatural alkyne analog by the cells endogenous machinery, and a copper-catalyzed 'click' reaction is performed to a fluorophore azide to form a covalent bond. In this manner, all of the prenylated proteins that receive this unnatural modification can be tagged with a fluorophore for futher study.

3.3.2 Metabolic Lableing in HeLa Cells and Response to Inhibitors

Initially, we set out to determine if these unnatural, alkyne containing, isoprenoids would be incorporated into cellular proteins by the cells own machinery. To test this, we grew cells in the presence of the unnatural analog at 50 μM for 24 h by simply adding either C10Alk or C15Alk to the cellular media. Following this incubation, the cells were washed to remove excess alkyne and were subsequently lysed. To the cell lysate, TAMRA-N_3, TCEP, TBTA, and $CuSO_4$ were added to perform the 'click' reaction between the alkyne moiety (now attached to a protein) and the fluorophore azide to form a covalent bond (Figure 3.1). After the click reaction, the excess reagents are removed by precipitating the proteins, so only protein remains following re-solubilization. The lysate is then run on an SDS-PAGE gel and the gel is scanned for fluorescence of the TAMRA fluorophore. Fluorescent bands in this gel correspond to labeled proteins in the sample.

After initial experiments showed promise with both compounds, more intense labeling was observed with the use of C15Alk, as it is a dual-substrate for two prenyltransferase and thus is incorporated to a greater extent (Figure 3.2, lane 2). Several bands are seen in lane 2 of Figure 3.2, indicating that incorporation of C15Alk is successful and that we are tagging proteins with a fluorophore through the click reaction. It can also be seen from lane 1 of this gel

that there is very little background labeling, which indicates that we are looking specifically at prenylated proteins and not non-specific labeling. Additionally, lanes 3 and 4 of Figure 3.2 have been co-treated with inhibitors of either FTase or GGTase I, respectively. Because these enzymes are necessary to incorporate the unnatural alkyne analog, inhibiting them should prevent incorporation of the probe and thus reduce the number and/or intensity of the labeled bands observed in the gel. As can be seen from Figure 3.2, there are several bands that disappear upon FTI treatment and some that diminish upon GGTI treatment. Surprisingly, one band (approximately 25 kDa) increases substantially upon FTI treatment, which is unexpected. It may be that this protein is alternatively geranylgeranylated in the presence of FTI, as when the GGTI is used the band is diminished. Regardless, these results show that specific incorporation of the alkyne analogs is occurring in cells.

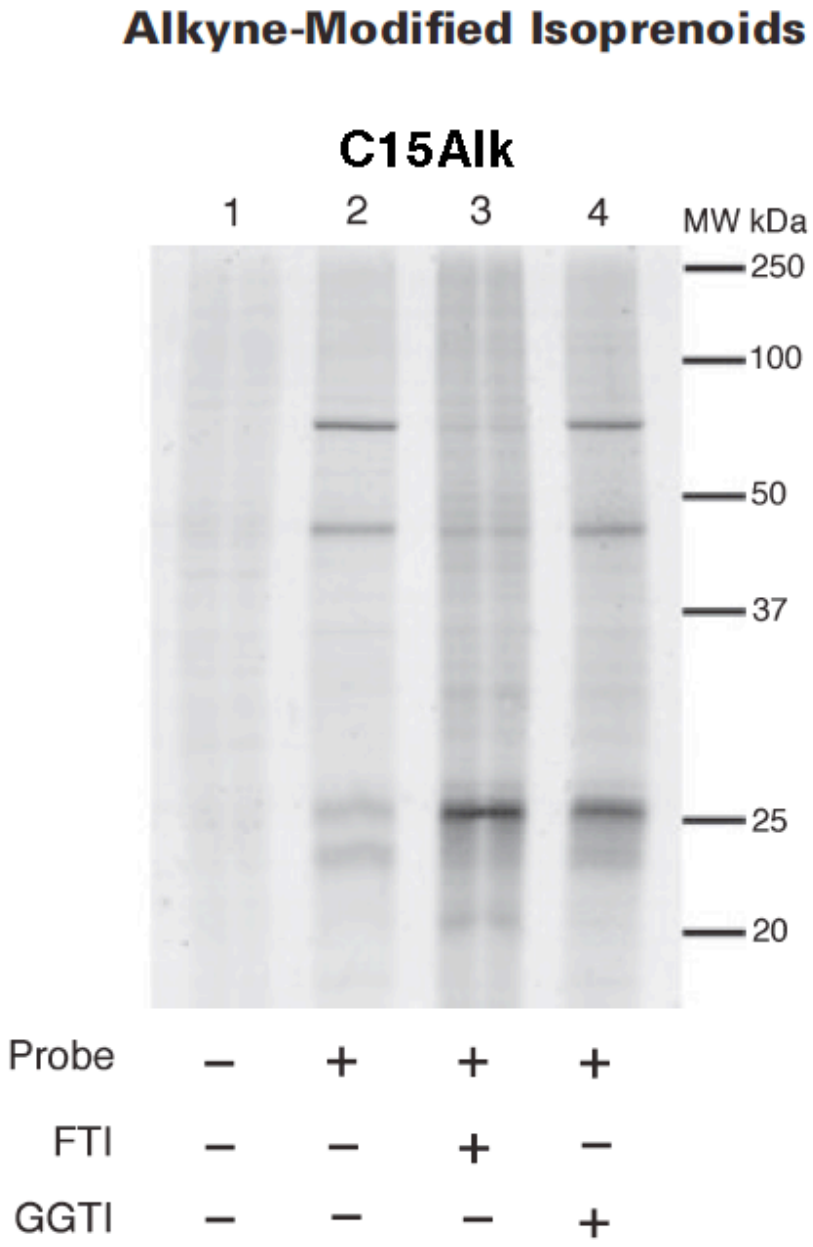

Figure 3.2. In-gel fluorescence analysis of prenylated proteins in HeLa cells. Cells were treated with C15Alk isoprenoid analog (50 μM) and reacted with TAMRA-azide. Lane 1: no treatment control; Lane 2: treatment with isoprenoid analog only; Lane 3: treatment with analog and farnesyltransferase inhibitor; Lane 4: treatment with analog and geranylgeranyltransferase inhibitor.

3.3.3 Effects of the Addition of Lovastatin During Metabolic Labeling

It was hypothesized that the incorporation of our unnatural analogs is not very effective because they must compete with the endogenous pool of natural isoprenoids in the cell. This may be an issue, especially because, as mentioned previously in chapter 2, the K_D of farnesyldiphosphate (the natural substrate) for FTase is 2 nM. One method to deplete the endogenous isoprenoids in the cells and thus maximize the incorporation of our probes is to use a statin, such as lovastatin. Lovastatin inhibits the HMG-CoA reductase enzyme in the mevalonate pathway and prevents the cell from synthesizing its own isoprenoids. Using lovastatin in conjunction with our probes should maximize their incorporation, as it will minimize the competition with the native substrate. To test this, cells were grown in the presence of lovastatin and either C10Alk or C15Alk for 24 h, lysed, clicked to TAMRA-N_3, and a gel was run of the lysate. Scanning the gel for fluorescence reveals that there is little difference between lovastatin treatment and not using lovastatin (Figure 3.3); the staining intensity is quite similar. Additionally, this data also highlights the more extensive labeling of C15Alk compared to C10Alk (compare lanes 3' to 1', for example). Overall, this data indicates that our unnatural compounds are being incorporated well without the need for lovastatin, so subsequent experiments were done in the absence of this compound.

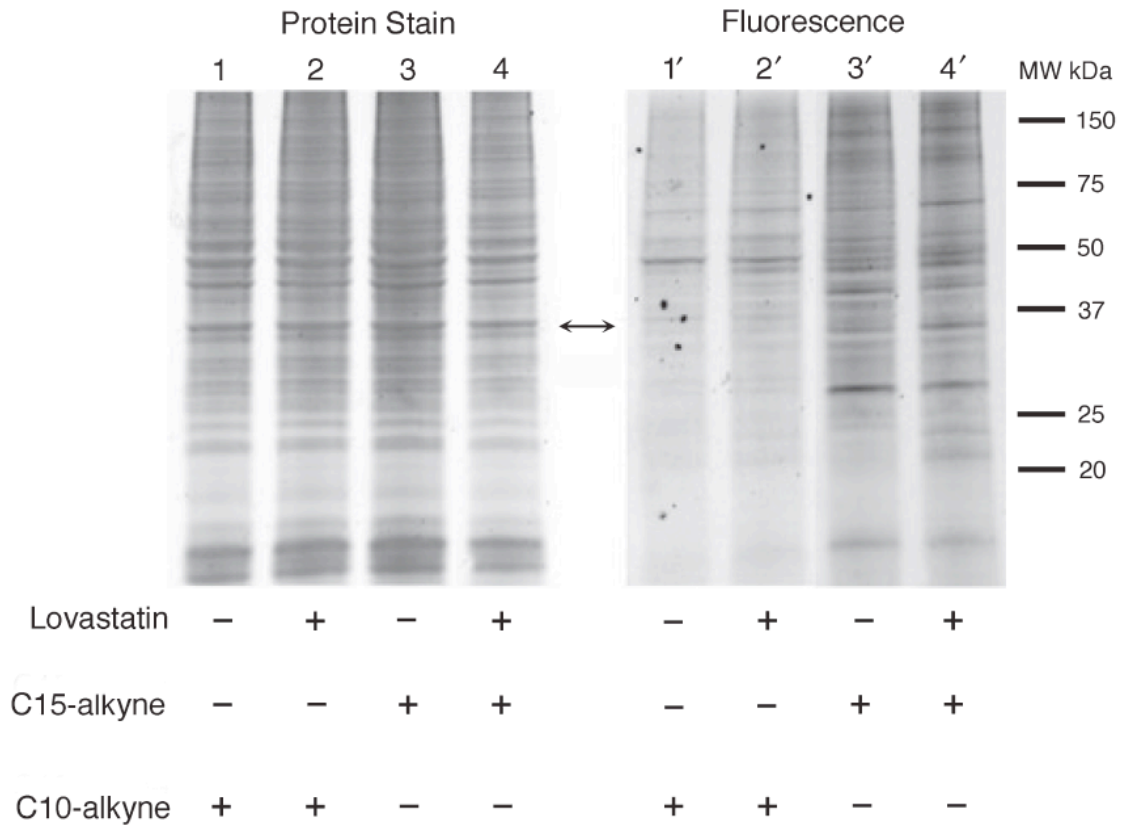

Figure 3.3. In-gel fluorescence analysis of prenylated proteins in HeLa cells in the absence and presence of lovastatin. Cells were grown in the presence of the C10Alk (lanes 1 / 1' and 2 / 2') or C15Alk (lanes 3 / 3' and 4 / 4'). Lanes 1–4 show total protein stain with Sypro Ruby. Lanes 1'–4' show fluorescently labeled proteins. Lanes 1 / 1' and 3 / 3' contain samples from cells not grown in the presence of lovastatin. Lanes 2 / 2' and 4 / 4' contain samples from cells treated with lovastatin. Following lysis, samples were treated with TAMRA-N_3 (50 μM) to allow the prenylated proteins to be visualized.

3.3.4 Identifying Proteins Labeled with Unnatural Isoprenoids

After establishing that visualization of prenylated proteins by fluorescent gel electrophoresis can be accomplished, we sought to determine specific proteins that were modified and that changed in response to inhibitor treatment. Our initial attempts to cut bands from this one-dimensional SDS-PAGE gel, digest them with trypsin, and submit them for mass spectrometry analysis proved unsuccessful, because even in a small band from this gel more than 100 proteins were identified. Using a crude lysate sample on this one-dimensional gel will likely not be successful because of the sample complexity. To circumvent this we turned to using two-dimensional gel electrophoresis, in which the proteins are first separated by their isoelectric point in one direction, followed by their molecular weight in another. This reduces the number of proteins contained in an individual spot and increases the chance of successful protein identification.

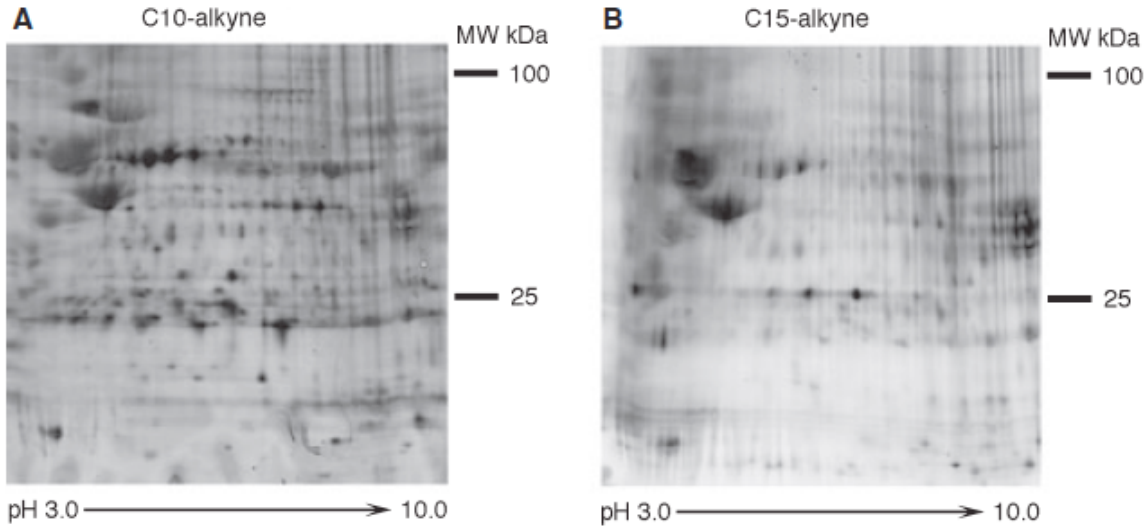

Figure 3.4. In-gel fluorescence analysis of prenylated proteins from HeLa cells after 2D electrophoretic separation: A: Two-dimensional gel of labeled proteins obtained from HeLa cells grown in the presence of C10Alk. B: Two-dimensional gel of labeled proteins obtained from HeLa cells grown in the presence of C15Alk.

Metabolic incorporation of C10Alk or C15Alk for 24 h, followed by cell lysis and two-dimensional gel electrophoresis allowed the resolution of single protein spots (Figure 3.4). The mass spectrometry facilities have the capability to pick spots from these gels with a robot, digest them, and analyze them by LC-MS/MS in an automated fashion. As a proof of principle, 20 spots were cut from the gel shown in Figure 3.4A with this automated system. The samples were trypsinized and subjected to LC-MS/MS analysis for protein identification. In this experiment, many proteins were identified at lower confidence, and 7 were identified with greater than 99% confidence (Table 3.1). Interestingly, several Rab proteins were identified. RabGGTase generally transferes two C15 isoprenoids onto the C-terminus of a protein, and it can be seen from the C-terminal sequence that these proteins contain two cysteine residues for this to occur. Whether these proteins are di-prenylated with C10Alk is unclear, but it lends support to the idea that RabGGTase is the most promiscuous of the prenyltransferase enzymes (see chapter 1 section 4). Additionally, the Annexin A3 protein was identified in this analysis and this is a bit unexpected, as the C-terminal sequence is not a typical CAAX sequence, but instead is a CAAAX sequence. Our *in vitro* attempts to prenylated this sequence on a short peptide have been unsuccessful (data not shown) and a recent study indicates that the Annexin proteins are not substrates for the prenyltransferase enzymes.[125] More work needs to be done to better understand the molecular targets of the prenyltransferase enzymes *in vivo*.

Table 3.1. Summary of proteins identified with proteomic analysis using C10Alk.

Protein	Accession number	C-terminal sequence	Number of peptides	Sequence coverage (%)
GNBP	gi 5729850 ref NP_006487.1	CGLY	3	7
Lamin B1	gi 5031877 ref NP_005564.1	CAIM	10	19
Rab 1B	gi 13569962 ref NP_112243.1	GGCC	8	38
Rab 2A	gi 4506365 ref NP_002856.1	GGCC	3	16
Rab 6A	gi 38679888 ref NP_942599.1	GCSC	4	24
Rab 7	gi 34147513 ref NP_004628.4	SCSC	3	15
Annexin A3	gi 4826643 ref NP_005130.1	CGGDD	6	19

3.4 Conclusions

This chapter discusses efforts to identify specific proteins that are prenylated and which proteins change in abundance in response to prenyltransferase inhibitor treatment. Towards this goal, the alkyne containing isoprenoids C10Alk and C15Alk were used in cell culture to metabolically label prenylated proteins and tag them with an alkyne moiety. Subsequent cell lysis and 'click' reaction to a fluorophore azide facilitated the tagging of prenylated proteins with a fluorophore. Separation of proteins by either one- or two-dimensional gel electrophoresis and scanning in the fluorescence channel allowed the prenylated proteins to be visualized. In addition, excision of these bands from the two-dimensional gel and subsequent LC-MS/MS analysis identified several prenylated proteins tagged with our unnatural isoprenoid analog. This method will serve as the foundation toward the better understanding of the effects of prenyltransferase inhibitors on the abundance of particular prenylated proteins. This information will prove useful for the development of specific inhibitors of a particular protein *in vivo*.

3.5 Experimental

3.5.1 General Materials

Protease inhibitor cocktail and benzonase were purchased from Sigma Aldrich

(St. Louis, MO, USA). PFTase inhibitor L-778 834 (FTI), PGGTase-I inhibitor GGTI-286 (GGTI), and ProteoExtract protein precipitation kits were obtained from Calbiochem (EMD Chemicals, Gibbstown, NJ, USA). TAMRA-azide was purchased from Invitrogen (Carlsbad, CA, USA). Detergent-compatible protein assay reagents and Tris–HCl sodium dodecylsulfate polyacrylamide gel electrophoresis (SDS-PAGE) Protean II Ready gels were obtained from Bio-Rad (Hercules, CA, USA). Immobline Dry-Strips and ampholyte buffer were purchased from GE Healthcare (Piscataway, NJ, USA). One-dimensional gels were visualized using a BioRad FX Molecular Imager. Two-dimensional electrophoresis was performed using an Ettan IPGphor IEF apparatus and the resulting fluorescent spots visualized using a Typhoon 8610 scanner, both obtained from GE Healthcare. Fluorescent spots were picked using an Investigator ProPic instrument (Genomic Solutions, Ann Arbor, MI, USA). The Paradigm Platinum Peptide Nanotrap precolumn and Magic C18 AQ RP column were purchased from Michrom Bioresources (Auburn, CA, USA). LC–MS/MS analysis was performed using Paradigm 2D capillary LC system (Michrom Bioresources) interfaced with a linear ion trap spectrometer (LTQ, Thermo Scientific, Waltham, MA, USA). For data analysis, Sequest embedded in BioWorks Browser (v 3.3) was obtained from Thermo Scientific and Scaffold (v2.00.03) was licensed from PROTEOME Software (Portland, OR, USA). Large-scale (1 L) growth of HeLa cell was performed by Biovest International Inc. / NCCC (Minneapolis, MN, USA). C10Alk[124] and C15Alk[123] were prepared as

previously described.

3.5.2 Cell Growth and Lysis

All cell lines except were routinely cultured in Dulbecco's modified Eagle's medium (DMEM) supplemented with 10% fetal bovine serum (FBS). For labeling experiments, cell media were supplemented with 25 μM lovastatin and 50 μM C10Alk or C15Alk. In some cases, the FTase inhibitor L-778,834 at 10 μM (FTI) or the GGTase-I inhibitor GGTI-286 (GGTI) at 5.0 μM were included in the cell media. The cells were allowed to reach 80–90% confluence (approximately 24 h) and then washed with phosphate-buffered saline (PBS). Cells were then suspended in PBS, placed in 1.5-mL microcentrifuge tubes, and pelleted by centrifugation at 2000x*g*, 4 °C, for 5 min. After discarding the supernatant, a PBS solution containing 0.10% SDS, 0.20% Triton X-100, protease inhibitor cocktail, benzonase, and 2.4 μM PMSF was added to the cell pellet. After vigorous vortexing, cell lysate was harvested by sonicating 4 times for 10 seconds each with 20 seconds intervals between sonication cycles. The concentration of protein in the lysate was determined using a detergent-compatible protein assay reagent kit.

3.5.3 Prenylation Changes Upon Inhibitor Exposure

To the cell lysate (1–2 mg ⁄ mL of protein) from one 60-mm dish of cells was added 50 μM TAMRA-azide, 50 mM TCEP, and 100 μM TBTA. After vortexing,

1.0 mM $CuSO_4$ was added, and the reaction was allowed to proceed at rt for 1 h. Excess reagents were removed by protein precipitation with a ProteoExtract protein precipitation kit. Protein pellets (200–300 μg of total protein) were suspended in 1x Laemmli SDS-PAGE loading buffer and sonicated in a water bath for 20 min to insure dissolution. A 12% SDS-PAGE gel was loaded with approximately 10 μg of protein for in-gel fluorescence scanning and visualized with a BioRad FX Molecular Imager.

3.5.4 Two-dimensional Gel Electrophoresis

Two-dimensional gel electrophoresis was performed at the Center for Mass Spectrometry and Proteomics, University of Minnesota, Twin Cities using a standard procedure.[126] In brief, the protein pellet was resuspended in IPG running buffer [7.0 M urea, 2.0 M thiourea, 2.0% CHAPS, bromophenol blue, 0.50% (v / v) ampholyte buffer, 1.0% n-dodecyl β-D-maltoside, and 12 mM dithiothreitol (DTT)]. Samples containing 800 μg of protein were rehydrated into 18 cm pH 3–10 Immobline_ DryStrips overnight under low current and resolved in an Ettan IPGphor IEF apparatus per manufacturer's protocol. Strips were then equilibrated in SDS equilibration buffer (50 mM Tris, pH 8.8, 8.0 M urea, 30% glycerol (v / v), 4.0% SDS, 1.0% DTT) for 0.5 h and resolved on 8–16% Tris–HCl SDS PAGE Protean II Ready gels. TAMRA labeled proteins on the gel were visualized with Typhoon 8610 scanner using an excitation wavelength of 532 nm and a 580BP30 emission filter (580 nm). Gel images were imported into a

Genomic Solutions Investigator Pro-Pic instrument for robotic excision and robotic trypsin digestion of excised spots.[127] Tryptic peptides were then lyophilized and stored at -20 °C prior to subsequent use.

3.5.5 Cell Growth and MS Analysis to Identify Prenylated Proteins

Large-scale (1 L) cultures of HeLa cells were grown in Joklik's modified MEM with 5.0% FBS. For metabolic labeling, cells at mid-log phase were treated with 25 μM Lovastatin and 50 μM C10Alk or C15Alk, and allowed to grow for 24 h. Cells were collected by centrifugation at 2500x*g*, followed by two washes in cold PBS (Ca/Mg free). Cell pellets were resuspended in PBS containing 1.0% SDS, protease inhibitor cocktail, and benzonase and sonicated on ice for 2 min in total (10 seconds pulse, 10 seconds rest). The concentration of protein in the lysate was determined using detergent-compatible protein assay reagents. Proteins in the lysate were precipitated using a trichloroacetic acid (TCA)/acetone protocol. Briefly, a 100% TCA solution (100 g TCA in 45.4 mL water) was added to the lysate so as to obtain a 10% final concentrationfof TCA in the solution that was vortexed and stored on ice for 1 h. HPLC-grade acetone (4x lysate volume) was then added to the mixture and maintained at -20 °C overnight. The lysate was then centrifuged at 10 000x*g* for 30 min to obtain a protein pellet. The supernatant was discarded, and the pellet was washed twice with acetone and air dried for 5 min. Precipitated proteins were resuspended in PBS containing 0.20% SDS by brief vortexing and sonication. Protein concentration was

measured using detergent compatible protein assay reagents. For protein labeling, 3.0 mg (1.9 mg / ml) of HeLa lysate protein was treated with TAMRA-azide, TCEP, and TBTA at final concentrations of 25 μM, 1.0 mM, and 100 μM, respectively. After vortexing, $CuSO_4$ (1.0 mM, final concentration) was added, and the reaction was allowed to proceed at rt for 1 h. Excess reagents were removed by protein precipitation using the above-mentioned TCA / acetone protocol, and the resulting protein pellet was stored at -20 °C prior to subsequent use.

LC-MS analysis was performed using a Michrom Bioresources Paradigm 2D capillary LC system interfaced with a linear ion trap spectrometer using a standard procedure.[126] Lyophilized tryptic peptides dissolved in water / CH_3CN/ formic acid (95:5:0.1) were desalted and concentrated with a Paradigm Platinum Peptide Nanotrap (Michrom Bioresources) precolumn and eluted onto a Magic C18 AQ RP column at a flow rate of approximately 250 nL / min. A 60-min (10–40% CH_3CN) linear gradient was used to separate the peptides. The peptides were ionized with a voltage of 2.0 kV applied distally on the column and analyzed on the LTQ instrument set to positive polarity and data-dependent acquisition method (one survey MS scan followed by MS/MS (relative collision energy of 35%) on the four most abundant ions detected in the survey scan). Dynamic exclusion was employed for 30-second time intervals.

The MS/MS data were searched with Sequest embedded in Bio-Works Browser (v 3.3, Thermo Scientific) against the database of human, mouse, and rat [NCBI

(http://www.ncbi.nlm.nih.gov)] nonredundant protein sequences, in addition to 179 common contaminant proteins (Thermo Scientific), for a total of 263,677 proteins. Fragment ion mass tolerance and parent ion tolerance were set at 1.00 Da. The search parameters were as follows: trypsin digestion, fixed carbamidomethyl modification of cysteine, and variable oxidation of methionine, three missed trypsin cleavage sites allowed. The dta / out files generated by Bioworks were analyzed in Scaffold (v2.00.03, PROTEOME Software) to validate MS / MS-based peptide and protein identifications. Peptide identifications were accepted if they could be established at >95.0% probability as specified by the Peptide Prophet algorithm.[128] Protein identifications were accepted if they could be established at > 99.0% probability by the Protein Prophet algorithm[129] and contained at least three identified peptides.

4. Imaging and Quantification of the Prenylome

4.1 Introduction

Chapter 3 detailed using a method involving unnatural alkyne analogs to identify specific prenylated proteins in living cells. This chapter describes the use of these same analogs to analyze the entire global prenylome (the subset of all prenylated proteins). Several methods have been recently developed to study various post-translational modifications of proteins using unnatural analogs that exploit metabolic labeling in concert with bioorthogonal chemistry (see reviews 130-133). Some of the most commonly employed methods include the use of glycosylation,[134-136] palmitoylation,[137-139] myristoylation,[140,141] and prenylation substrates[142-144] that incorporate bioorthogonal functionality that can be derivatized via the copper catalyzed click reaction (3+2 Huisgen cycloaddition) or the strain-promoted alkyne-azide cycloaddition (SPAAC). To date, these methods have mainly been employed to metabolically incorporate the unnatural analog and follow the fate of individual proteins in *ex vivo* cell culture or animal models including zebrafish and mice, with glycosylation being the most studied.[145-148] Despite the numerous reports using such strategies, there have only been a small number reported that allow for the examination of prenylated proteins, and even fewer that allow for the levels of prenylated proteins to be quantified. Historically, in the prenylation field, the most common method for quantification has been through the use of radioactive assays employing tritiated forms of farnesyl diphosphate, geranylgeranyl diphosphate, or mevalonic acid. Even as

late as 2006, the only method for quantifying prenylated proteins was still a radioactive based assay.[149] The inherent problem with tritium-based radiochemical methods is their low inherent sensitivity; autoradiography can require exposure times as long as several months.[150] As an alternative method, a tagging-via-substrate approach was employed by Chan and coworkers in which an azide isoprenoid substrate was metabolically incorporated into proteins in mammalian cells, which allowed for several geranylgeranylated proteins to be identified by mass spectrometry after a click reaction to an alkyne fluorophore and band excision from a two-dimensional SDS-PAGE gel.[151] The difficulty with this method is that using excess alkyne fluorophore leads to substantial background labeling.[144] Circumventing this problem, Nguyen and coworkers developed a mass spectrometry based method to quantify prenylated proteins using an unnatural biotin isoprenoid analog.[28] This approach was able to detect low levels of prenylated proteins, however, in order to achieve incorporation of the biotin analog the authors had to perform site directed mutagenesis of farnesyl and geranylgeranyltransferase to accept the substrate, thus requiring the labeling to be performed on cell lysates instead of in physiologically active cells. Significant perturbation of the isoprenoid substrate structure may also result in compensatory changes in protein substrate specificity.[23] To gain an accurate picture of the complete prenylome *in vivo*, a method that relies on native cellular machinery is needed.

Our group and others have previously reported on the development and use of alkyne isoprenoid analogues to study various aspects of protein prenylation[123,124] through the Huisgen 1,3 dipolar cycloaddition, also known as the click reaction.[152] In our earlier work, the focus was on the identification of prenylated proteins present within cells. In this chapter, we extend the use of these alkyne-containing alternative substrates by describing a method that allows for imaging and quantification of the global prenylome through the use of the click reaction in situ (Figure 4.1).

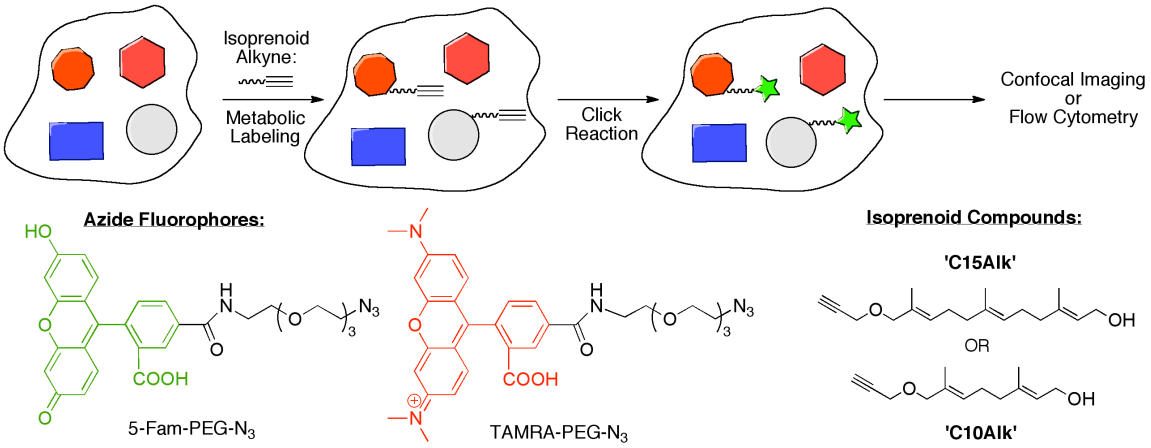

Figure 4.1. Metabolic incorporation of alkyne isoprenoid analogs in living cells and subsequent derivitization to a fluorophore for further analysis, allowing global prenylome monitoring.

This method allows for localization studies of prenylated proteins in various cell types, with our results highlighting the distribution of most of the labeled prenylated proteins in the endoplasmic reticulum. In addition, we show that various types of cells from different tissues have drastic differences in the level of prenylated proteins. Also, the extent of prenylated protein labeling was explored with respect to alkyne concentration, incubation time and permeabilization time. Furthermore, co-incubation with farnesol or inhibitors of farnesylation leads to a concomitant reduction in labeling, illustrating the specificity of the alkyne isoprenoids for prenylated proteins. Lastly, using this method and an ATG7 autophagy knockdown cellular model of aging, we show that the levels of prenylated proteins are increased in a cellular model of aging. This may indicate a potential involvement of protein prenylation in aging disorders such as Alzheimers and Parkinsons disease.

4.2 Research Objectives

The aim of the work in this chapter is to develop a method to quantify the global prenylome through the use of unnatural isoprenoid analogs. This will allow for a better understanding of protein prenylation and how this process may be involved in several neurodegenerative diseases.

4.3 Results and Discussion

4.3.1 Characterization of Alkyne Substrates

In chapter 3 it was demonstrated that the incorporation of the unnatural isoprenoid alkyne analogs using fluorescently scanned SDS-PAGE gels was successful. To support this hypothesis it was necessary to show incorporation of the alkyne analogs into specific proteins. In support of this and prior to performing the click reaction on mammalian cells to investigate prenylated proteins, we sought to determine whether the C10 and C15 alkyne isoprenoids (C10Alk and C15Alk, respectively) could be efficiently incorporated into the H-Ras protein in cell culture. Previous studies have shown that a related isoprenoid azide can be efficiently incorporated into H-Ras, a prototypical farnesylated protein,[153] however, no data is available for the alkyne isoprenoid analogues. Accordingly, COS-1 cells were incubated with lovastatin, an HMG-CoA reductase inhibitor, to deplete the endogenous isoprenoids in the cells. The consequence of this treatment is that prenylated proteins, such as H-Ras, are unable to be processed (prenylated, proteolyzed and methylated) and a shift to unprocessed H-Ras (Figure 4.2, top band 'U') was observed by western blot. Even though a high concentration of lovastatin was used, the processing of H-Ras cannot be completely abolished, but only reduced to approximately 45% unprocessed protein (Figure 4.2, lane 2), compared to approximately 90% of H-Ras being processed under normal conditions (Figure 4.2, lane 1, and Figure 4.3). When lovastatin was administered in combination with farnesol, the precursor to the native substrate FPP, H-Ras processing was completely rescued (Figure 4.2,

lane 3) to levels seen in the negative control. When giving lovastatin in combination with C10Alk (Figure 4.2, lane 4) or C15Alk (Figure 4.2, lane 5), H-Ras became 60% and 70% processed, respectively. It is clear from this data that C10Alk is not incorporated as well as C15Alk in cell culture, at least in the H-Ras protein, but also that C15Alk cannot completely rescue H-Ras processing. This is not altogether unexpected, since this unnatural analog is not as good of a substrate as FPP; C10Alk is incorporated approximately 12-fold slower than FPP[124] while C15Alk has an approximately 8-fold higher K_M value for FTase than does FPP.[123] Despite the lower incorporation, it is clear that significant amounts of the alkyne isoprenoids are metabolically incorporated rendering them suitable for cellular studies of prenylated proteins.

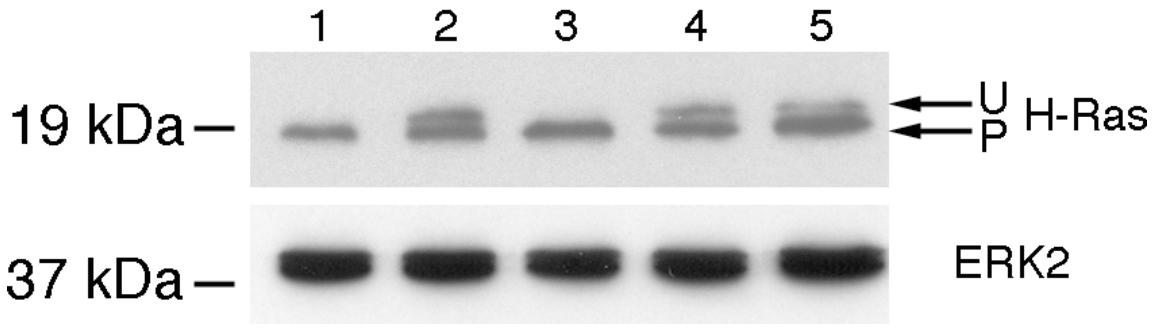

Figure 4.2. Incorporation of C10Alk and C15Alk into H-Ras in COS-1 cells. COS-1 cells were treated with either DMSO (0.05% v/v, lane 1), 25 μM lovastatin (lane 2), 25 μM lovastatin & 100 μM farnesol (lane 3), 25 μM lovastatin & 100 μM C10Alk (lane 4), or 25 μM lovastatin & 100 μM C15Alk (lane 5). After 24h, whole cell lysates were prepared and 40 μg of protein was resolved by 15% SDS-PAGE. The proteins were transferred to a PVDF membrane and incubated with an antibody against H-Ras. Note the faster mobility of processed Ras (P) compared with unprocessed Ras (U). Total ERK2 levels were measured as a loading control as they should not change in response to treatment with lovastatin or alkyne isoprenoids.

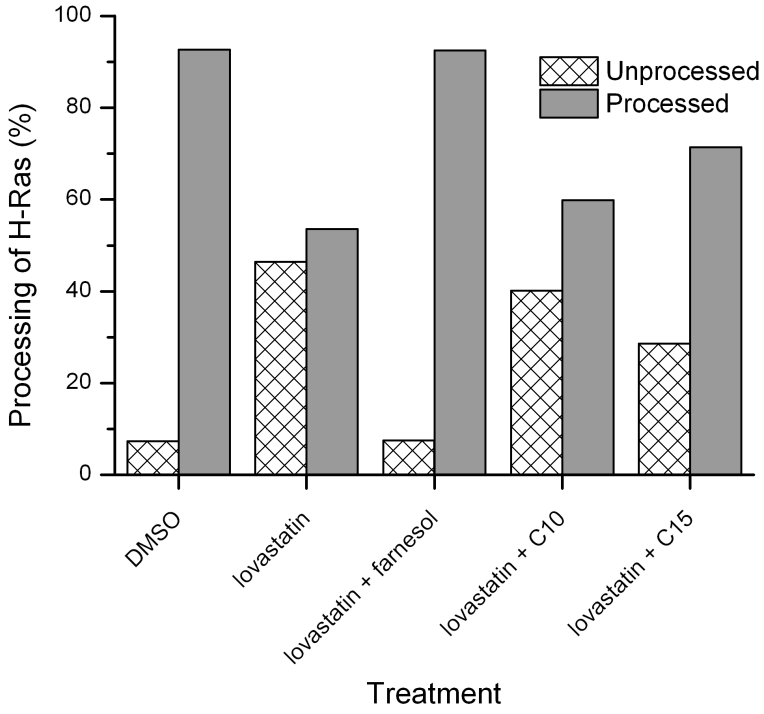

Figure 4.3. Incorporation of the C10Alk and C15Alk into H-Ras in COS-1 cells. ImageJ was used to quantify the amount of processing of H-Ras by densitometry of the western blot in Figure 4.2.

4.3.2 Cellular Labeling and Visualization of Prenylated Proteins

After confirming that the alkyne isoprenoids were incorporated into H-Ras, we set out to determine if it was possible to use the click reaction to image the distribution of prenylated proteins in a mammalian cell. Our methodology (Figure 4.1) consists of using either C10Alk or C15Alk to metabolically label a culture of mammalian cells. As noted above, previous work by our group has demonstrated that these unnatural isoprenoid analogs are used efficiently by protein prenyltransferases.[123,124] Upon metabolic incorporation of the alkyne into naturally prenylated proteins, the cells are fixed and permeabilized in preparation for the click reaction with a fluorophore azide. Following the click reaction, the cells can be imaged with confocal microscopy or analyzed by flow cytometry to quantify the total amount of prenylated proteins in the cells.

Two fluorophore azides were used: 5-Fam-PEG-N_3, which was synthesized as previously described,[154] and TAMRA-PEG-N_3, which was synthesized in an analogous manner. Briefly, TAMRA-succinimidyl ester was reacted with 11-Azido-3,6,9-trioxaundecan-1-amine in the presence of diisopropylethylamine to afford the desired product. It is important to note that the choice of fluorescent azide is critical to the experiment, as using an azide that replaces the flexible ethylene glycol-based hydrophilic linker used here with a less flexible or shorter, hydrophobic linker results in a large amount of background labeling (data not shown).

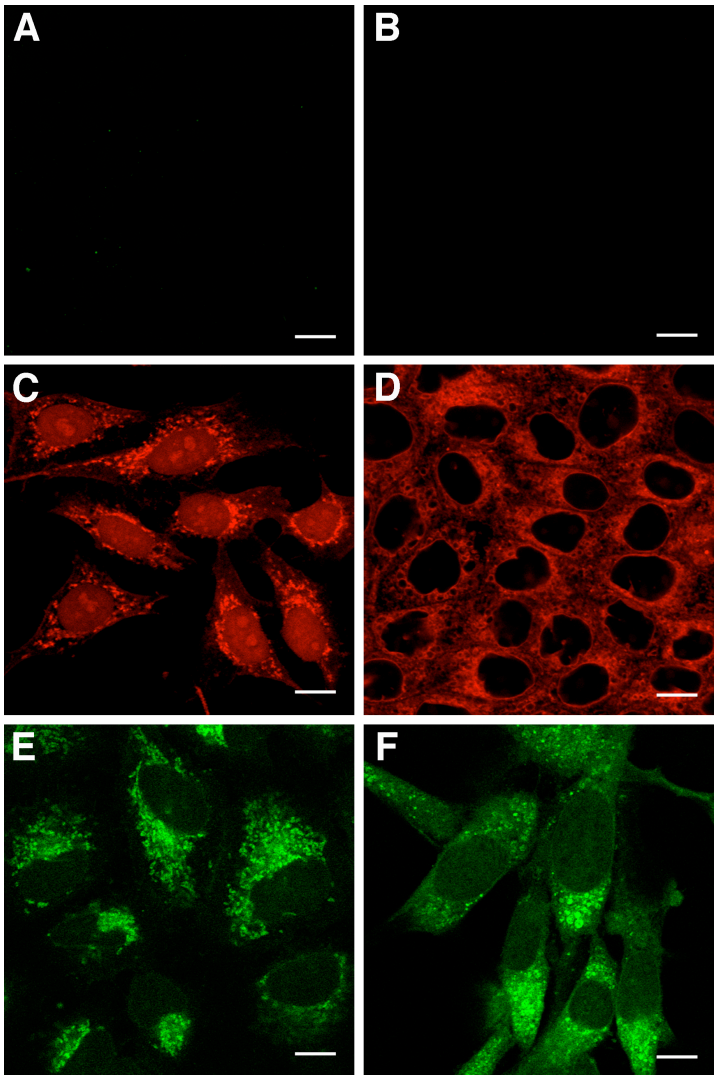

Figure 4.4. Imaging of prenylated proteins in mammalian cells with confocal microscopy. Various types of cells were treated with 50 μM C15Alk for 24 h, followed by fixation with paraformaldehyde and permeabilization with Triton X-100. After several rinses, the cells were subjected to the click reaction for 1 h with either TAMRA-PEG-N_3 or 5-Fam-PEG-N_3. A) Control reaction in which A549 cells were treated with DMSO only and were subjected to the click reaction with 5-Fam-PEG-N_3. B) Same as A) using MDCK cells and TAMRA-PEG-N_3 as the fluorophore, demonstrating the low level of background labeling. C) HeLa cells clicked to TAMRA-PEG-N_3. D) MDCK cells clicked to TAMRA-PEG-N_3. E) A549 cells clicked to 5-Fam-PEG-N_3. F) NIH/3T3 cells clicked to 5-Fam-PEG-N_3. Size bar represents 20 μm.

To investigate the feasibility of this method we first incubated various types of cells with C15Alk at 50 μM for 24 h to allow maximum incorporation of the alkyne isoprenoid. Following the incubation, the cells were fixed in paraformaldehyde and permeabilized with Triton-X-100 to remove unincorporated alkyne. Next, the click reaction was performed *in situ* by adding the reagents for the click reaction (TCEP, TBTA, and $CuSO_4$) directly to the cells for 1 h together with either TAMRA-PEG-N_3 or 5-Fam-PEG-N_3. The cells were then rinsed several times to remove excess fluorescent reagent and imaged using confocal microscopy (Figure 4.4). These experiments resulted in a large amount of labeling in each cell type, regardless of which fluorophore azide was used. Importantly, the background labeling (Figures 4.4A and 4.4B) is almost non-existent, which is essential to verify that we are not simply imaging nonspecific labeling of the fluorophore azide in the cells. Interestingly, it also appears that in HeLa cells (Figure 4.4C) and to a lesser extent in NIH/3T3 (Figure 4.4F) that a small amount of labeling is present in the nucleus.

The fluorescence observed in the cells shown in Figure 4.4 appears to be both punctate in nature but also clustered around the nucleus in a specific location, indicating a large portion of proteins were present in this area. It is known that prenylated proteins receive the isoprenoid modification in the cytosol and are subsequently trafficked to the endoplasmic reticulum and golgi for further processing.[155] To explore if this was indeed what was being observed, HeLa cells

were incubated with C10Alk or C15Alk for 24 h, followed by the click reaction to 5-Fam-PEG-N_3 for 1 h. Following this, the cells were counterstained with ER Tracker Red to visualize the endoplasmic reticulum (Figure 4.5). The results show almost complete co-localization between the green and red fluorescence, indicating a significant localization of the labeled proteins in the endoplasmic reticulum, consistent with the established mechanism of prenylated protein transport.

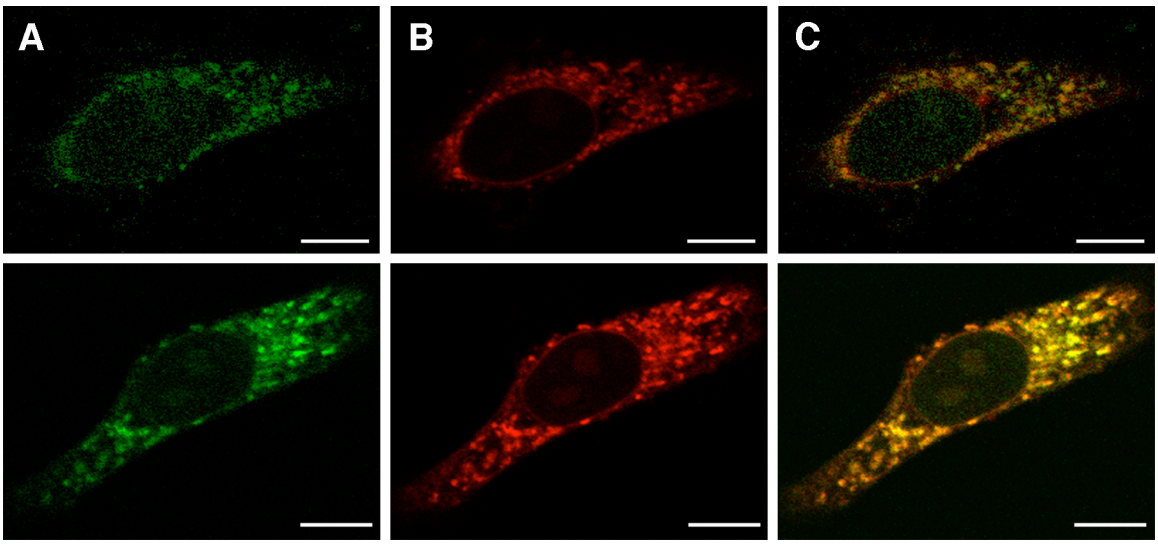

Figure 4.5. Localization of the labeled prenylated proteins in mammalian cells. HeLa cells were treated with either 50 μM C10Alk (top row) or 50 μM C15Alk (bottom row) for 24 h, followed by fixation with paraformaldehyde and permeabilization with Triton X-100. After several rinses, the cells were subjected to the click reaction for 1 h with 5-Fam-PEG-N_3, followed by staining with ER Tracker Red at 1 μM for 10 min. A) Green channel showing prenylated proteins 'clicked' to 5-Fam-PEG-N_3. B) Red channel showing staining of endoplasmic reticulum by ER Tracker Red. C) Overlay of images from A) and B) showing significant colocalization of the green and red fluorescence. Size bar represents 10 μm.

4.3.3 Quantitative Analysis of Prenylated Protein Levels Using Flow Cytometry in Different Cell Types

Having established the ability to label prenylated proteins in cells, we next sought to quantify the total labeling in order to measure dynamic changes in levels of prenylation. To do this, the method described above consisting of incubating cells with C10Alk or C15Alk followed by fixation and permeabilization was again employed except that this was done with the cells in solution and not attached to the culture plate. The click reaction was performed with 5-Fam-PEG-N_3 for 1 h and the cells were rinsed and analyzed by flow cytometry to count the fluorescence intensity in each cell. Initially, we investigated the effects of both the alkyne isoprenoid incubation time as well as concentration on the total amount of labeling. The results from those experiments show that increasing the incubation time of the cells with the isoprenoid leads to an increase in the amount of labeling with C15Alk (Figure 4.6A). Curiously, C10Alk labeling does not change in a similar manner. This may reflect the lower abundance of labeled proteins with this compound, as only farnesylated proteins can be directly labeled with C10Alk, whereas C15Alk can label farnesylated proteins as well as geranylgeranylated proteins.[123] In addition to increasing the incubation time, increasing the concentration of alkyne isoprenoid also increases the amount of observed labeling (Figure 4.6B). To maximize the extent of labeling while minimizing the

amount of alkyne isoprenoid used in the experiments, we chose to label with 50 μM C15Alk for 24 h in most of the subsequent experiments.

In addition to varying the alkyne isoprenoid incubation time and concentration, the effects of the permeabilization step on the labeling was also examined. In experiments using two different detergents, the amount of labeling was greater with Tween 20 versus Triton-X-100 when times less than 5 min were used for permeabilization (Figure 4.7) However, more variation in labeling was observed using Tween 20. Because more consistent labeling was obtained with Triton-X-100 in the ranges tested, a 2 min permeabilization with this detergent was chosen for subsequent experiments.

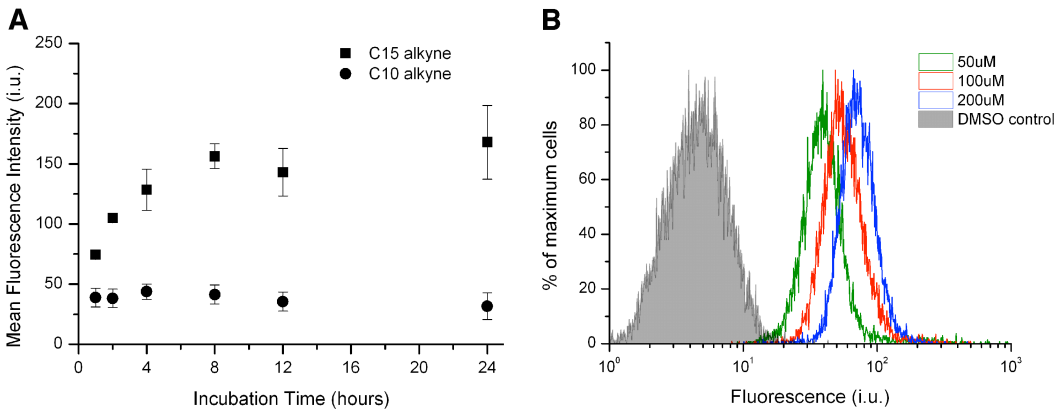

Figure 4.6. Quantifying the incorporation of C10Alk and C15Alk in HeLa cells. In (A), HeLa cells were incubated with 50 μM C10Alk or C15Alk for various times. In (B), HeLa cells were incubated with various concentrations of C15Alk for 2 h. The cells were then fixed, permeabilized for 2 min, rinsed, and subjected to the click reaction with 5-Fam-PEG-N_3 for 1 h. After several additional rinses, the cells were analyzed by flow cytometry and the results are expressed as the mean fluorescence intensity of 10,000 cells ± standard error of the mean of at least three replicates (A) or the percentage of maximum cell count (B). The data in (B) were done in triplicate and showed similar results.

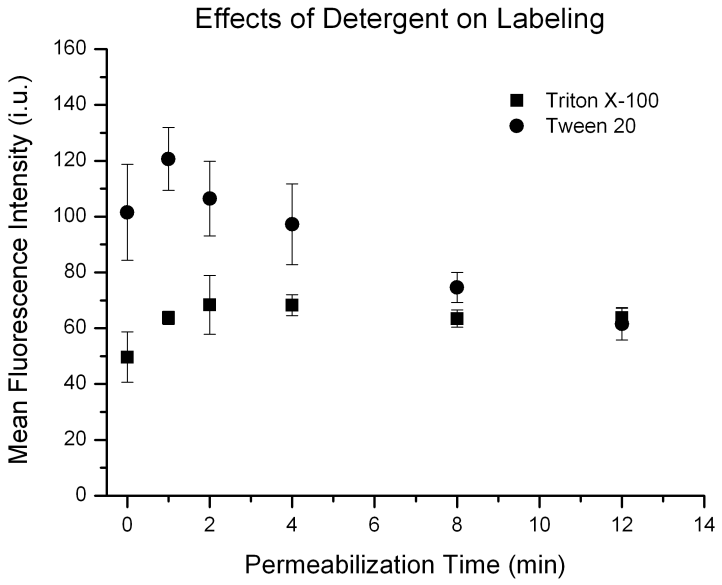

Figure 4.7. Flow cytometry data of HeLa cells that have been incubated with C15Alk at 50 μM for 24 h. The cells were then fixed, permeabilized for various times with different detergents, rinsed, and subjected to the click reaction with 5-Fam-PEG-N_3 for 1 h. After several additional rinses, the cells were analyzed by flow cytometry and the results are expressed as the mean fluorescence intensity of 10,000 cells ± standard error of the mean of at least three replicates.

In addition to quantifying the levels of prenylated proteins in HeLa cells, it was desirable to compare the extent of labeling in a variety of different cell types since differences in cell type may result in differences in the abundance of prenylated proteins. Using the flow cytometry method described here, the results show that there are indeed large differences in the levels of prenylated proteins, depending on cell type (Figure 4.8**,** left panel). HeLa cells show the largest extent of labeling, while A549 cells, derived from human lung adenocarcinoma, have a significantly lower amount of labeling than all other cells tested, in some cases manifesting a 3-fold decrease in the overall level of prenylated proteins. Interestingly, the MCF10A cell line (breast epithelial cells) shows a larger amount of labeling than does the same cell line engineered to constitutively overexpress H-Ras (MCF10A H-Ras). Because Ras is overexpressed in these cells it might be expected to observe higher levels of prenylated proteins; however, this is not the case. It is important to consider that some of the differences in the levels of prenylated proteins between cells could simply reflect a difference in cell size. An analysis of the cell area using confocal microscopy shows that there are very minor differences in size between these cell types, which indicates that these measurements highlight differences in protein prenylation and not simply cell size (Figure 4.8, right panel). Of particular interest, A549 cells are the same size as HeLa and MCF10A cells but display a more than three-fold lower amount of

prenylated proteins. Additionally, MCF10A H-Ras expressing cells are larger than their parental line, MCF10A, but also have a lower level of prenylated proteins.

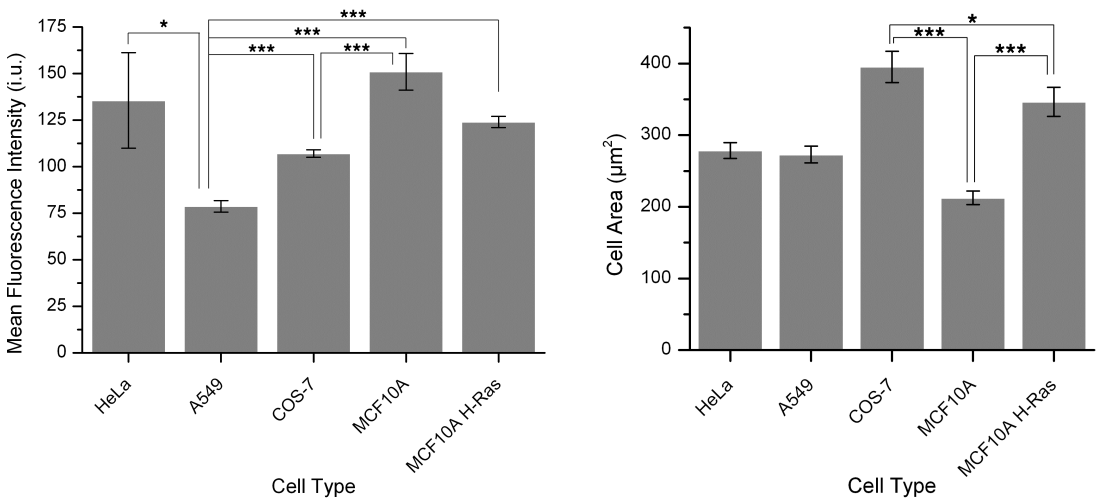

Figure 4.8. The levels of prenylated proteins varies widely depending on cell type, regardless of cell size. Left panel: flow cytometry data of various cell types that have been incubated with C15Alk at 50 μM for 24 h. The cells were then fixed, permeabilized for 2 minutes, rinsed, and subjected to the click reaction with 5-Fam-PEG-N_3 for 1 h. After several additional rinses, the cells were analyzed by flow cytometry and the results are expressed as the mean fluorescence intensity of 10,000 cells ± standard error of the mean of at least three replicates. Right panel: the plasma membrane of various types of cells was stained with wheat germ agglutinin-AlexaFluor 594 conjugate (following manufacturers protocols) and the area of the cell was calculated using ImageJ software. The results are expressed as the mean cell area ± standard error of the mean of at least 40 measured cells. * = $p < 0.05$, ** = $p < 0.01$, *** = $p < 0.001$

To further demonstrate the utility of this method, we also explored its application to primary cells; such cells are often superior to immortalized cell lines for studying cellular phenomena. For this, primary neurons were isolated from mice and the levels of prenylated proteins in them were quantified using the methods outlined above (Figure 4.9). Results from those experiments indicate that these primary neuronal cells had a low level of labeling, possibly because these cells are a fraction of the size of immortalized cells; it may also indicate that these cells are not as metabolically active as immortalized cells and thus don't incorporate the alkyne isoprenoids as efficiently. Despite this, the signal from the prenylated proteins is consistent and more than 2-fold over background. Taken together, these results highlight the highly variable nature of protein prenylation in various cell types and the ability of the method reported here to quantify prenylated proteins in a wide spectrum of systems.

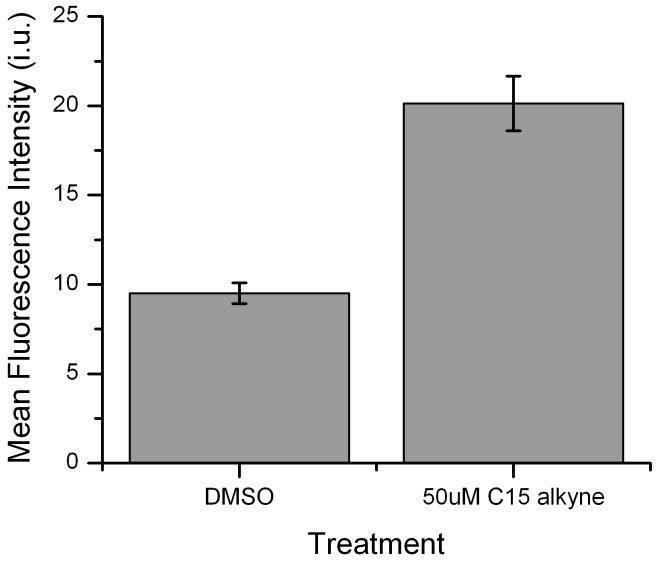

Figure 4.9. Quantifying the incorporation of C15Alk in primary mouse neuron cells. Primary cells from the brains of mice were isolated and selected for neurons by cytosine arabinoside treatment. The primary neuron cells were then incubated with 50 μM C15Alk for 24 h, after which they were fixed, permeabilized for 2 minutes, rinsed, and subjected to the click reaction with 5-Fam-PEG-N_3 for 1 h. After several additional rinses, the cells were analyzed by flow cytometry and the results are expressed as the mean fluorescence intensity of 10,000 cells ± standard error of the mean of three replicates.

4.3.4 Effects of Prenylation Inhibitors on the Extent of Labeling

Having established the ability to measure the levels of prenylated proteins in different cells and under various conditions, it was important to verify the specificity of the labeling that was being observed. One way to investigate this is to use inhibitors of the prenyltransferase enzymes as well as protein synthesis inhibitors. In a first set of experiments, two different farnesyltransferase inhibitors were employed and their effects on the levels of prenylated proteins were monitored. Manumycin A is a natural product that has been shown to act as a competitive inhibitor of farnesyltransferase with an *in vivo* K_i of 1.2 μM.[156] Additionally, α-hydroxyfarnesyl phosphonic acid (HFPA) is a non-hydrolyzable analog of farnesyl diphosphate that acts as a competitive inhibitor of farnesyltransferase with an *in vitro* IC_{50} of 30 nM.[157] Either Manumycin A or HFPA were co-incubated with cells containing 25 μM C15Alk for 24 h, followed by fixation, permeabilization, and click reaction with 5-Fam-PEG-N_3. The cells were then analyzed by flow cytometry to measure the fluorescence in each cell and thus the levels of prenylated proteins. Treatment with either Manumycin A or HFPA showed a reduction in the amount of prenylated proteins by approximately 25% (Figure 4.10). This is consistent with what is expected, as inhibiting farnesyltransferase with these compounds decreases the ability of the cell to incorporate the isoprenoid analog into proteins, thus resulting in a reduction in labeling. Interestingly, the reduction in labeling is only 25% compared to the non-

inhibitor treated cells. The likely reason for this is because C15Alk can act as an analog for both farnesyltransferase and geranylgeranyltransferase type I and II. By inhibiting farnesyltransferase with these compounds, the alkyne isoprenoid can still be utilized by both type I and II geranylgeranyltransferase and thus the labeling is only reduced but not eliminated.

In addition to using inhibitors of farnesyltransferase to show the isoprenoid alkyne is being incorporated in prenylated proteins, we also incubated HeLa cells with 25 μM C15Alk along with 50 μM farnesol, the precursor to the natural enzyme substrate farnesyl diphosphate. Using the natural substrate precursor for farnesyltransferase should out-compete the labeling of the unnatural alkyne isoprenoid since the enzyme utilizes FPP more efficiently. A reduction in labeling of approximately 40% was observed when using farnesol in conjunction with C15Alk, consistent with the expectation noted above (Figure 4.10). Lastly, the effect of a global protein synthesis inhibitor, cycloheximide (CHX), on cellular labeling by C15Alk was examined. Incubation of HeLa with CHX for 24 h prior to 25 μM C15Alk incubation for 4 h leads to a reduction in labeling of approximately 30% (Figure 4.10). This is consistent with the observation that by inhibiting protein synthesis, the target proteins of farnesyltransferase are reduced and so is the incorporation of C15Alk.

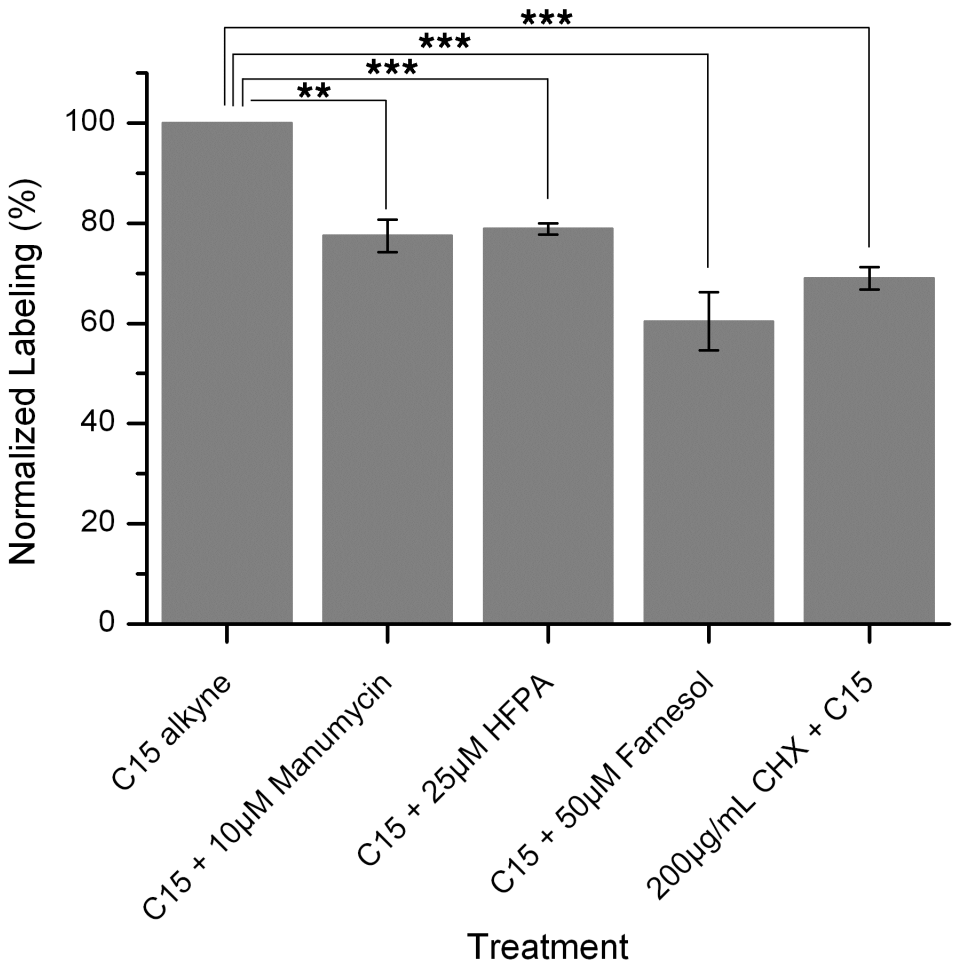

Figure 4.10. A decrease in the levels of prenylated proteins is observed when adding Inhibitors of farnesyltransferase or addition of the native isoprenoid substrate. Flow cytometry data of HeLa cells that have been incubated with C15Alk at 25 μM for 24 h along with inhibitors indicated (with the exception of the cycloheximide treatment, in which the cells were pre-treated with CHX for 24 h followed by 4 h incubation with 50 μM C15Alk). The cells were then fixed, permeabilized for 2 min, rinsed, and subjected to the click reaction with 5-Fam-PEG-N_3 for 1 h. After several additional rinses, the cells were analyzed by flow cytometry and the results are expressed as the normalized fluorescence intensity (in relation to the C15Alk treatment) of 10,000 cells ± standard error of the mean of at least three replicates. * = $p < 0.05$, ** = $p < 0.01$, *** = $p < 0.001$

4.3.5 Measurement of Prenylation Levels in a Cellular Model for Aging

With the validation of the abovementioned method for determining the levels of prenylated proteins established, we next sought to quantify the levels of such proteins in a cellular model for aging. The rationale for studying prenylation levels in aging cells is based on the finding that there are higher levels of FPP and GGPP in the brains of those suffering from Alzheimer's disease;[32] One consequence of such higher levels of isoprenoid diphosphates could be higher levels of prenylated proteins. To study this phenomenon, a cell culture model of aging was chosen that was produced by knocking down the cellular genes for autophagy, the process responsible for protein and organelle degradation via the lysosome. It has been shown in several mammalian systems that defects in autophagy lead to age-related disorders such as neurodegeneration, cardiomyopathy, and cancer.[158-161] ATG7 has been identified as the main gene responsible for autophagy in mammalian cells[162] and knockdown of this gene with siRNA provides the neurodegenerative phenotype. Thus, L6 rat myoblast cells were transfected with siRNA against the ATG7 gene for 4 h, followed by a 24 h incubation period to maximize gene knockdown. The cells were then incubated with 50 μM C15Alk for 24 h followed by fixation, permeabilization, and click reaction with 5-Fam-PEG-N_3, at which point the cells were analyzed by flow cytometry to quantify the prenylated proteins. The L6 cells in which the ATG7 gene was knocked down ('Aging' L6) showed an increase in the levels of

prenylated proteins by almost 50% (Figure 4.11). This result may indicate that individuals with neurodegenerative disorders have an increase in the levels of prenylated proteins, possibly because of an increase in the levels of available FPP or GGPP, because the genes expressing the prenyltransferases are upregulated, or because the activity of the prenyltransferases themselves is amplified. Currently, there are several studies providing contradicting results as to the effects of statins and farnesyltransferase inhibitors in Alzheimer's disease. For instance, Hoof and coworkers found that the levels of Aβ abundance did not change with farnesyltransferase inhibition in an APP695 expressing SH-SY5Y cell line.[163] Aβ levels themselves are not the only modulator of Alzheimer's disease pathology, however, and increasing the levels of α-secretase activity precludes the production of Aβ,[164] leading to another therapeutic route. Pedrini and coworkers found that use of a farnesyltransferase inhibitor stimulated α-secretase and increased the levels of the α fragment of APP, which precludes the ability of Aβ to form.[165]

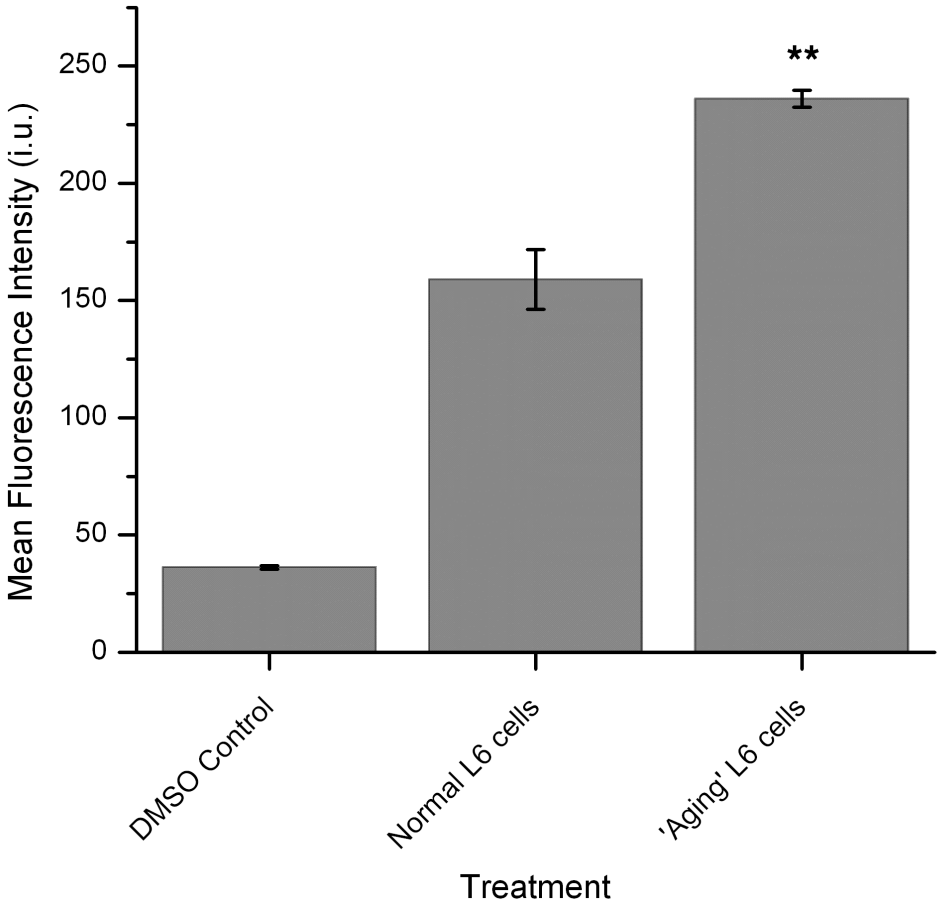

Figure 4.11. An increase in the amount of prenylated proteins in a cellular model of aging is demonstrated. L6 rat myoblast cells were incubated with C15Alk at 50 μM for 24 h, followed by fixing, permeabilizing, and the click reaction to 5-Fam-PEG-N_3 and analysis by flow cytometry. In the aging cell model, the ATG7 gene controlling autophagy was knocked down with siRNA for 24 h prior to C15Alk exposure. The cells were then fixed, permeabilized for 2 minutes, rinsed, and subjected to the click reaction with 5-Fam-PEG-N_3 for 1 h. After several additional rinses, the cells were analyzed by flow cytometry and the results are expressed as the mean fluorescence intensity of 10,000 cells ± standard deviation of at least three replicates. There is a statistically significant increase in the amount of prenylated proteins in the cell aging model. * = $p < 0.05$, ** = $p < 0.01$, *** = $p < 0.001$

4.4 Conclusions

It is clear that statins may have some therapeutic benefit in ameliorating the symptoms and pathology of Alzheimer's disease.[166-168] Indeed, research has shown a correlation between increased cholesterol levels and the incidence of Alzheimer's disease.[169,170] Further, inhibiting isoprenoid synthesis with a statin increases the long term potentiation in neurons in mice, directly due to a reduction in farnesylated proteins and/or FPP.[35] More work must to be done to elucidate the cellular mechanisms underlying Alzheimer's disease pathology and, more specifically, the role of protein prenylation in the course of this disease. Importantly, the method we have developed allows the quantification of the total level of prenylated proteins in various types of cells. We have shown that the majority of the labeled prenylated proteins localize to the ER and that different types of cells have significant differences in their levels of prenylated proteins. Furthermore, we have shown that the levels of prenylated proteins are increased by almost 50% in a cellular aging model, pointing to a possible connection between protein prenylation and aging disorders such as Alzheimer's and Parkinson's disease. Additional studies with this method utilizing mouse models of Alzheimer's disease may help elucidate the role that isoprenoids and protein prenylation play in neurodegenerative diseases.

4.5 Experimental

4.5.1 General Materials

HeLa cells were the generous gift of Dr. Audrey Minden (Department of Chemical Biology, Rutgers University); all other cell lines were purchased from ATCC. 100mm tissue culture treated dishes were from Corning Scientific. Petri dishes (35 mm) fitted with microwells (14 mm) and a No. 1.5 coverglass were from MatTek Corporation. Tissue culture treated 6-well multiwell plates and 5mL polystyrene round bottom tubes (12x75mm) were from BD Biosciences. DMEM (Dulbecco's Modified Eagle Medium), ER Tracker Red, wheat germ agglutinin-AlexaFluor 594 conjugate, Lipofectamine 2000, Stealth ATG7 RNAi, Stealth RNAi Universal Negative Control, Opti-MEM, neurobasal medium, B27 supplement, and glutamine were from Invitrogen. Manumycin A and α-hydroxyfarnesyl phosphonic acid (HFPA) were from Cayman Chemical. Fetal bovine serum (FBS) was from Intergen Company. 70μm cell strainers and SuperSignal West Pico Chemiluminescent Substrate were from ThermoFisher Scientific. Immobilon-P PVDF membranes were from Millipore, Anti-H-ras rabbit polyclonal and anti-ERK2 rabbit polyclonal antibodies were from Santa Cruz Biotechnology. Anti-rabbit IgG horseradish peroxidase-linked secondary antibody was from Cell Signaling. Vydac 218TP54 and 218TP1010 columns were used for analytical and preparative RP-HPLC, respectively. All analytical and preparative RP-HPLC solvents, water and CH_3CN, contained 0.10% TFA and were of HPLC grade. 5-Carboxyfluorescein succinimidyl ester and TAMRA-succinimidyl ester were from AnaSpec. All other reagents were from Sigma Aldrich.

General cell culture:

Cells were seeded in culture dishes at the following densities prior to experimentation: HeLa 3.1 x 10^4 cells/cm^2, MDCK 2.5 x 10^4 cells/cm^2, A549 3.0 x 10^4 cells/cm^2, NIH/3T3 2.5 x 10^4, MCF10A and MCF10A-HRas 3.3 x 10^4 cells/cm^2, and L6 2.3 x 10^3 cells/cm^2. HeLa, MDCK, NIH/3T3, and L6 were maintained in DMEM supplemented with 10% FBS. A549 were maintained in RPMI supplemented with 10% FBS. MCF10A and MCF10A H-Ras were maintained in DMEM/F12 supplemented with 5% horse serum, 0.5 μg/mL hydrocortisone, 10 μg/mL insulin, 20 ng/mL EGF, and 0.1 μg/mL cholera toxin. All cells were grown at 37°C with 5.0% CO_2.

4.5.2 Western Blot Analysis

Cell lysates were prepared using the following buffer: 50 mM Tris-HCl, pH 7.4, 1% NP-40, 0.25% Na-deoxycholate, 150 mM NaCl, 1 mM EDTA, 1 mM PMSF, 1 mg/mL aprotinin, 1 mg/mL leupeptin, 1 mM Na_3VO_4, 1 mM NaF, 20 mM b-glycerophosphate. Lysates were cleared by centrifugation (16,000 x g, 10 min, 4 °C). 40 µg of protein was resolved using 15% SDS-polyacrylamide minigels, and then transferred to Immobilon-P PVDF membrane. After blocking in a TBST/5% milk solution, immunoblots were incubated overnight at 4 °C using the following primary antibodies: anti-H-ras rabbit polyclonal (1:500) and anti-ERK2 rabbit polyclonal (1:2000). Following this, the membranes were incubated with an anti-rabbit IgG horseradish peroxidase-linked secondary antibody. The immunoblots

were visualized using the SuperSignal West Pico Chemiluminescent Substrate following manufacturers protocols.

4.5.3 Imaging Prenylated Proteins

HeLa, A549, MDCK, or NIH/3T3 cells were seeded (see above for density) in 35 mm glass bottomed culture dishes and grown to approximately 50% confluency (24 h). The cells were rinsed twice with phosphate buffered saline (PBS), followed by the addition of 50 μM C15Alk in 2mL complete DMEM media. After 24 h probe incubation, the cells were rinsed twice with PBS, fixed with 4% paraformaldehyde (PFA) in PBS for 10 min at RT, permeabilized with 0.1% Triton X-100 in PBS for 2 min at RT, and subsequently rinsed three times with PBS. The following reagents were added, in order, at the specified concentration (typically 300 uL total volume in PBS): TAMRA-PEG-N_3 or 5-Fam-PEG-N_3 (0.1 mM), *tris*(2-carboxyethyl)phosphine (TCEP, 1 mM), *tris*[(1-benzyl-1H-1,2,3-triazol-4-yl)methyl] amine (TBTA, 0.2 mM), $CuSO_4$ (1 mM). Following 1 h incubation at RT, the cells were rinsed four times with PBS and Hoescht 34580 nuclear stain was added at a final concentration of 1 μg/mL for 10 min. Additionally, for the colocalization experiments, ER Tracker Red was added at 1 μM for 10 min. The cells were rinsed twice with PBS and imaged using an Olympus FluoView 1000 confocal microscope with a 60X objective.

4.5.4 Quantifying the Prenylome

Cells were seeded in 6-well multiwell culture dishes and grown to approximately 50% confluency (24 h). The cells were rinsed twice with PBS, followed by the addition of the desired alkyne isoprenoid probe in 2 mL complete DMEM media (typically between 25-200 μM).

In the inhibitor treatment experiments, 10 μM Manumycin A, 25 μM HFPA, or 50 μM farnesol was added immediately following C15Alk. For cycloheximide (CHX) treatment, 200 μg/mL CHX was pre-treated with cells for 24 h, followed by addition of C15Alk for 4 h.

After incubation C15 Alk and/or inhibitors for various times (typically 24h), the cells were rinsed twice with PBS and trypsinzed for 5 min. After addition of 1.8 mL complete DMEM and transfer to a centrifuge tube, the cells were pelleted by centrifugation at 100 g for 5 min, hereafter referred to as 'spun'. The media was aspirated from the pellet and the cells were fixed with 4% paraformaldehyde (PFA, in PBS) for 10 min at RT, spun, and permeabilized with 0.1% Triton X-100 (in PBS) for 2 min at RT. After spinning, PBS was added and the cells were spun again. This was repeated three times to rinse the cells. Next, the following reagents were added, in order, at the specified concentration (100 uL total volume in PBS): 5-Fam-PEG-N_3 (0.1 mM), *tris*(2-carboxyethyl)phosphine (TCEP, 1 mM), *tris*[(1-benzyl-1H-1,2,3-triazol-4-yl)methyl] amine (TBTA, 0.2 mM), $CuSO_4$ (1 mM). Following 1 h incubation at RT, the cells were spun, liquid removed, and PBS added (150 μL). This was repeated four times to rinse the cells. Cells were added to a 12 x 75 mm test tube (1.5 mL in PBS) for flow cytometry analysis. A

total of 10,000 events (cell counts) for each sample were analyzed using a BD FACSCalibur (BD Biosciences).

4.5.5 L6 Aging Model

L6 rat myoblast cells were seeded 12-well tissue culture dishes (see above for density) and grown to approximately 50% confluency (24 h). The cells were then transfected with 80 pmol each of Stealth ATG7 RNAi or Stealth RNAi Universal Negative Control using 1 mL of plating medium and 100 uL of Opti-MEM dilution media with Lipofectamine 2000. The media was exchanged for fresh antibiotic-free media after 4 h of incubation with the transfection reagents. 24 h after the transfection, the cells were incubated with 50 μM of C15Alk. The prenylated proteins were then quantified using the same method described above (see 'Quantifying the Prenylome').

4.5.6 Primary Neuron Preparation

The brains were removed from embryos at gestational day E16 – E18 of C3H/C57BL/6 mice and placed in 1x Hanks balanced salt solution (HBSS). Cortices and hippocampi were dissected out and meninges removed. The tissues were cut into 1 mm^3 pieces with a sterile disposable scalpel, transferred to a conical tube with 1x trypsin in HBSS, and incubated in a 37 °C water bath for 15 minutes. A stop solution, containing 4% FBS and 0.2 mg/ml DNase I in HBSS, was added and the incubation extended for an additional 30 seconds at 37 °C.

The tissue mixture was centrifuged for 5 minutes at room temperature and the supernatant was carefully aspirated from the tube. DMEM containing 10% FBS was added to the cell pellet and the mixture was triturated 20 times to dissociate cells. The cell suspension was passed through a 70 µm cell strainer to achieve single cell suspension. The total cell number and viability were determined with a hemacytometer by adding 10 µL of cell suspension and 90 µL of trypan blue. Approximately 1.5-2.0 x 10^6 cells were plated into each well of a 6-well plate, which had been previously coated with 0.1 mg/ml poly lysine. Neurons were cultured initially in DMEM with 10% of FBS at 37 °C with 5% of CO_2, and 24 hours later, the medium was changed to neurobasal medium containing 2% B27 supplement, 2 mM glutamine, and 5 µM of cytosine arabinoside to limit the growth of non-neuronal cells. After 5 days in culture, the neurons were subjected to isoprenoid labeling reactions (see 'Quantifying the Prenylome' in Materials and Methods).

4.5.7 TAMRA-PEG-N_3 Synthesis

TAMRA-PEG-N_3 was synthesized similar to a previously described method.[154] TAMRA-succinimidyl ester (25.0 mg, 47.4 µmol) was dissolved in 0.4 mL *N,N*-dimethylformamide (DMF). To this solution, 11-Azido-3,6,9-trioxaundecan-1-amine (14.1 µL, 71.1 µmol) and diisopropylethylamine (4.1 µL, 23.7 µmol) were added. The reaction was stirred overnight at RT in the dark. The reaction was diluted with 10 volumes of 0.1% aqueous TFA, filtered through a 0.2 µm syringe

filter, and purified by RP-HPLC on a C_{18} column using a gradient of 1% B per minute (solvent A: 0.1% aqueous trifluoroacetic acid (TFA), solvent B: 0.1% TFA in CH_3CN), affording a dark red solid. Yield: 15.6 mg (52.1%), product eluted at 36% CH_3CN. Deconvoluted ESI-MS calculated for $C_{33}H_{39}N_6O_7$ = 631.3, found 631.3.

5. Fluorescently Labeled Prenylated Peptides for *in vivo* analysis

5.1 Introduction

As mentioned previously, studies detailing the role of prenylation in membrane association,[18] protein-protein interactions,[171] as well as its effects on signal transduction[172,173] have been undertaken, with most studies having been conducted *in vitro*. Even with an abundant knowledge of prenylation *in vitro*, much remains unclear about the process as it occurs in living cells. For example, prenylation takes place in the cytosol but the resulting proteins are translocated to the plasma membrane via the secretory pathway;[174] additionally, prenylated proteins appear to cycle in a dynamic fashion between the plasma membrane and the Golgi. Peptides can provide useful information concerning protein prenylation, but to date, most peptides have been microinjected into cells.[175] To gain insight into the processing and localization of prenylated proteins, we have sought to create cell permeable prenylated peptides that can be used to study prenylation in living cells. Recently, our group reported on the preparation and cellular distribution of a class of prenylated peptides that freely enter HeLa

cells.[176] Those molecules, based on the C-terminus of CDC42 include a geranylgeranylated cysteine residue embedded within the CAAX-box sequence CVLL, thus mimicking the C-terminus of a naturally geranylgeranylated protein and rendering them substrates for RCE1 and ICMT. In this chapter, I will discuss my efforts to extend that work to peptides that incorporate the CAAX-box sequences CVLS and CVIM that are present in farnesylated proteins. Flow cytometry and confocal laser scanning microscopy (CLSM) were used to quantify the levels and evaluate the localization patterns of farnesylated peptides in HeLa cells. Several additional cell lines including COS-1 (African green monkey kidney cells), NIH/3T3 Fibroblast (Swiss mouse embryo fibroblasts), D1TNC1 astrocytes (rat astrocyte cell line), and PC-12 cells (derived from rat adrenal pheochromocytoma[177]) were also evaluated for their ability to take up these peptides. These specific cell lines were chosen both for their common laboratory use as well as their utility for future experiments with these peptides. Finally, a peptide incorporating a lipid linked to the CAAX-box cysteine residue thiol via a disulfide was prepared and evaluated for its cell penetrating ability. Entry of such a probe into cells should result in reductive cleavage of the lipid to reveal a CAAX-box containing peptide that can serve as a substrate for protein farnesyltransferase and the subsequent modifying enzymes.

5.2 Research Objectives

The goal of this work was, as mentioned in the previous section, to develop fluorescently labeled peptides that can naturally penetrate the membrane of cells. Once inside the cells, we can use these peptides as tools to study the enzymology of the prenyltransferase enzymes in living cells. This work serves to develop new peptides with cell-penetrating ability and to develop a new peptide to allow for *in vivo* enzymology studies.

5.3 Results and Discussion

5.3.1 Peptide Synthesis

Acm protected peptides (**1a** and **1b**):

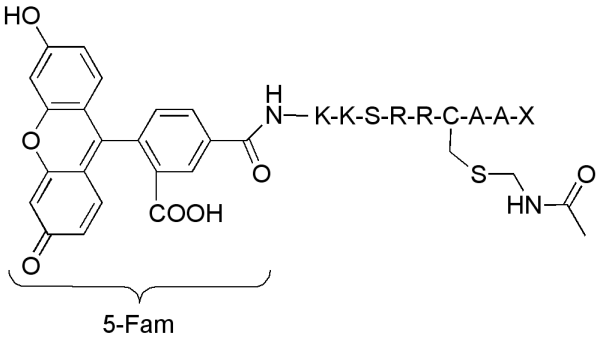

Scm protected peptides (**2a** and **2b**):

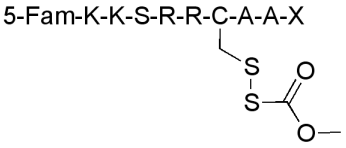

a = 5-Fam-KKSRRCVIM
b = 5-Fam-KKSRRCVLS

Free thiol peptides (**3a** and **3b**):

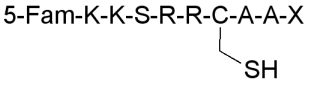

Farnesylated CAAX peptides (**4a** and **4b**):

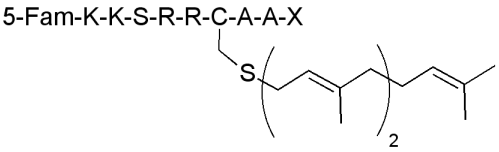

Disulfide linked CAAX peptides (**5a** and **5b**):

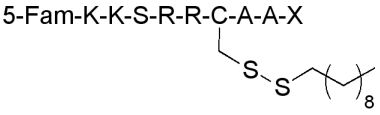

In all cases, the 'a' series of peptides contain the CVIM sequence (A_1=V, A_2=I, X=M). The 'b' series of peptides contain the CVLS sequence (A_1=V, A_2=L, X=S)

Figure 5.1. Fluorescently labeled prenylated peptides for *in vivo* analysis. In all cases, the 'a' series of peptides contain the CVIM sequence while the 'b' series of peptides contain the CVLS sequence.

A total of ten peptides were synthesized en route to producing cell-permeable molecules (Figure 5.1). The synthesis of peptides **1a** and **1b** was accomplished via standard SPPS with an automated synthesizer utilizing HBTU coupling. After SPPS, on-resin addition of 5-Fam was accomplished in one step using peptide coupling conditions (HOBt, DIC) followed by removal of the acid labile protecting groups and cleavage from the resin with Reagent K.[178] It is important to note that the acetamidomethyl (Acm) protecting group on cysteine is not removed during this treatment, which allowed its later conversion to an *S*-carbomethoxysulfenyl (Scm) group. Conversion of Acm protected peptides **1a** and **1b** to the Scm protected peptides **2a** and **2b** was accomplished using a previously described method.[176]

In route to peptides **4a** and **4b,** the free thiol precursors **3a** and **3b** were first generated by reducing the Scm disulfide protecting groups of **2a** and **2b** with DTT. After reduction, farnesylation of **3a** and **3b** was conducted using an acidic, aqueous medium and zinc acetate catalyzed coupling conditions as described by Xue *et al.*[179] The disulfide linked lipidated peptides **5a** and **5b** were also generated starting with the Scm protected peptides **2a** and **2b**. In those cases, disulfide exchange with decanethiol was used to complete the synthesis of **5a** and **5b**.

5.3.2 Peptide Design and Uptake in HeLa Cells

In earlier work, we investigated the cell penetrating ability of a number of different peptides based on the naturally geranylgeranylated protein CDC42 containing the C-terminal sequence KKSRRCVLL. Here we sought to expand the range of cell penetrating prenylated peptides that can be studied to include sequences that mimic those present in farnesylated proteins. Accordingly, the CAAX box sequences CVIM and CVLS were chosen as they are present in the naturally occurring oncogenic proteins K or N-Ras and H-Ras, respectively.[180] The same sequence upstream of the CAAX box in CDC42 was used in the design of these new peptides to facilitate comparison of their uptake characteristics with those previously reported for peptides bearing geranylgeranylation sequences (Figure 5.1).

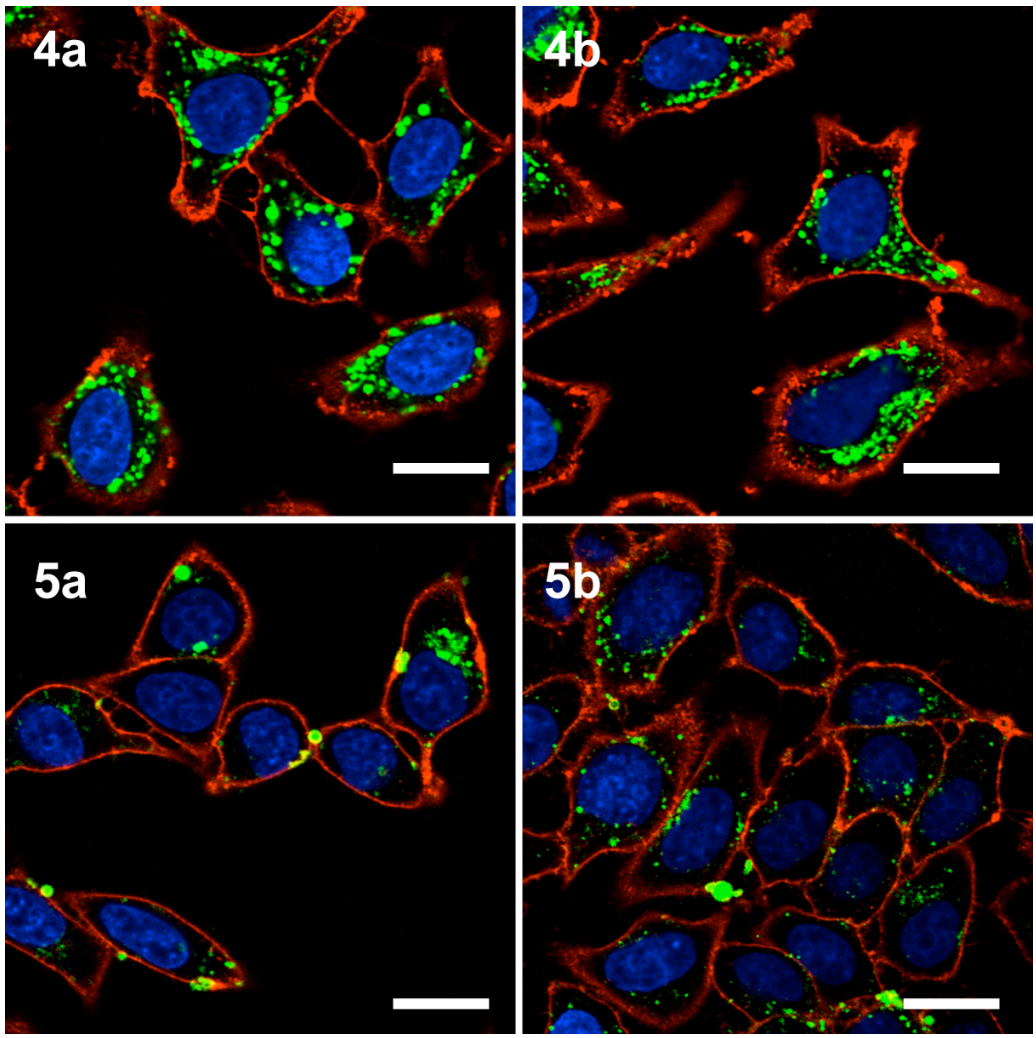

Figure 5.2. Confocal laser scanning microscopy (CLSM) images of live HeLa cells after incubation with various peptides. Peptides 4a and 4b were incubated for 2 h at 3 μM while peptides 5a and 5b were incubated for 1 h at 1 μM. Hoechst 34850 was used to stain the nucleus blue and wheat germ agglutinin Alexa Fluor 594 conjugate was used to stain the plasma membrane red. The peptide is visualized as green fluorescence. Size bar represents 20 μm.

Initially, confocal laser scanning microscopy (CLSM) was used to monitor the uptake of the peptides in HeLa cells (Figure 5.2). Inspection of the CLSM images in Figure 5.2 clearly indicates significant uptake into HeLa cells for **4a** and **4b** as well as for the disulfide linked peptides **5a** and **5b** (all other synthesized peptides showed no cellular uptake). The punctate fluorescence in the cytoplasm is similar to what has been observed previously in images of live cells treated with related geranylgeranylated peptides.[176] Next, flow cytometry was used to quantify the uptake of the peptides in live HeLa cells. Cells were incubated with peptides at various concentrations for 1 h, followed by trypsinization for 15 minutes to remove any surface bound peptide and thereby allow the measurement of only the internalized peptide.[181] As the concentration of peptide was increased, the uptake increased, although not in a linear fashion (Figure 5.3). It was previously noted for related geranylgeranylated peptides that longer incubation times result in increased uptake,[176] and this trend was observed here for the farnesylated peptides as well (data not shown). Uptake was also compared to a peptide that has a similar sequence but is geranylgeranylated rather than farnesylated (Figure 5.3, peptide **GG**, sequence: Ac-K(5-Fam)AKKSRRC(gg)VLL where 'gg' represents a geranylgeranyl moiety). While there is a small difference in the sequence, the uptake of the geranylgeranylated peptide at a similar concentration (1 μM) is approximately 4

times greater than that of the farnesylated peptide. Increased uptake is presumed to be because of the more hydrophobic geranylgeranyl group.

To explore this idea, octanol/water partition coefficient (LogP) values were measured for peptides **4b** and **GG**. With a LogP value of -0.81 ± 0.26, the geranygeranylated peptide **GG** is noticeably more hydrophobic than the farnesylated peptide **4a**, with a LogP of -1.37 ± 0.37. While this difference is small compared to the uptake difference, it is important to note that previous studies by our group have shown that the hydrophobic moiety on cysteine is crucial for uptake, regardless of peptide sequence.[176,182] Furthermore, peptide **4b** was synthesized with D amino acids and uptake was measured by flow cytometry (data not shown). The resulting uptake was similar to that of the standard L amino acid peptide. This data, coupled with the aforementioned observations, indicates that uptake is likely not dependent on a transport system. Lastly, both peptide **4a** and **4b** exhibit similar uptake; however, because methionine is prone to oxidation to methionine sulfoxide,[183] peptide **4b** was used in subsequent experiments.

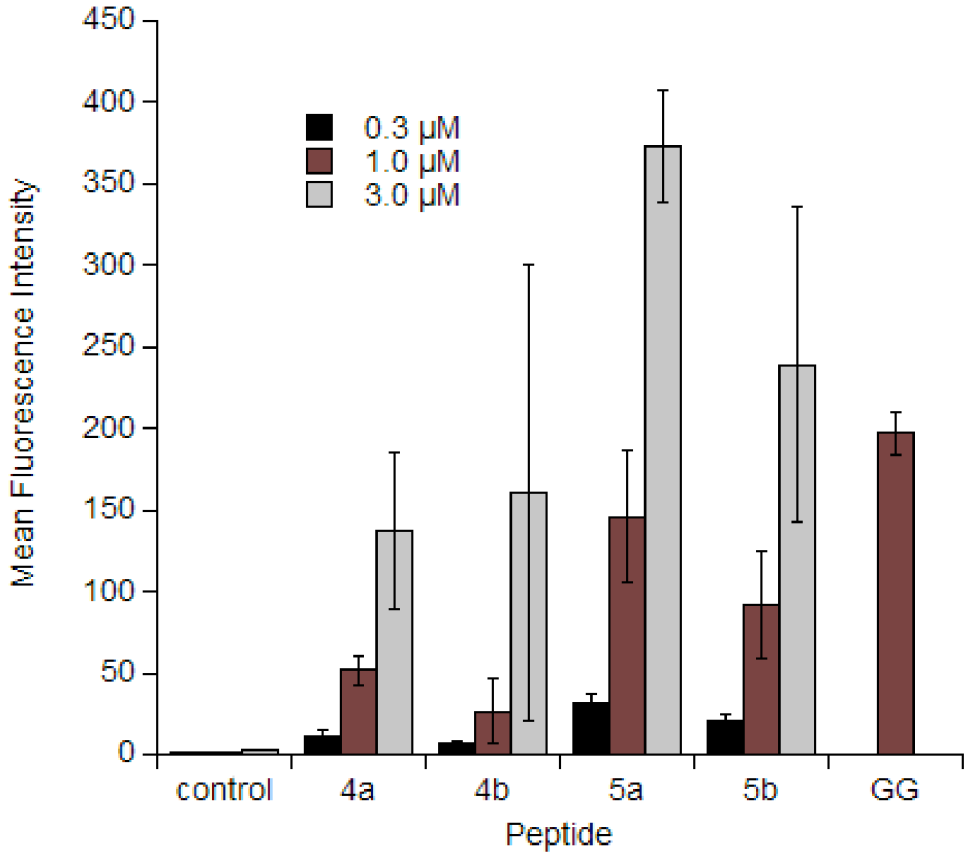

Figure 5.3. Flow cytometry analysis of fluorescently labeled prenylated peptides incubated with HeLa cells at 37°C for 1 h at varying concentrations. After incubation, cells were trypsinized for 15 min to remove membrane-bound peptide. Each bar represents the geometric mean fluorescence of internalized peptide in 10,000 cells. Peptide GG represents a similar sequence that is geranylgeranylated for comparison (sequence Ac-K(Fam)-AKKSRRC(gg)VLL; because peptide characterization and synthesis has been previously described,[176] only the 1 *µ*M concentration was used for comparison).

5.3.3 Utility of the Peptides in Diverse Cell Types

Previous studies investigating cell penetrating prenylated peptides have focused solely on HeLa cells, concluding that the uptake of the prenylated peptides is ATP-independent, possibly relying on a diffusional process across the cell membrane.[176] It is likely that various cells types exhibit different membrane compositions; even within cell cultures themselves the composition of membranes is highly affected by cell–cell contact and culture density.[184] To explore the utility of these cell penetrating peptides beyond HeLa cells (a cervical cancer cell line), their ability to enter a diverse range of cell types was studied by both CLSM and flow cytometry. Initial incubation of **4b** with COS-1 and NIH/3T3 fibroblast cells showed moderate uptake (Figure 5.4, panels A and B). Subsequent experiments used D1TNC1 astrocytes and PC-12 cells, which are used as a model of neurons. Both cell lines showed significant uptake (Figure 5.4, panels C and D). Live cells were used for the above study as it has been shown that cell fixation can cause an artificial redistribution of cell penetrating peptides in the cytoplasm.[181]

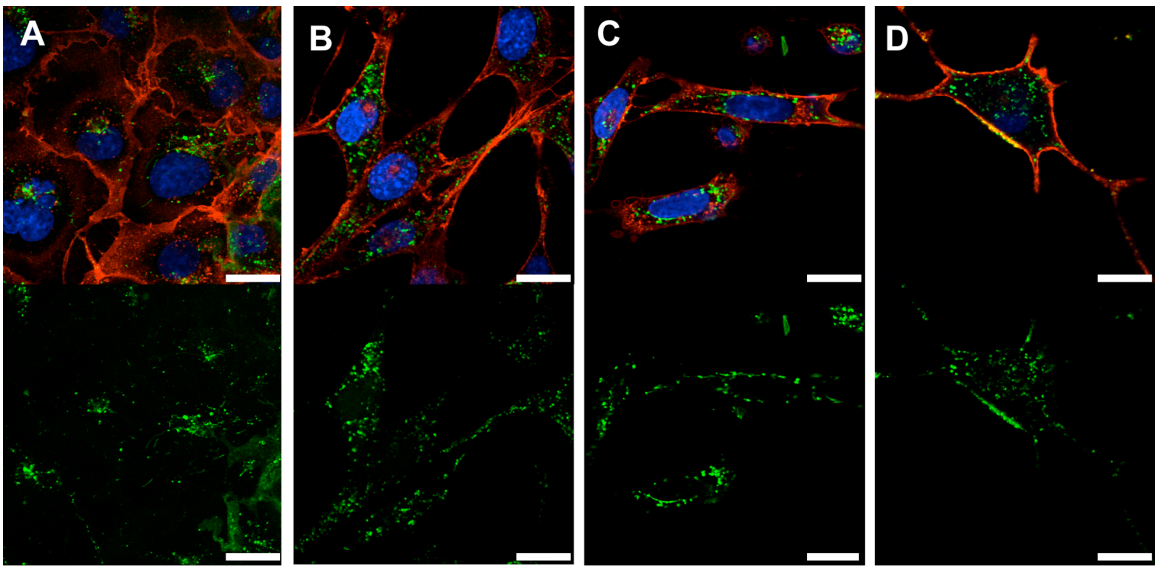

Figure 5.4. CSLM images of various live cells after incubation with peptide 4b at 1 μM for 2 h. A) COS-1 cells. B) NIH/3T3 fibroblasts. C) D1 astrocytes. D) PC-12 differentiated neurons. The top panel is an overlay of all fluorescence channels, while the bottom panel represents only the green channel for clarity. Hoechst 34850 was used to stain the nucleus blue and wheat germ agglutinin Alexa Fluor 594 conjugate was used to stain the plasma membrane red. The peptide is visualized as green fluorescence. Size bar represents 20 μm.

The uptake pattern of the prenylated peptides reported here can be characterized as punctate (see Figures 5.2 and 5.4), which is often indicative of an endocytotic process.[185] To explore this issue, flow cytometry was performed under ATP depletion conditions in all cell lines and compared with uptake data obtained under normal conditions (no ATP depletion); a comparison for each cell type is given in Figure 5.5. No significant difference was observed with uptake under ATP depletion conditions in HeLa and COS-1 cells, suggesting that farnesylated peptide **4b** enters in an ATP-independent, non-endocytotic manner similar to what was observed with the aforementioned geranylgeranlyated peptides. In contrast, reduced uptake under ATP depleting conditions was observed in NIH/3T3 and PC-12 cells. The significance of these latter results are unclear since many of the cells did not survive the depletion conditions; additionally, ATP depletion in astrocytes resulted in essentially complete cell death, possibly because this rapidly growing cell is not able to survive extended periods without ATP. Thus, it is possible that entry of **4b** into NIH/3T3, PC-12 and astrocytes involves an ATP-dependent process although this appears unlikely in view of the results obtained in the other cell lines. Finally, it is also noteworthy that the amount of peptide that entered both the astrocytes and the PC-12 cells appears to be significantly higher than was observed in the other cell lines tested. This may be significant, suggesting that these cells are more permeable or it may simply reflect the larger size and internal volume of the cells themselves.

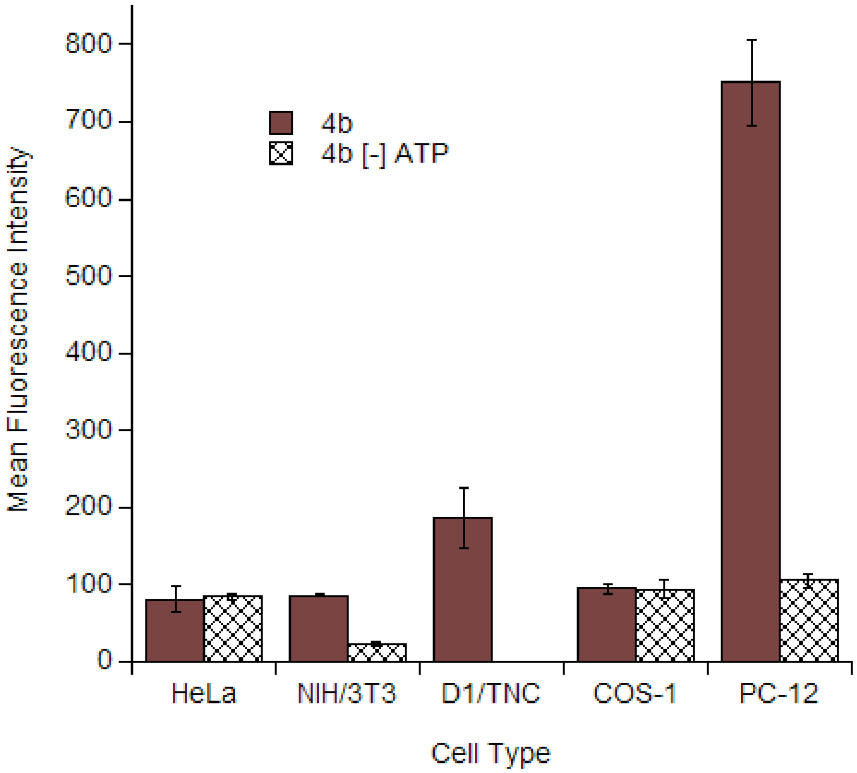

Figure 5.5. Flow cytometry analysis of peptide 4b incubated with various cells at 1 μM for 2 h. Cells were incubated at either 37°C or under conditions of ATP depletion. After incubation, cells were trypsinized for 15 min to remove membrane-bound peptide. Each bar represents the geometric mean fluorescence of 10,000 cells. Experiments performed in triplicate with the results expressed as the mean fluorescence intensity ± standard deviation.

5.3.4 Evaluation of a Probe to Study in vivo Prenylation

From the experiments described above, we demonstrated that peptides containing farnesylation sequences were introduced into living cells. We next sought to develop a peptide that could serve as a substrate for protein farnesyltransferase. If this could be accomplished, it would then be possible to monitor the complete processing of prenylated peptides that includes prenylation, proteolysis and methylation. Accordingly, the disulfide linked peptides **5a** and **5b** (see Figure 5.1) were constructed to explore the cell penetrating ability of probes containing a lipid group that would be reductively cleaved upon entry into the reducing environment of the cytoplasm.[186] Such a process would reveal a complete CAAX sequence suitable for subsequent modification by the endogenous prenylation machinery.[155]

The uptake of the disulfide-linked peptides **5a** and **5b** into HeLa cells was studied by flow cytometry analysis. As can be seen in Figure 5.3, the disulfide linked peptides **5a** and **5b** have greater uptake than the corresponding farnesylated peptides even though they contain only a 10 carbon alkyl chain compared with the farnesyl group (15 carbons) present in **4a** and **4b**. This may be a result of the straight alkyl chain having more favorable interactions with similarly structured saturated lipids in the plasma membrane, while the isoprenoid chain contains branches and elements of unsaturation that may render it less likely to integrate with and pass through the membrane. In support of this

hypothesis, the calculated octanol/water partition coefficient (ClogP) value of N-acetylcysteine methyl ester with a farnesyl group is lower (3.82) than that of the same amino acid conjugated to a disulfide linked decyl group (5.31), suggesting that the decyl group is more hydrophobic and may have more favorable membrane interactions.

Finally, the significant cell penetrating capability of these disulfide-linked peptides led us to investigate their ability to enter other cell types. Flow cytometry analysis was used to quantify their entry into astrocytes and PC12 cells (Figure 5.6). Interestingly, **5b** was able to enter these cells with efficiency comparable to that observed with HeLa cells. In light of this finding, both astrocytes and PC-12 cells were used in these experiments. The finding that the disulfide linked peptides **5a** and **5b** are able to enter these cells (Figure 5.6) opens the door for studies of prenylation in the central nervous system in order to better understand the molecular mechanisms underlying the prenylation state in Alzheimer's Disease. Experiments using this probe to study prenylation in live cells are underway.

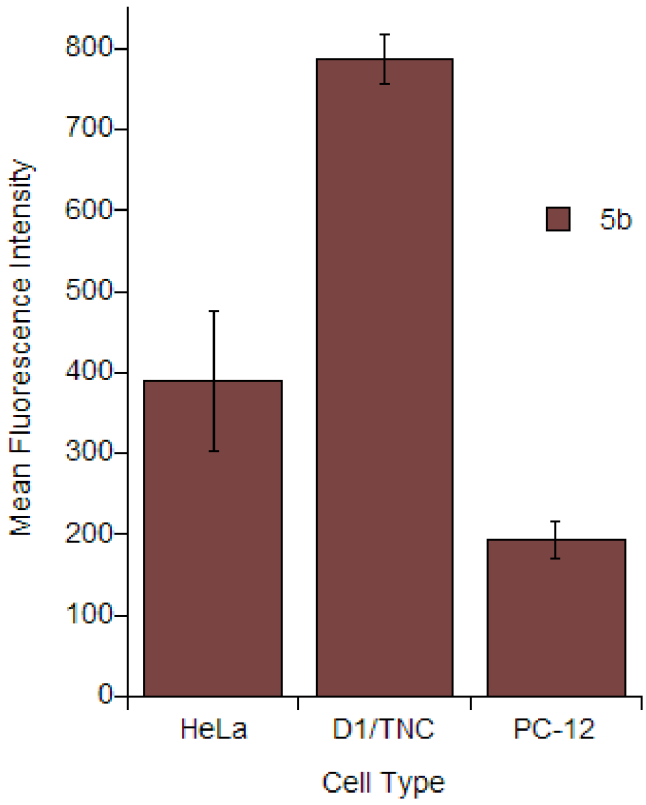

Figure 5.6. Flow cytometry analysis of peptide 5b incubated with various cells at 1 μM for 2 h at 37°C. After incubation, cells were trypsinized for 15 min to remove membrane-bound peptide. Each bar represents the geometric mean fluorescence of 10,000 cells. Experiments performed in triplicate with the results expressed as the mean fluorescence intensity ± standard deviation.

5.4 Conclusions

This chapter describes results that fluorescently labeled farnesylated peptides based on the C-terminus of CDC42 are able to translocate the membrane of live cells in an ATP-independent manner. The peptides are also able to enter diverse cell types, suggesting that they will be useful for a variety of different types of studies. Of particular interest, peptides **5a** and **5b**, which contain a 10 carbon alkyl chain linked through a disulfide bridge in place of the isoprenoid, are able to efficiently enter live cells. In previous work by Krylov and coworkers, fluorescently labeled peptides were used to study the kinetics of farnesyltransferase as well as to detect the processing steps of prenylation in single cells.[187-189] However, using single cell methods, the authors were not able to detect the processing of the substrate peptide, probably because the uptake of the peptide was insufficient. Using peptides **5a** and **5b** should allow this limitation to be overcome and will expand the available tools for examining prenyl processing *in vivo*. In addition to applications in cancer biology, recent studies have indicated that the levels of farnesyl diphosphate and geranygeranyl diphosphate are elevated in the brains of patients with Alzheimers Disease, suggesting that prenylation may play some role in the neuropathophysiology of this disease.[32] Thus, we are currently employing the peptides reported in this chapter to probe the process of prenylation in both cancer and neuronal cells.

5.5 Experimental

5.5.1 General Materials

HeLa cells were the generous gift of Dr. Audrey Minden (Department of Chemical Biology, Rutgers University). Petri dishes (35 mm) fitted with microwells (14 mm) and a No. 1.5 coverglass were from MatTek Corporation. Wheat germ agglutinin Alexa Fluor 594 conjugate, Hoechst 34850, and DMEM (Dulbecco's Modified Eagle Medium) were from Invitrogen. Fetal bovine serum (FBS) was from Intergen Company. Horse Serum (HS) was from Fischer Scientific. F12K media was from ATCC. Mouse β-Nerve Growth Factor was purchased from Raybiotech. Vydac 218TP54 and 218TP1010 columns were used for analytical and preparative RP-HPLC, respectively. All analytical and preparative RP-HPLC solvents, water and CH3CN, contained 0.10% TFA and were of HPLC grade. PAL-PEG-PS was from Applied Biosystems. Preloaded CLEAR-Acid resins were from Peptides International. 5-Carboxyfluorescein was from Berry & Associates. All other reagents were from Sigma Aldrich.

5.5.2 Synthesis

Peptides were synthesized on an Applied Biosystems 433A automated synthesizer according to manufacturer protocols. 5-Carboxyfluorescein was coupled to the peptide while still on resin in the following manner: In a small test tube, 2.0 equivalents of 1-Hydroxybenzotriazole (HOBt, 0.2 mmol), 2.0 equivalents of *N,N′*-Diisopropylcarbodiimide (DIC, 0.2 mmol), and 2.1 equivalents

of 5-carboxyfluorescein (5-Fam, 0.2 mmol) were pre-incubated for 5 min in 1.2 mL *N,N*-Dimethylformamide (DMF). This solution was added to the peptide on resin in a syringe with a fritted filter and reacted overnight on a rotisserie wrapped in aluminum foil. The resin was then rinsed with DMF (5x, 3.0 mL each) followed by CH_2Cl_2 (5x, 3.0 mL each). After drying the crude peptide *in vacuo* for 2 h, it was cleaved from the resin using freshly prepared Reagent K[178] (TFA/phenol/thioanisole/water/ethanedithiol, 82.5:5:5:5:2.5) for 2 h. Following resin cleavage, the peptide was precipitated by the addition of 50 mL diethyl ether (Et_2O), centrifuged to form a pellet which was rinsed twice with Et_2O, and frozen at -20°C until later purification.

5-Fam-KKSRRC(Acm)VIM (**1a**)

Synthesized on Fmoc protected methionine CLEAR Acid Resin. The peptide was purified by RP-HPLC on a C_{18} column using a gradient of 1% B per minute (solvent A: 0.1% aqueous TFA, solvent B: 0.1% TFA in CH_3CN) affording a light yellow solid. Product eluted at 31% B, verified with mass spectrometry (deconvoluted ESI-MS calculated for $C_{70}H_{104}N_{18}O_{18}S_2$ 1548.7, found 1547.7).

5-Fam-KKSRRC(Scm)VIM (**2a**)

A 0.27 M stock solution of methoxycarbonylsulfenyl chloride was prepared by adding 5.0 µL of methoxycarbonylsulfenyl chloride to 200 µL acetonitrile; the stock solution was cooled on ice. The concentration of the peptide used was determined by UV spectroscopy of the 5-Fam chromophore (ε_{492}=79,000 $M^{-1}cm^{-1}$, 492 nm, pH=9.0); this method was used throughout the synthesis to calculate

peptide concentration. After the peptide concentration was determined, 1 equivalent of solid peptide (15.1 mg, 9.7 µmol) was dissolved in a 1:1 mixture of DMF and CH_3CN (7.0 mL total, approximately 1.0 mL solvent per 1.0 mg peptide). The peptide solution was cooled on ice and 3 equivalents of the 0.27 M methoxycarbonylsulfenyl chloride stock solution (108 µL, 29.2 µmol) was added. The reaction was stirred at rt for 3h in the dark and purified by RP-HPLC on a C_{18} column using a gradient of 1% B per minute (solvent A: 0.1% aqueous TFA, solvent B: 0.1% TFA in CH_3CN) yielding a green solid (9.3 mg, 58%). Product eluted at 30.5% B and was verified with mass spectrometry (deconvoluted ESI-MS calculated for $C_{69}H_{101}N_{17}O_{19}S_3$ 1567.7, found 1567.3).

5-Fam-KKSRRCVIM (**3a**)

1.0 mg of Scm-protected peptide **2a** was dissolved in 10 mL of 20 mM Tris (pH=8.0). To this peptide solution, approximately 0.5 mg of solid dithiothreitol (DTT) was added. The reaction was stirred at rt in the dark for approximately 30 min. The product was purified by RP-HPLC on a C_{18} column using a gradient of 1% B per minute (solvent A: 0.1% aqueous TFA, solvent B: 0.1% TFA in CH_3CN) yielding a green solid (0.9 mg, 83%). Product eluted at 28% B and was verified with MS (deconvoluted ESI-MS calculated for $C_{67}H_{99}N_{17}O_{17}S_2$ 1477.7, found 1477.5).

5-Fam-KKSRRC(farnesyl)VIM (**4a**)

100 mM $Zn(OAc)_2$ stock solution was prepared by dissolving 22.0 mg $Zn(OAc)_2$ in 1.0 mL of 0.1% aq. TFA. 1.0 equivalent of **3a** (0.6 mg, 0.4 µmol) was

dissolved in 600 µL of solvent (DMF/1-butanol/0.1% aqueous TFA, 2:1:1), to which 20.1 µL of the 100 mM stock $Zn(OAc)_2$ solution (5.0 eq., 2.0 µmol) was added. To this solution, 0.4 µL (4.0 eq., 1.6 µmol) of farnesyl bromide was added. The solution was stirred at rt, in the dark, overnight and purified by RP-HPLC on a C_{18} column using a gradient of 1% B per minute (solvent A: 0.1% aqueous TFA, solvent B: 0.1% TFA in CH_3CN) which afforded a light green solid (0.07 mg, 11.7%). Product eluted at 55%B and was verified with high-resolution ESI-MS (deconvoluted ESI-MS for $C_{82}H_{123}N_{17}O_{17}S_2$ 1681.8724, found 1681.8888).

5-Fam-KKSRRC(S-decyl)VIM (**5a**)

A 7.0 mM decanethiol solution was prepared by adding 1.4 µL of decanethiol to 1.0 mL DMF. A 17 mM $Zn(OAc)_2$ stock solution was also prepared by dissolving 3.7 mg of $Zn(OAc)_2$ in 1.0 mL water. Peptide **2a** (1.0 eq., 0.5 µmol, 0.7 mg) was dissolved in 100 µL DMF. To the peptide solution, 64.3 µL of the 7.0 mM stock decanethiol solution was added (1.0 eq., 0.5 µmol). After cooling this solution on ice, 132.4 µL of the 17 mM $Zn(OAc)_2$ stock solution was slowly added (5.0 eq., 2.3 µmol). The reaction was stirred at rt in the dark for 4 h and was purified by RP-HPLC on a C_{18} column using a gradient of 1% B per minute (solvent A: 0.1% aqueous TFA, solvent B: 0.1% TFA in CH_3CN) yielding a light green solid (0.08 mg, 11.4%). Product eluted at 52%B and was verified with high-resolution ESI-MS (deconvoluted ESI-MS for $C_{77}H_{119}N_{17}O_{17}S_3$ 1649.8132, found 1649.8288).

5-Fam-KKSRRC(Acm)VLS (**1b**)

Prepared similar to **1a** using Fmoc-L-Ser(tBu)-PEG-PS resin. Product eluted at approximately 28% B, verified with mass spectrometry (deconvoluted ESI-MS calculated for $C_{68}H_{100}N_{18}O_{19}S$ 1504.7, found 1504.8).

5-Fam-KKSRRC(Scm)VLS (**2b**)

Prepared similar to **2a**. Reaction scale = 5.7 mg, 3.8 µmol peptide. Yield 3.4 mg (58.9%). Product eluted at 30% B and was verified with ESI-MS (deconvoluted ESI-MS calculated for $C_{67}H_{97}N_{17}O_{20}S_2$ 1523.7, found 1523.2).

5-Fam-KKSRRCVLS (**3b**)

Prepared similar to **3a**. Reaction scale = 1.5 mg, 1.0 µmol peptide. Yield 1.4 mg (95.7%). Product eluted at 28% B and was verified with MS (deconvoluted ESI-MS calculated for $C_{65}H_{95}N_{17}O_{18}S$ 1433.7, found 1433.8).

5-Fam-KKSRRC(farnesyl)VLS (**4b**)

Prepared similar to **4a**. Reaction scale = 0.3 mg, 0.2 µmol. Yield 0.04 mg (11.1%). Product eluted at 50%B and was verified with MS (deconvoluted ESI-MS calculated for $C_{80}H_{119}N_{17}O_{18}S$ 1637.9, found 1637.8).

5-Fam-KKSRRC(S-decyl)VLS (**5b**)

Prepared similar to **5a**. Reaction scale = 1.3 mg, 0.9 µmol. Yield 0.4 mg (29.2%). Product eluted at 48%B and was verified with MS (deconvoluted ESI-MS calculated for $C_{75}H_{115}N_{17}O_{18}S_2$ 1605.8, found 1605.4).

5.5.3 Cell Experiments

For cell experiments involving HeLa, COS-1, NIH/3T3, and D1TNC1 astrocyte cells, 7.8 x 10^3 cells/cm^2 were seeded in culture dishes and grown to approximately 50% confluency (generally 24 h); PC-12 cells were seeded at 3.9 x 10^3 cells/cm^2. PC-12 cells were differentiated into neurons before analysis (see below). HeLa cells were maintained in DMEM supplemented with 10% FBS; PC-12 were maintained in F12K supplemented with 10% HS and 5% FBS.

Microscopy:

The cells were washed twice with PBS (1 mL), followed by the addition of serum-free DMEM (or F12K + 1% HS for PC-12) and incubated for either 1h or 2h at 37°C with 5.0% CO_2 with the desired peptide at the desired concentration (typically 1 or 3 μM). Hoechst 34580 nucleus stain was added to a final concentration of 1 μg/mL during the final 20 min of incubation. Additionally, wheat germ agglutinin Alexa Fluor 594 conjugate was added to a final concentration of 5 μg/mL during the final 10 min of incubation. After the incubation period all cells were washed twice with PBS (1mL) and placed back in serum-free DMEM (F12K + 1% HS for PC-12). The cells were then imaged using an Olympus FluoView 1000 confocal microscope with a 60X objective. The fluorophores were monitored at their maximum emission wavelengths of 520 nm, 450 nm, and 620 nm for 5-Fam, Hoechst 34580 nuclear stain, and wheat germ agglutinin Alexa Fluor 594 conjugate, respectively.

Flow cytometry:

The cells were rinsed twice with PBS (1 mL) and incubated for 1 h at 37°C with 5.0% CO_2 with the desired peptide in serum-free DMEM (or F12K + 1% HS for PC-12) at varying concentrations. Following incubation, the media was aspirated and the cells rinsed with PBS (2X, 1 mL each). The cells were removed from the plate by trypsinization for 15 min (to remove membrane bound peptide) at 37°C with 5.0% CO_2 (0.2 mL of a 0.0625% trypsin/versene solution). Cells were re-suspended in 1.8 mL complete DMEM (or F12K for PC-12) and transferred to a 15 mL falcon tube. The cells were pelleted by centrifugation at 100 g for 5 min. The media was aspirated from the cells followed by the addition of 2 mL PBS to resuspend the pellet. Cells were added to a 12 x 75 mm test tube for flow cytometry analysis. A total of 10,000 events for each sample were analyzed using a BD FACSCalibur (BD Biosciences). For ATP depletion, cells were washed twice with glucose-free, serum-free DMEM and then incubated for 2 h at 37°C and 5.0% CO_2 in glucose-free, serum-free DMEM supplemented with 12 μM rotenone and 15 mM 2-deoxyglucose;[190] then the peptides were added and incubation proceeded as above.

Neuron Differentiation for PC-12:

PC-12 cells were differentiated similarly to previously described methods [177]. Briefly, PC-12 cells were seeded at 3.9 x 10^3 cells/cm^2 on poly lysine coated plates [191] and grown 24 h at 37°C with 5.0% CO_2. Cells were serum starved for 24h with F12K + 1% HS. Addition of F12K media containing 1% HS and 100

ng/mL of β-NGF initiated neuron differentiation. Incubation with β-NGF proceeded for 6-8 days; fresh media was added every 2 days.

5.5.4 Octanol/water (LogP) Measurement

LogP values were measured following a previously established procedure.[192] Briefly, 100 μL of a peptide solution (50 or 100 μM) in 10mM Tris (pH=7.4) was added to 100 μL octanol in a microtube (1.5 mL). A buffered Tris solution was used to ensure the peptide was kept in a state similar to physiological pH. The solution was vortexed for 2 min and centrifuged for 2 min. 25 μL of each layer was removed and diluted either in 100 μL 3:1 methanol/Tris or methanol/octanol for a final composition of 3:1:1 methanol/octanol/Tris. The aqueous layer was further diluted 2-4 fold so the absorbance (at 492 nM for 5-Fam) was in the linear range of the instrument. For measurements at lower concentration, the octanol absorbance was measured directly. The log (A_{492} of the organic layer/A_{492} of the aqueous layer) yielded logP. This was repeated twice to yield a mean logP ± standard deviation.

6. Prenylated Peptides Lacking a Fluorophore for *in vivo* analysis

6.1 Introduction

Chapter 5 discussed the development of a series of peptides that are based on the C-terminus of the naturally geranylgeranylated protein CDC42. These peptides were functionalized with a fluorophore and a geranylgeranyl group and found to have intrinsic cell-penetrating ability, by a mechanism that was energy independent.[176] This study also demonstrated that without the geranylgeranyl group, the peptides were unable to enter cells; related experiments demonstrated that farnesylated peptides derived from CDC42 can also enter a wide variety of cell types. A further study examining the role of the positively charged amino acids in the sequence found that these amino acids were not necessary for uptake, and that a peptide as short as two amino acids was able to penetrate cells, provided the geranylgeranyl group was present.[182] This chapter describes work that serves to elucidate the role of the 5-carboxyfluorescein (5-Fam) fluorophore on the uptake of these peptides. The benefit of this class of cell penetrating prenylated peptides is that they enter cells

by a non-endocytotic, ATP independent mechanism that allows accumulation into the cytosol of cells. These peptides may prove useful in cell-penetrating applications in which the cargo can be easily released in the cytosol. Additionally, make the peptide as minimalist as possible will allow for a more accurate study of protein prenylation in living systems.

6.2 Research Objectives

It has long been thought that the reason the cell penetrating prenylated peptides could diffuse through the plasma membrane of cells was because of the fluorophore on the peptide. We have shown previously that the prenyl group is necessary for uptake, but this work serves to elucidate the role the fluorophore plays in the peptide uptake.

6.3 Results and Discussion

6.3.1 Peptide Synthesis

For this study, the peptides (Figure 6.1) were synthesized using standard Fmoc coupling conditions on an automated synthesizer with Rink-amide resin to afford the C-terminal amide peptides. While still on resin, the N-terminal lysine side chain (ε amine) was acetylated, followed by acylation with an alkyne-containing acid (4-pentynoic acid) on the α amino group to give the resulting N-terminal alkyne. Geranylgeranylation of that peptide was performed in solution

using acidic $Zn(OAc)_2$ coupling conditions[179] to afford peptide **1.** Peptide **2** was prepared in an analogous manner except that the ε-amino group of the N-terminal lysine was acylated with 5-Fam. Thus, peptide **1** contains an alkyne but no fluorophore whereas peptide **2** contains both an alkyne and a fluorophore.

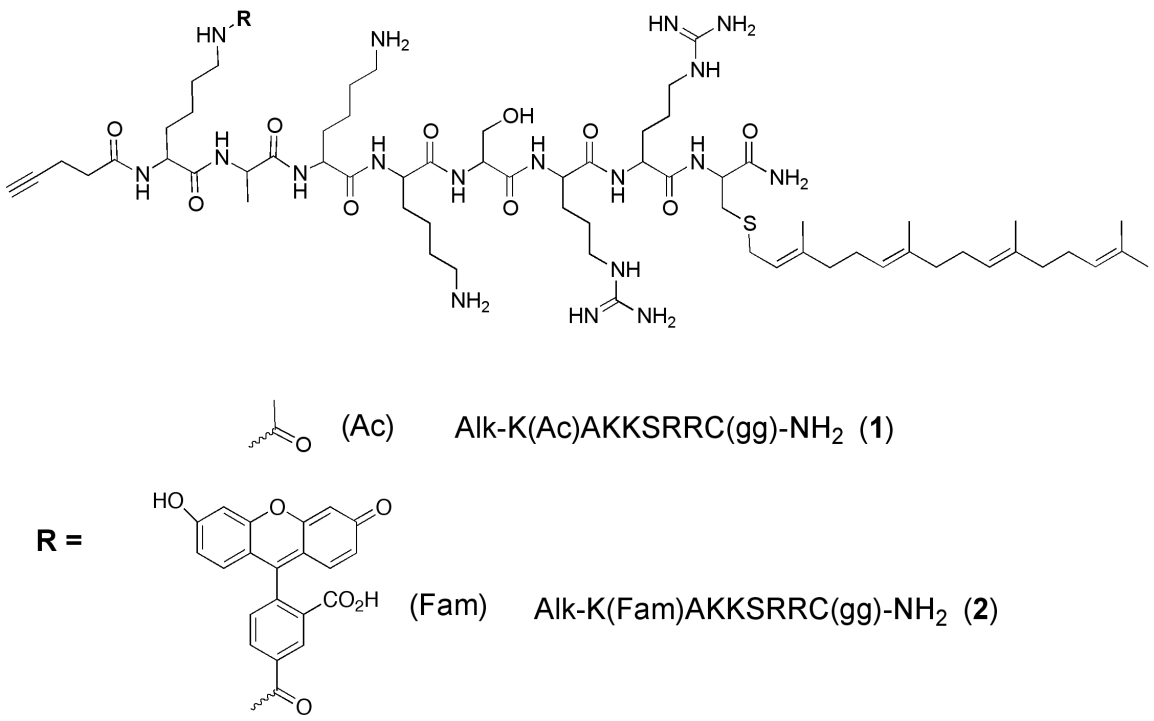

Figure 6.1. Sequences of the peptides used to study the requirement of the 5-Fam fluorophore on peptide uptake. The alkyne moiety on the N-terminus was included so a 'click' reaction would enable visualization inside cells.

6.3.2 Uptake studies in HeLa cells

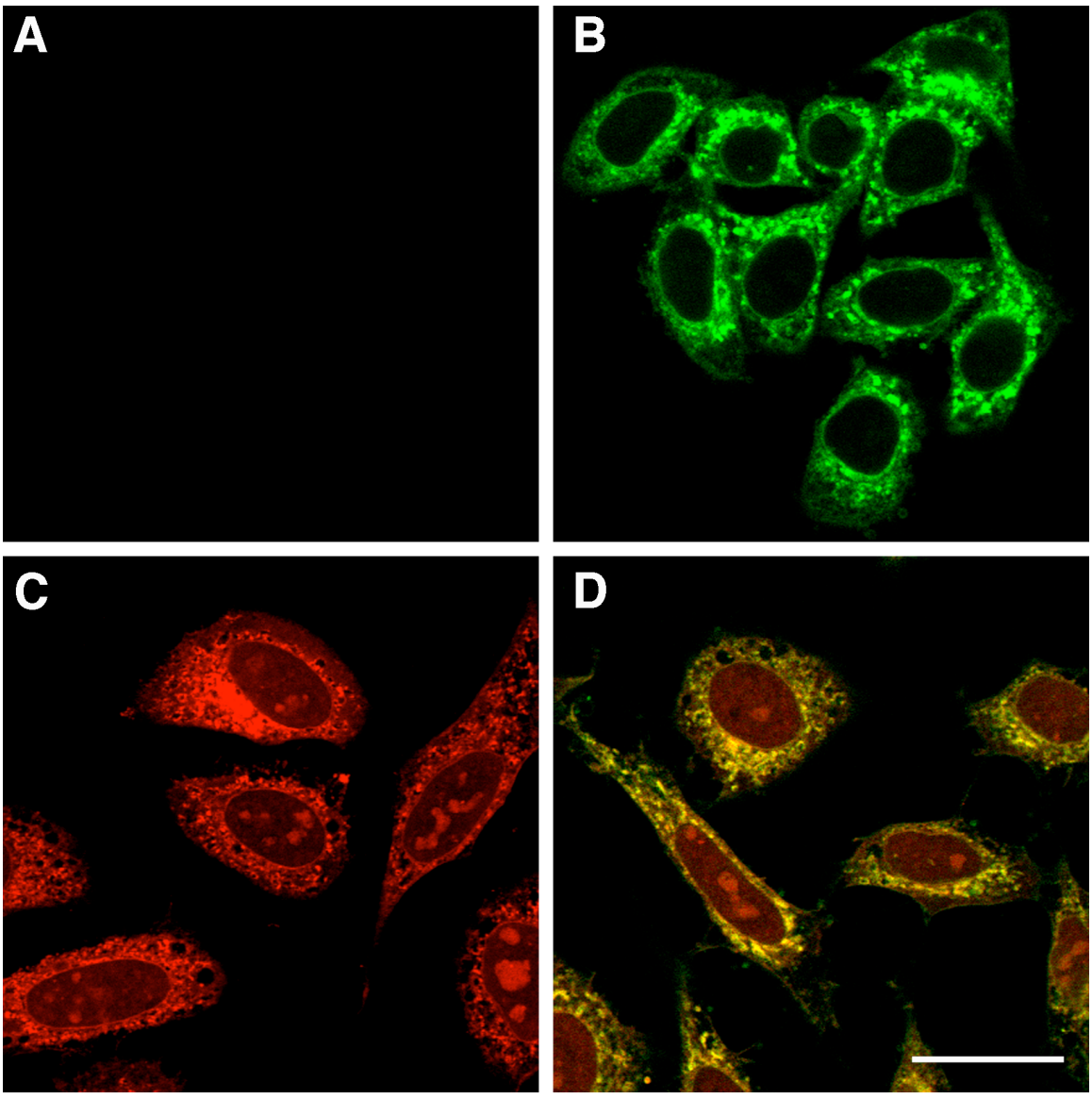

Figure 6.2. HeLa cells incubated with peptides 1 or 2 at 1 μM for 2 h. Panel A) Click reaction performed on cells that were not treated with an alkyne peptide, showing no background labeling by TAMRA-N_3. Panel B) Peptide 2 visualized with green 5-Fam fluorescence. Panel C) Peptide 1 monitored by click reaction with TAMRA-N_3 on fixed cells. Panel D) Peptide 2 monitored by click reaction with TAMRA-N_3 on fixed cells and green 5-Fam fluorescence; the yellow color indicates co-localization of 5-Fam and TAMRA fluorophores, now present on the same peptide. The size bar represents a distance of 25 μm.

The ability of both of these peptides to enter cells was first established using confocal laser scanning microscopy (CLSM). Because peptide **2** contains the 5-Fam fluorophore, visualization after uptake in HeLa cells is easily accomplished after a 2 h incubation of the peptide at 1 μM (Figure 6.2 B). To investigate whether the 5-Fam fluorophore is necessary for uptake, peptide **1** was synthesized lacking the fluorophore. Following cellular incubation of **1** at 1 μM for 2 h, HeLa cells were rinsed three times with PBS and fixed with 4% paraformaldehyde, followed by permeabilization with 0.1 % Triton X-100. A copper catalyzed click reaction was then conducted using tetramethylrhodamine azide (TAMRA-N_3) to form a covalent triazole linkage between the peptide-alkyne and the tetramethylrhodamine (TAMRA) fluorophore; when **1** enters cells, it can be visualized through the TAMRA fluorophore using CLSM (Figure 6.2 C). Thus, it can be seen that the peptide lacking a fluorophore is still able to efficiently cross the membrane of HeLa cells. While control experiments in which HeLa cells were treated with TAMRA-N_3 (without prior peptide treatment) manifested no background labeling (Figure 6.2 A), we wanted to compare the localization pattern obtained by direct visualization of 5-Fam with that observed from the TAMRA-N_3 labeling. Incubation of **2** with HeLa cells and subsequent click reaction to TAMRA-N_3 resulted in strong co-localized fluorescence in the cells (yellow color, Figure 6.2 D); this observation also confirms that little background reaction occurs in the TAMRA-N_3 labeling process since the red TAMRA

fluorophore is only present where the green 5-Fam of the peptide is observed. The Mander's overlap coefficient of the cells is 0.901 when the nucleus is included in the analysis and 0.960 when it is excluded, indicating there is significant overlap of green and red fluorescence, even when the nucleus is considered (a Mander's coefficient of 1 indicates perfect overlap[193]).

6.3.3 Localization of Peptides Inside Cells

It is important to note that it appears there is some nuclear labeling when HeLa cells are incubated with **1**. To explore this issue, we incubated peptide **1** with HeLa cells, followed by a subsequent click reaction to either TAMRA-N_3 or 5-Fam-PEG-N_3. This will help establish if the nuclear localization is an artifact of the fixation or of the fluorophore used. Regardless of the fluorophore used, nuclear staining is observed when incubating HeLa cells with **1** (Figure 6.3). This effect is absent when performing the click reaction on cells that were not treated with alkyne peptide (see Figure 6.2 A), and is also absent in cells treated with **2** (see Figure 6.2 B). This suggests that peptide **1** that lacks the fluorophore partitions differently within cells and is able to enter the nucleus whereas peptide **2** does not; however, it should be noted that the amount of nuclear localization is small compared to the amount of peptide distributed throughout the remainder of the cell. Overall, the localization patterns of **1** and **2** are quite similar and appear to be cytosolic.

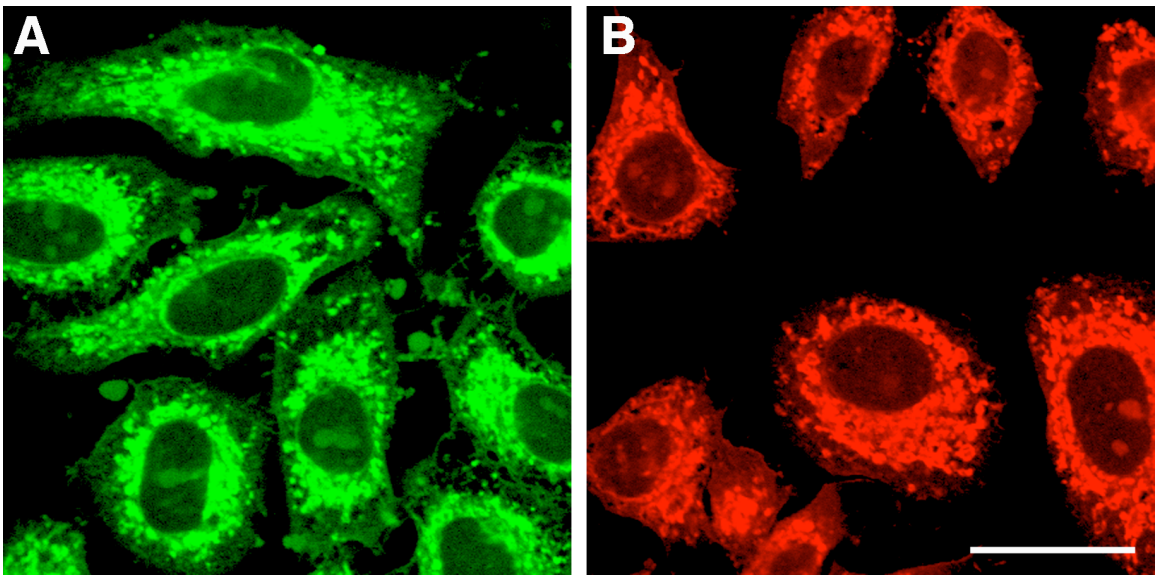

Figure 6.3. HeLa cells incubated with peptide 1 at 1 μM for 2 h and intentionally overexposed and saturated to highlight the nuclear labeling. Panel A) Peptide 1 visualized by click reaction with 5-Fam-PEG-N_3 on fixed cells. Panel B) Peptide 1 visualized by click reaction with TAMRA-N_3 on fixed cells. Regardless of the fluorophore used, nuclear staining is observed in both cases. This effect is not seen in cells that are subjected to the click reaction but not treated with peptide; this indicates that peptide 1 has a small amount of nuclear localization. The size bar represents a distance of 25 μm.

6.3.4 Quantification of Peptide Uptake

Having visually established that peptide **1** can enter HeLa cells, we next sought to quantify the differences in uptake between **1** and **2**. Accordingly, a reagent containing 5-Fam linked to an azide moiety was synthesized for this purpose. This reagent was designed so that the fluorescence of the two peptides could be more directly compared since both peptides would be labeled by the same fluorophore. A succinimidyl ester of 5-Fam was reacted with 11-Azido-3,6,9-trioxaundecan-1-amine in the presence of diisopropylethylamine overnight at room temperature. Following purification by reverse phase HPLC, 5-Fam-PEG-N_3 was isolated and used as the subsequent azide for click chemistry. HeLa cells were incubated with **1** or **2** at various concentrations for 1 h. Both sets of cells were rinsed, fixed and permeabilized. Cells treated with peptide **1** were subjected to the click reaction with 5-Fam-PEG-N_3 for 1 h followed by several rinses, and subsequent flow cytometry analysis. Cells treated with peptide **2** were analyzed directly by flow cytometry without click reaction. Based on those experiments, peptide **1** appears to enter the cells to a lesser extent (2-3-fold) than **2** (Figure 6.4) at all concentrations tested. This could indicate that **1** is indeed not as efficient at penetrating the cellular membrane compared to **2** since it lacks the fluorophore. Alternatively, this result could be an artifact of the analysis; the click reaction may not quantitatively label all of the available alkyne-functionalized peptide during the course of the reaction. It is also plausible that if **1** enters the

cells and localizes to an internal membrane (endoplasmic reticulum localization is natural for geranylgeranylated proteins[194]) that the N-terminal alkyne becomes buried in the membrane and is inaccessible for the click reaction. These latter two possibilities would both lead to an artificially lower mean fluorescence value. Regardless of which explanation is correct for the reduced fluorescence of cells treated with **1** versus **2**, the important conclusion remains – peptide **1** lacking a fluorophore is able to efficiently enter HeLa cells. This further substantiates the importance of the hydrophobic geranylgeranyl group for peptide uptake; without that moiety, the peptide is unable to enter cells.[176]

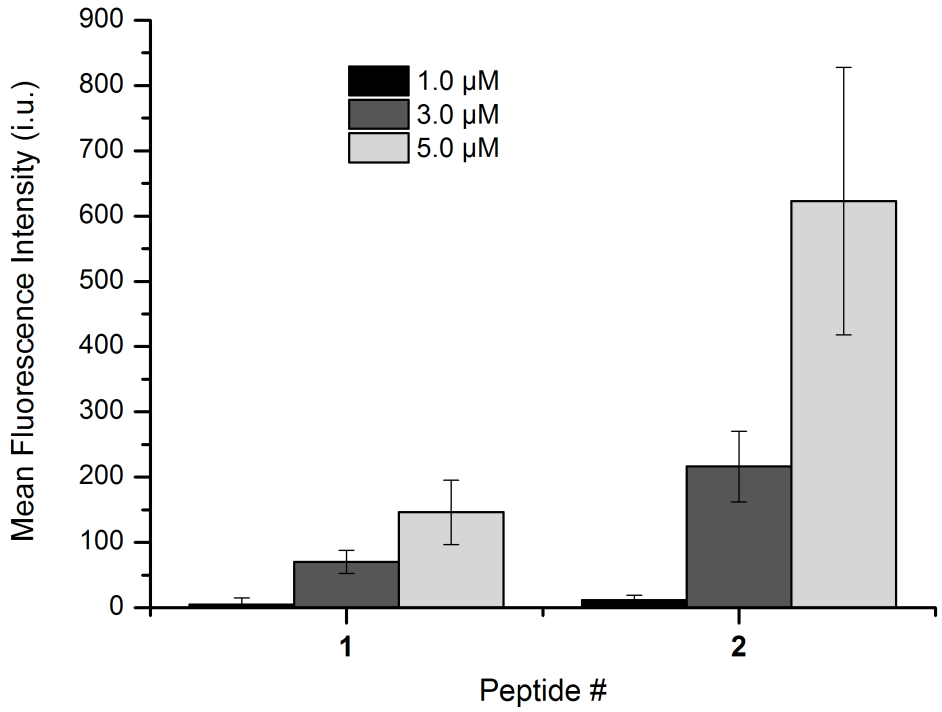

Figure 6.4. Flow cytometry analysis of peptides 1 and 2 incubated for 1 h at various concentrations. Each bar represents the geometric mean fluorescence of 10,000 cells, with the background fluorescence subtracted from each sample. Each experiment was performed in at least triplicate, expressed as the geometric mean ± standard deviation.

6.4 Conclusions

In chapter 5 and previous work by our group we have shown that peptide sequences containing a geranylgeranyl group are efficiently taken into cells in an energy-independent manner, regardless of positive charge in the sequence. The findings reported here demonstrate that the presence of the hydrophobic fluorophore 5-Fam in such peptides has minimal effect on their cell penetrating ability, further underscoring the importance of the isoprenoid moiety. This information may be useful for applications utilizing cell-penetrating peptides to deliver cargo across membranes. Using the smallest molecule for a CPP has the benefit of facile synthesis as well as minimum disturbance of the cell during cargo delivery. The non-endocytotic mechanism that functions in the uptake of these peptides may also prove to be useful since it avoids potential endosomal localization/degradation of cargo. For instance, Medintz and coworkers attached a CPP to a quantum dot and a fluorescent protein to study the internalization of cargo, finding that microinjection of the conjugate into cells was necessary to avoid endosomal uptake.[195] Finally, we note the novel method for visualizing cell penetrating peptides described herein. To date, most studies of cell penetrating peptides and related materials have employed fluorophores linked to the compounds themselves to report on cellular entry. The incorporation of bulky, hydrophobic fluorescent groups inevitably perturbs the chemical and physical

properties of the molecules under study and hence complicates structure/function analysis. For example, the addition of the 5-Fam fluorophore to a lysine residue alters the calculated partition coefficient (CLogP) by 3 units, illustrating a large change in the hydrophobic properties of the parent molecule (Figure 6.5). The method reported here provides a simple solution to this problem. The incorporation of a small alkyne-containing moiety into the peptide results in minimal alteration of the properties of the parent peptide. The CLogP value of Lys(5-Fam) with either an acetylated N-terminus or an N-terminal alkyne differs by only approximately 0.5 units, indicating the addition of the alkyne is a rather benign change to the hydrophobicity of the peptide (see Figure 6.6). However, the presence of the alkyne allows for facile visualization via click-mediated fluorescent labeling when desired. Furthermore, the alkyne group may be used in a variety of click reactions beyond fluorophore attachment. This approach should be quite useful for a variety of studies of cell penetrating molecules.

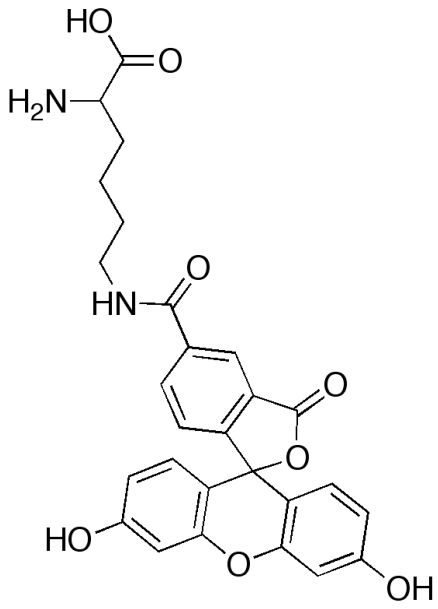

CLogP: -1.0188

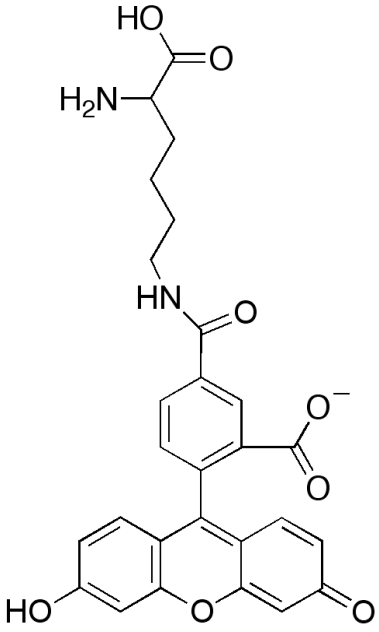

CLogP: -4.3885

Figure 6.5. Structures of Lys(Ac) and Lys(5-Fam) with calculated partition coefficient values (CLogP), showing a large difference in the hydrophobicity of the peptide with the addition of the fluorophore.

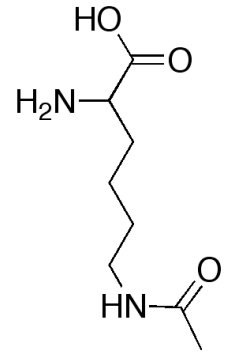

CLogP: -3.838

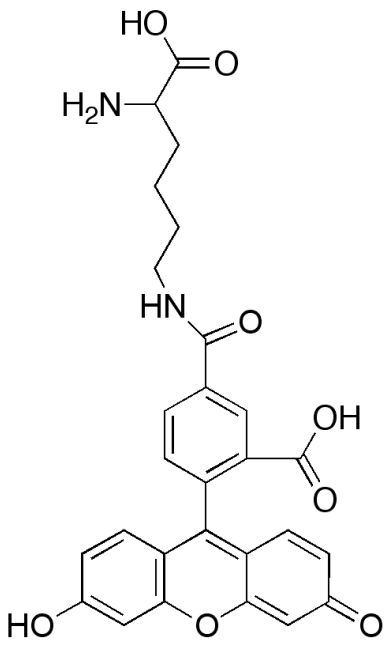

CLogP: -0.8461

Figure 6.6. Structures of Lys(5-Fam) and calculated partition coefficient values (CLogP) with and without alkyne on N-terminus, illustrating the marginal affect of the alkyne group on the hydrophobicity of the peptide.

6.5 Experimental

6.5.1 General

HeLa cells were the generous gift of Dr. Audrey Minden (Department of Chemical Biology, Rutgers University). Hoechst 34850, tetramethylrhodamine 5-carboxamido-(6-azidohexanyl) 5-isomer (TAMRA-N_3), and DMEM (Dulbecco's Modified Eagle Medium) were from Invitrogen. Fetal bovine serum was from Intergen Company. Culture dishes (100 and 35mm) were from Corning; 6-well plates were from BD Biosciences. Glass-bottomed 35mm culture dishes for imaging were from MatTek. Vydac 218TP54 and 218TP1010 columns were used for analytical and preparative RP-HPLC, respectively. All analytical and preparative RP-HPLC solvents, water and CH_3CN, contained 0.10% TFA and all solvents were HPLC grade. DIEA and TFA were of Sequalog/peptide synthesis grade from Fisher. Rink Amide resin and Fmoc amino acids were purchased from Peptides International. C18 SepPak® cartridges were from Waters (WAT023635). 5-Fam-succinimidyl ester was from AnaSpec. All other reagents were from Sigma Aldrich. All procedures involving fluorescent derivatives were protected from light as much as possible in order to avoid bleaching the fluorophore.

6.5.2 Solid-Phase Peptide Synthesis

Synthesis of PynKAK(Boc)K(Boc)S(tBu)R(Pbf)R(Pbf)C(Trt)-Rink Amide resin:

The sequence AK(Boc)K(Boc)S(tBu)R(Pbf)R(Pbf)C(Trt)-Rink Amide resin (0.37 mmol/g, 0.15 mmol) was synthesized on the ABI 433 by the FastMoc® procedure, with HCTU as coupling reagent. The resin was then transferred to a manual solid phase reaction syringe. FmocLys(ivDde) (172 mg, 0.30 mmol) and Bop (133 mg, 0.30 mmol) were dissolved in DMF (5 mL) and DIEA (104 mL, 0.60 mmol) was added. The solution was added to the resin, and the syringe was allowed to tumble for 5 h. The resin was washed with DMF, the Fmoc group removed [piperidine-DMF, [(1:4), 5 mL, 15 min], followed by washing with DMF. In a test tube, 4-pentynoic acid (59 mg, 0.60 mmol), HCTU (248 mg. 0.60 mmol), and HOBt (92 mg. 0.60 mmol) were dissolved in DMF (5 mL) and then DIEA (209 mL. 1.2 mmol) added. The solution was added to the resin and allowed to react for 1 h. After washing with DMF, the ivDde group was removed by treatment with anhydrous hydrazine in DMF [(1:9), 5 mL] for 15 min. The resin was washed with DMF and CH_2Cl_2, dried, and divided into two portions.

Synthesis of PynK(5-Fam)AKKSRRC-NH_2:

PynKAK(Boc)K(Boc)S(tBu)R(Pbf)R(Pbf)C(Trt)-Rink Amide resin (0.075 mmol) was swollen by washing with DMF. In a test tube, 5-Fam (56 mg, 0.15 mmol) and HOBt (23 mg, 0.15 mmol) were dissolved in DMF (2 mL), then DIC (23 mL, 0.15 mmol) was added. The solution was added to the resin, and the reaction was allowed to tumble 4 h. After washing with DMF, the resin was

treated with 20% piperidine in DMF for 15 min to remove any 5-Fam that may have coupled to the phenolic hydroxyl of 5-Fam. Without this added deprotection step, an impurity is often observed that contains a mass consistent with di-5-Fam incorporation (an M + 318 impurity). The resin was then washed with DMF and CH_2Cl_2, and dried in a vacuum desiccator. The peptide was cleaved from the resin with freshly prepared Reagent K for 2 h, precipitated with ether, and centrifuged to form a pellet. The pellet was washed twice with ether, dissolved in 0.1% aqueous TFA, filtered, and purified by preparative HPLC. Yield: 37 mg (35%), T_r = 29 min., purity by RP-HPLC: 94%, deconvoluted ESI-MS: calculated 1412.7, found 1412.6.

Synthesis of PynK(Ac)AKKSRRC-NH_2:

PynKAK(Boc)K(Boc)S(tBu)R(Pbf)R(Pbf)C(Trt)-Rink Amide resin (0.075 mmol) was swollen in DMF (3 mL). To the swollen resin was added acetic anhydride (35 mL, 0.38 mmol) and DIEA (130 mL, 0.75 mmol), and the reaction was allowed to tumble 2 h. The resin was then washed with DMF and CH_2Cl_2, and dried in a vacuum desiccator. The peptide was cleaved from the resin with freshly prepared Reagent K for 2 h, precipitated with ether, and centrifuged to form a pellet. The pellet was washed twice with ether, dissolved in 0.1% aqueous TFA, filtered, and purified by preparative HPLC. Yield: 20 mg (24%), T_r = 16 min., purity by RP-HPLC: 95%, deconvoluted ESI-MS: calculated 1096.6, found 1096.6.

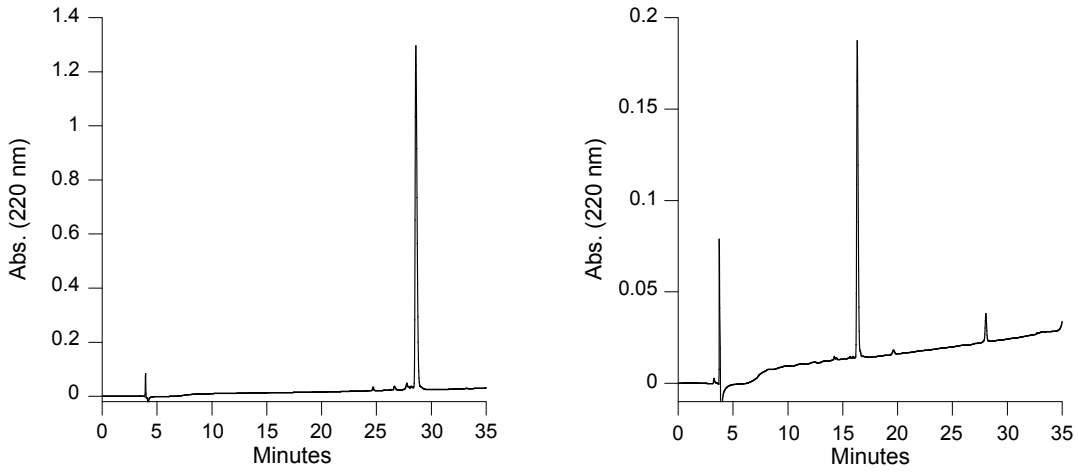

Figure 6.7. Left panel, HPLC chromatogram of purified PynK(5-Fam)AKKSRRC-NH_2. Right panel, HPLC chromatogram of purified PynK(Ac)AKKSRRC-NH_2. Gradient: 0-30% CH_3CN over 30 min. The small peak at 29 min. on the right panel is carryover of PynK(5-Fam)AKKSRRC-NH_2, which was injected in the prior run.

Synthesis of PynK(Ac)AKKSRRC(Gg)-NH_2 (1):

A C18 SepPak® column was equilibrated by passing 10 mL of 5% CH_3CN in 0.1% aqueous TFA through the column. Geranylgeranyl bromide (16 mg, 46 μmol) dissolved in 0.50 mL of DMF was loaded onto the column. The column was washed with 10 mL of 5% CH_3CN in 0.1% aqueous TFA, followed by 10 mL of 30% CH_3CN in 0.1% aqueous TFA. The geranylgeranyl bromide was then eluted directly into a flask that contained PynK(Ac)AKKSRRC-NH_2 (10 mg, 91 μmol), dissolved in DMF/*n*-butanol [(4:2), 4 mL], with 5.0 mL of DMF. Then $Zn(OAc)_2 \cdot 2H_2O$ (10 mg, 45 μmol) dissolved in 0.50 mL of 0.1% aqueous TFA was added to the reaction. The reaction was allowed to stir 1 h protected from light. The solvents were removed *in vacuo*. The residue was dissolved in 3 M guanidine hydrochloride (about 25 mL). The solution was filtered through a 0.45 mm filter disk. Small amounts of DMF (0.5 mL) were used to dissolve peptide precipitate observed on the filter disk. The peptide was purified by preparative HPLC on a C18 column. Yield: ~ 1.5 mg (12%), T_r = 50 min., purity by RP-HPLC: 85%, deconvoluted ESI-MS: calculated 1368.8, found 1368.8.

Synthesis of PynK(5-Fam)AKKSRRC(Gg)-NH_2 (2):

A C18 SepPak® column was equilibrated by passing 10 mL of 5% CH_3CN in 0.1% aqueous TFA through the column. Geranylgeranyl bromide (15 mg, 0.044 mmol) dissolved in 0.50 mL of DMF was loaded onto the column. The column was washed with 10 mL of 5% CH_3CN in 0.1% aqueous TFA, followed by

10 mL of 30% CH_3CN in 0.1% aqueous TFA. The geranylgeranyl bromide was then eluted directly into a flask that contained PynK(5-Fam)AKKSRRC-NH_2 (12 mg, 0.0087 mmol), dissolved in DMF/n-butanol [(4:2), 4 mL], with 5.0 mL of DMF. Then $Zn(OAc)_2$ dihydrate (10 mg, 0.045 mmol) dissolved in 0.50 mL of 0.1% aqueous TFA was added to the reaction. The reaction was allowed to stir 1 h protected from light. The solvents were removed *in vacuo*. The residue was dissolved in 3 M guanidine hydrochloride (about 25 mL). The solution was filtered through a 0.45 mm filter disk. Small amounts of DMF (0.5 mL) were used to dissolve peptide precipitate observed on the filter disk. The peptide was purified by preparative HPLC on a C18 column. Yield: ~ 1 mg (~ 7%), T_r = 52 min., purity by RP-HPLC: 94%, deconvoluted ESI-MS: calculated 1684.8, found 1684.8.

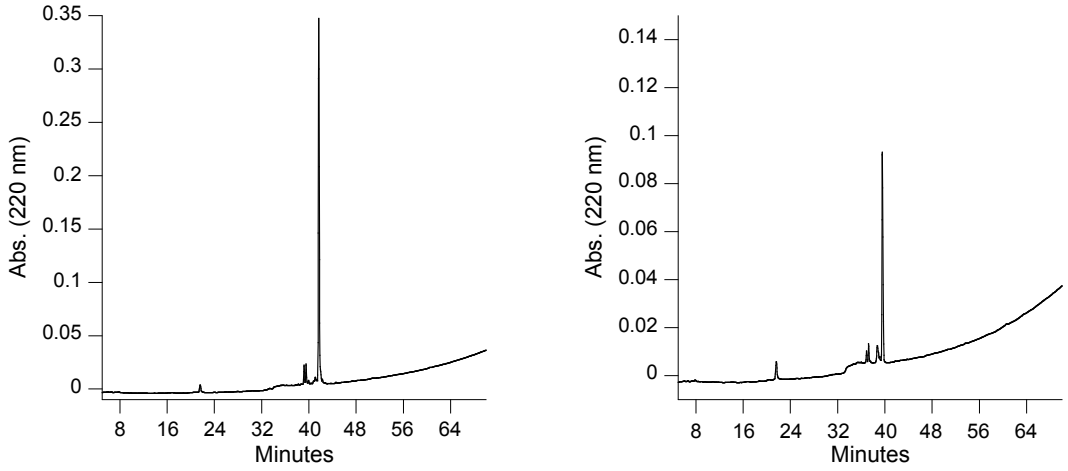

Figure 6.8. Left panel, HPLC chromatogram of purified PynK(5-Fam)AKKSRRC(gg)-NH_2. Right panel, HPLC chromatogram of purified PynK(Ac)AKKSRRC(gg)-NH_2. Gradient: 10-70% CH_3CN over 60 min.

Synthesis of geranylgeranyl bromide:

To a solution of polymer bound triphenylphosphine (68 mg, 0.20 mmol, 3.0 mmol/g substitution) and carbon tetrabromide (68 mg, 0.20 mmol) in dry CH_2Cl_2 was added geranylgeraniol (56 mL, 0.17 mmol), and the reaction was stirred for 2 h. The polymeric reagent was removed by filtration and the solvents removed *in vacuo*. This crude product is stable overnight in the freezer, but was generally used directly in the Zn^{2+} catalyzed geranylgeranylation reactions after purification on a C18 SepPak® column. The SepPak® purification removes an unknown impurity that greatly increases the amount of undesirable disulfide peptide dimer formed instead of the desired geranylgeranylation of cysteine.

6.5.3 Fluorophore Synthesis

5-Fam-succinimidyl ester (20.0 mg, 42.2 mmol) was dissolved in 1.5 mL DMF. To this solution, 11-Azido-3,6,9-trioxaundecan-1-amine (8.4 mL, 42.2 mmol) and DIEA (3.7 mL, 21.1 mmol) were added. The reaction was stirred overnight at rt in the dark. The reaction was diluted with 10 volumes of 0.1% aqueous TFA, filtered through a 0.2 mm syringe filter, and purified by RP-HPLC on a C18 column. Yield: 6.1 mg (25.1%), Product eluted at 30% CH_3CN. Deconvoluted ESI-MS: calculated 576.2, found 576.5.

6.5.4 Cell culture

HeLa cells were grown in DMEM supplemented with 10% fetal bovine serum at 37 °C with 5% CO_2. For all experiments, 2.8 x 10^4 cells/cm^2 were seeded in 35mm culture dishes and grown for 24 h to approximately 50% confluency prior to incubation with the peptides. For microscopy, glass bottomed 35mm culture dishes were used, while normal plastic 35mm dishes were used for flow cytometry.

6.5.5 Confocal Laser-Scanning Microscopy

The cells were washed twice with PBS (1.0 mL), followed by the addition of serum-free DMEM and incubated for 2 h at 37°C with 5.0% CO_2 with the desired peptide at 1 μM. The cells were rinsed twice with PBS (1.0 mL) and fixed with 4% paraformaldehyde in PBS (0.5 mL) for 10 min. The cells were rinsed once with PBS (1.0 mL) and permeabilized with 0.1% Triton X-100 in PBS for 2 min. After rinsing the cells an additional three times with PBS (1.0 mL), the click reaction was performed on the cells (300 mL total volume) by adding the following reagents, in order (final reaction concentration): 267 mL PBS (1X), TAMRA-N_3 (0.1 mM), tris(2-carboxyethyl)phosphine (TCEP, 1.0 mM), tris[(1 - benzyl - 1H - 1,2,3 - triazol - 4 - yl)methyl] amine (TBTA, 0.2 mM), copper (II) sulfate (1.0 mM). After a 1h reaction, the cells were rinsed three times with PBS (1.0 mL) and Hoechst 34580 nuclear stain was added to a final concentration of 1 mg/mL in PBS. The cells were washed twice with PBS (1.0 mL) and placed back in PBS (1.0 mL) for imaging. The cells were imaged using an Olympus FluoView 1000

confocal microscope with a 60X oil objective. The fluorophores were excited and monitored at the following excitation/emission wavelengths of 488/519 nm, 405/461 nm, and 543/567 nm for 5-Fam, Hoechst 34580 nuclear stain, and TAMRA, respectively.

6.5.6 Flow cytometry

The cells were washed twice with PBS (1.0 mL), followed by the addition of serum-free DMEM and incubated for 1h at 37°C with 5.0% CO_2 with the desired peptide at various concentrations. The cells were rinsed twice with PBS (1.0 mL) and were removed from the plate by trypsinization for 10 min (to remove membrane bound peptide) at 37°C with 5.0% CO_2 (0.2 mL of a 0.0625% trypsin/versene solution). Cells were re-suspended in 1.8 mL complete DMEM and transferred to a 15 mL falcon tube. The cells were pelleted by centrifugation at 100 g for 5 min. After removing the media from the cell pellet, the cells were fixed with 4% paraformaldehyde in PBS (150 mL) for 10 min. The cells were spun at 100 g for 4 min, liquid removed, and permeabilized with 0.1% Triton X-100 in PBS (150 mL) for 2 min. The cells were spun at 100 g for 4 min, liquid removed, and PBS (200 mL) was added to rinse the cells; this was repeated an additional two times. Next, the click reaction was performed on the cells (100 mL total volume) by adding the following reagents, in order (final reaction concentration): 90 mL PBS (1X), TAMRA-N_3 (50.0 μM), tris(2-carboxyethyl)phosphine (TCEP, 1.0 mM), tris[(1 - benzyl - 1H - 1,2,3 - triazol - 4 - yl)methyl] amine (TBTA, 0.2

mM), copper (II) sulfate (1.0 mM). After a 1h reaction, the cells were spun at 100 g for 4 min, liquid removed, and PBS (200 mL) was added to rinse the cells; this was repeated three additional times. The cells were transferred to a 12 x 75 mm test tube for flow cytometry analysis with a final volume of 1.5 mL PBS. A total of 10,000 events for each sample were analyzed using a BD FACSCalibur (BD Biosciences).

References:

1 C. T. Walsh, S. Garneau-Tsodikova and G. J. Gatto, Protein Posttranslational Modifications: The Chemistry of Proteome Diversifications, *Angew. Chem. Int. Ed.*, 2005, **44**, 7342-7372.

2 M. Mann and O. N. Jensen, Proteomic analysis of post-translational modifications, *Nat Biotech*, 2003, **21**, 255-261.

3 C. C. Farnsworth, S. L. Wolda, M. H. Gelb and J. A. Glomset, Human lamin B contains a farnesylated cysteine residue, *J. Biol. Chem.*, 1989, **264**, 20422-20429.

4 C. C. Farnsworth, M. H. Gelb and J. A. Glomset, Identification of geranylgeranyl-modified proteins in HeLa cells, *Science*, 1990, **247**, 320-2.

5 W. Benetka, M. Koranda and F. Eisenhaber, Protein Prenylation: An (Almost) Comprehensive Overview on Discovery History, Enzymology, and Significance in Physiology and Disease, *Monatsh. Chem.*, 2006, **137**, 1241-1281.

6 P. J. Casey, Biochemistry of protein prenylation, *J. Lipid Res.*, 1992, **33**, 1731-40.

7 S. Clarke, Protein isoprenylation and methylation at carboxyl-terminal cysteine residues, *Annu. Rev. Biochem.*, 1992, **61**, 355-86.

8 N. Berndt, A. D. Hamilton and S. M. Sebti, Targeting protein prenylation for cancer therapy, *Nat Rev Cancer*, 2011, **11**, 775-791.

9 J. L. Hougland, K. A. Hicks, H. L. Hartman, R. A. Kelly, T. J. Watt and C. A. Fierke, Identification of Novel Peptide Substrates for Protein Farnesyltransferase Reveals Two Substrate Classes with Distinct Sequence Selectivities, *J. Mol. Biol.*, 2010, **395**, 176-190.

10 J. L. Hougland, C. L. Lamphear, S. A. Scott, R. A. Gibbs and C. A. Fierke, Context-Dependent Substrate Recognition by Protein Farnesyltransferase, *Biochemistry*, 2009, **48**, 1691-1701.

11 C. L. Lamphear, E. A. Zverina, J. L. Hougland and C. A. Fierke, *Global identification of protein prenyltransferase substrates: defining the prenylated proteome*. 2011; Vol. 29, p 207-234.

12 I. Jordens, M. Marsman, C. Kuijl and J. Neefjes, Rab Proteins, Connecting Transport and Vesicle Fusion, *Traffic*, 2005, **6**, 1070-1077.

13 E. A. Stigter, G. Triola, R. S. Goody and H. Waldmann, *Inhibition of Rab prenylation*. Elsevier: 2011; Vol. 30, p 179-203.

14 L. Desnoyers, J. S. Anant and M. C. Seabra, Geranylgeranylation of Rab proteins, *Biochem. Soc. Trans.*, 1996, **24**, 699-703.

15 M. R. Lackner, R. M. Kindt, P. M. Carroll, K. Brown, M. R. Cancilla, C. Chen, H. de Silva, Y. Franke, B. Guan, T. Heuer, T. Hung, K. Keegan, J. M. Lee, V. Manne, C. O'Brien, D. Parry, J. J. Perez-Villar, R. K. Reddy, H. Xiao, H. Zhan, M. Cockett, G. Plowman, K. Fitzgerald, M. Costa and P.

Ross-Macdonald, Chemical genetics identifies Rab geranylgeranyl transferase as an apoptotic target of farnesyl transferase inhibitors, *Cancer Cell*, 2005, **7**, 325-336.

16 J. S. Taylor, T. S. Reid, K. L. Terry, P. J. Casey and L. S. Beese, Structure of mammalian protein geranylgeranyltransferase type-I, *EMBO J.*, 2003, **22**, 5963-5974.

17 F. Ghomashchi, X. Zhang, L. Liu and M. H. Gelb, Binding of prenylated and polybasic peptides to membranes: affinities and intervesicle exchange, *Biochemistry*, 1995, **34**, 11910-11918.

18 M. C. Seabra, Membrane association and targeting of prenylated Ras-like GTPases, *Cell. Signalling*, 1998, **10**, 167-172.

19 W. W. Epstein, D. Lever, L. M. Leining, E. Bruenger and H. C. Rilling, Quantitation of prenylcysteines by a selective cleavage reaction, *Proc. Natl. Acad. Sci.* , 1991, **88**, 9668-70.

20 R. Roskoski Jr, Protein prenylation: a pivotal posttranslational process, *Biochem. Bioph. Res. Co.*, 2003, **303**, 1-7.

21 K. Alexandrov, Y. Wu, W. Blankenfeldt, H. Waldmann and R. S. Goody, Organization and Function of the Rab Prenylation and Recycling Machinery. In *The Enzymes*, Fuyuhiko Tamanoi, C. A. H.; Martin, O. B., Eds. Academic Press: 2011; Vol. Volume 29, pp 147-162.

22 Z. Guo, Y.-W. Wu, D. Das, C. Delon, J. Cramer, S. Yu, S. Thuns, N. Lupilova, H. Waldmann, L. Brunsveld, R. S. Goody, K. Alexandrov and W. Blankenfeldt, Structures of RabGGTase-substrate/product complexes provide insights into the evolution of protein prenylation, *EMBO J.*, 2008, **27**, 2444-2456.

23 A. J. Krzysiak, D. S. Rawat, S. A. Scott, J. E. Pais, M. Handley, M. L. Harrison, C. A. Fierke and R. A. Gibbs, Combinatorial Modulation of Protein Prenylation, *ACS Chem. Biol.*, 2007, **2**, 385-389.

24 A. J. Krzysiak, A. V. Aditya, J. L. Hougland, C. A. Fierke and R. A. Gibbs, Synthesis and screening of a CaaL peptide library versus FTase reveals a surprising number of substrates, *Bioorg. Med. Chem. Lett.*, 2010, **20**, 767-770.

25 A. J. Krzysiak, S. A. Scott, K. A. Hicks, C. A. Fierke and R. A. Gibbs, Evaluation of protein farnesyltransferase substrate specificity using synthetic peptide libraries, *Bioorg. Med. Chem. Lett.*, 2007, **17**, 5548-5551.

26 N. London, C. L. Lamphear, J. L. Hougland, C. A. Fierke and O. Schueler-Furman, Identification of a novel class of farnesylation targets by structure-based modeling of binding specificity, *PLoS Comput. Biol.*, 2011, **7**, e1002170.

27 O. Pylypenko, A. Rak, R. Reents, A. Niculae, V. Sidorovitch, M.-D. Cioaca, E. Bessolitsyna, N. H. Thoma, H. Waldmann, I. Schlichting, R. S. Goody

and K. Alexandrov, Structure of Rab Escort Protein-1 in Complex with Rab Geranylgeranyltransferase, *Mol. Cell*, 2003, **11**, 483-494.

28 U. T. T. Nguyen, Z. Guo, C. Delon, Y. Wu, C. Deraeve, B. Franzel, R. S. Bon, W. Blankenfeldt, R. S. Goody, H. Waldmann, D. Wolters and K. Alexandrov, Analysis of the eukaryotic prenylome by isoprenoid affinity tagging, *Nat. Chem. Biol.*, 2009, **5**, 227-235.

29 P. J. Casey, P. A. Solski, C. J. Der and J. E. Buss, p21ras is modified by a farnesyl isoprenoid, *Proc. Natl. Acad. Sci.*, 1989, **86**, 8323-8327.

30 J. H. Jackson, C. G. Cochrane, J. R. Bourne, P. A. Solski, J. E. Buss and C. J. Der, Farnesol modification of Kirsten-ras exon 4B protein is essential for transformation, *Proc. Natl. Acad. Sci.*, 1990, **87**, 3042-3046.

31 Z. Liu, R. K. Meray, T. N. Grammatopoulos, R. A. Fredenburg, M. R. Cookson, Y. Liu, T. Logan and P. T. Lansbury, Jr., Membrane-associated farnesylated UCH-L1 promotes α-synuclein neurotoxicity and is a therapeutic target for Parkinson's disease, *Proc. Natl. Acad. Sci. U. S. A.*, 2009, **106**, 4635-4640.

32 G. P. Eckert, G. P. Hooff, D. M. Strandjord, U. Igbavboa, D. A. Volmer, W. E. Mueller and W. G. Wood, Regulation of the brain isoprenoids farnesyl- and geranylgeranylpyrophosphate is altered in male Alzheimer patients, *Neurobiol. Dis.*, 2009, **35**, 251-257.

33 G. P. Hooff, N. Patel, W. G. Wood, W. E. Mueller, G. P. Eckert and D. A. Volmer, A rapid and sensitive assay for determining human brain levels of farnesyl-(FPP) and geranylgeranylpyrophosphate (GGPP) and transferase activities using UHPLC-MS/MS, *Anal. Bioanal. Chem.*, 2010, **398**, 1801-1808.

34 G. P. Hooff, D. A. Volmer, W. G. Wood, W. E. Mueller and G. P. Eckert, Isoprenoid quantitation in human brain tissue: a validated HPLC-fluorescence detection method for endogenous farnesyl- (FPP) and geranylgeranylpyrophosphate (GGPP), *Anal. Bioanal. Chem.*, 2008, **392**, 673-680.

35 R. A. Mans, L. L. McMahon and L. Li, Simvastatin-mediated enhancement of long-term potentiation is driven by farnesyl-pyrophosphate depletion and inhibition of farnesylation, *Neuroscience*, 2012, **202**, 1-9.

36 M. Schlitzer, R. Ortmann and M. Altenkämper, CaaX-Protein Prenyltransferase Inhibitors. In *Drug Design of Zinc-Enzyme Inhibitors*, John Wiley & Sons, Inc.: 2009; pp 813-857.

37 M. Schlitzer, Structure based design of benzophenone-based non-thiol farnesyltransferase inhibitors, *Curr. Pharm. Des.*, 2002, **8**, 1713-1722.

38 C. E. McKenna, B. A. Kashemirov, K. M. Blazewska, I. Mallard-Favier, C. A. Stewart, J. Rojas, M. W. Lundy, F. H. Ebetino, R. A. Baron, J. E. Dunford, M. L. Kirsten, M. C. Seabra, J. L. Bala, M. S. Marma, M. J. Rogers and F. P. Coxon, Synthesis, Chiral High Performance Liquid Chromatographic Resolution and Enantiospecific Activity of a Potent New

Geranylgeranyl Transferase Inhibitor, 2-Hydroxy-3-imidazo[1,2-a]pyridin-3-yl-2-phosphonopropionic Acid, *J. Med. Chem.*, 2010, **53**, 3454-3464.

39 Z. Guo, Y.-W. Wu, K.-T. Tan, R. S. Bon, E. Guiu-Rozas, C. Delon, U. T. Nguyen, S. Wetzel, S. Arndt, R. S. Goody, W. Blankenfeldt, K. Alexandrov and H. Waldmann, Development of selective RabGGTase inhibitors and crystal structure of a RabGGTase-inhibitor complex, *Angew. Chem. Int. Ed.*, 2008, **47**, 3747-3750.

40 N. E. Kohl, F. R. Wilson, S. D. Mosser, E. Giuliani, S. J. DeSolms, M. W. Conner, N. J. Anthony, W. J. Holtz, R. P. Gomez and a. et, Protein farnesyltransferase inhibitors block the growth of ras-dependent tumors in nude mice, *Proc. Natl. Acad. Sci.* , 1994, **91**, 9141-5.

41 E. C. Lerner, Y. Qian, A. D. Hamilton and S. M. Sebti, Disruption of oncogenic K-Ras4B processing and signaling by a potent geranylgeranyltransferase I inhibitor, *J. Biol. Chem.*, 1995, **270**, 26770-3.

42 D. J. Augeri, S. J. O'Connor, D. Janowick, B. Szczepankiewicz, G. Sullivan, J. Larsen, D. Kalvin, J. Cohen, E. Devine, H. Zhang, S. Cherian, B. Saeed, S.-C. Ng and S. Rosenberg, Potent and Selective Non-Cysteine-Containing Inhibitors of Protein Farnesyltransferase, *J. Med. Chem.*, 1998, **41**, 4288-4300.

43 M. L. Curtin, A. S. Florjancic, J. Cohen, W.-Z. Gu, D. J. Frost, S. W. Muchmore and H. L. Sham, Novel and selective imidazole-containing biphenyl inhibitors of protein farnesyltransferase, *Bioorg. Med. Chem. Lett.*, 2003, **13**, 1367-1371.

44 C. J. Dinsmore and I. M. Bell, Inhibitors of farnesyltransferase and geranylgeranyltransferase-I for antitumor therapy: substrate-based design, conformational constraint and biological activity., *Curr. Top. Med. Chem.*, 2003, **3**, 1075-1093.

45 J. Sun, M. A. Blaskovich, D. Knowles, Y. Qian, J. Ohkanda, R. D. Bailey, A. D. Hamilton and S. M. Sebti, Antitumor Efficacy of a Novel Class of Non-thiol-containing Peptidomimetic Inhibitors of Farnesyltransferase and Geranylgeranyltransferase I, *Cancer Res.*, 1999, **59**, 4919-4926.

46 H. Peng, D. Carrico, V. Thai, M. Blaskovich, C. Bucher, E. E. Pusateri, S. M. Sebti and A. D. Hamilton, Synthesis and evaluation of potent, highly-selective, 3-aryl-piperazinone inhibitors of protein geranylgeranyltransferase-I, *Org. Biomol. Chem.*, 2006, **4**, 1768-1784.

47 M. Watanabe, H. D. G. Fiji, L. Guo, L. Chan, S. S. Kinderman, D. J. Slamon, O. Kwon and F. Tamanoi, Inhibitors of Protein Geranylgeranyltransferase I and Rab Geranylgeranyltransferase Identified from a Library of Allenoate-derived Compounds, *J. Biol. Chem.*, 2008, **283**, 9571-9579.

48 K. W. Cheng, J. P. Lahad, W.-l. Kuo, A. Lapuk, K. Yamada, N. Auersperg, J. Liu, K. Smith-McCune, K. H. Lu, D. Fishman, J. W. Gray and G. B. Mills,

The RAB25 small GTPase determines aggressiveness of ovarian and breast cancers, *Nat. Med.*, 2004, **10**, 1251-1256.

49 W.-W. Dong, Q. Mou, J. Chen, J.-T. Cui, W.-M. Li and W.-H. Xiao, Differential expression of Rab27A/B correlates with clinical outcome in hepatocellular carcinoma, *World J. Gastroenterol.*, 2012, **18**, 1806-1813.

50 K. Croizet-Berger, C. Daumerie, M. Couvreur, P. J. Courtoy and M.-F. van den Hove, The endocytic catalysts, Rab5a and Rab7, are tandem regulators of thyroid hormone production, *Proc. Natl. Acad. Sci.*, 2002, **99**, 8277-8282.

51 G. A. Rodan and A. A. Reszka, Bisphosphonate mechanism of action, *Curr. Mol. Med.*, 2002, **2**, 571-577.

52 A. A. Reszka and G. A. Rodan, Bisphosphonate mechanism of action, *Curr. Rheumatol. Rep.*, 2003, **5**, 65-74.

53 A. A. Reszka and G. A. Rodan, Nitrogen-containing bisphosphonate mechanism of action, *Mini-Rev. Med. Chem.*, 2004, **4**, 711-719.

54 F. P. Coxon, F. H. Ebetino, E. H. Mules, M. C. Seabra, C. E. McKenna and M. J. Rogers, Phosphonocarboxylate inhibitors of Rab geranylgeranyl transferase disrupt the prenylation and membrane localization of Rab proteins in osteoclasts in vitro and in vivo, *Bone*, 2005, **37**, 349-358.

55 F. P. Coxon, K. Thompson and M. J. Rogers, Recent advances in understanding the mechanism of action of bisphosphonates, *Curr. Opin. Pharmacol.*, 2006, **6**, 307-312.

56 M. S. Marma, Z. Xia, C. Stewart, F. Coxon, J. E. Dunford, R. Baron, B. A. Kashemirov, F. H. Ebetino, J. T. Triffitt, R. G. G. Russell and C. E. McKenna, Synthesis and Biological Evaluation of α-Halogenated Bisphosphonate and Phosphonocarboxylate Analogues of Risedronate, *J. Med. Chem.*, 2007, **50**, 5967-5975.

57 R. A. Baron, R. Tavare, A. C. Figueiredo, K. M. Blazewska, B. A. Kashemirov, C. E. McKenna, F. H. Ebetino, A. Taylor, M. J. Rogers, F. P. Coxon and M. C. Seabra, Phosphonocarboxylates Inhibit the Second Geranylgeranyl Addition by Rab Geranylgeranyl Transferase, *J. Biol. Chem.*, 2009, **284**, 6861-6868.

58 R. S. Bon, Z. Guo, E. A. Stigter, S. Wetzel, S. Menninger, A. Wolf, A. Choidas, K. Alexandrov, W. Blankenfeldt, R. S. Goody and H. Waldmann, Structure-Guided Development of Selective RabGGTase Inhibitors, *Angew. Chem. Int. Ed.*, 2011, **50**, 4957-4961.

59 W. R. Schafer, R. Kim, R. Sterne, J. Thorner, S. H. Kim and J. Rine, Genetic and pharmacological suppression of oncogenic mutations in ras genes of yeast and humans, *Science*, 1989, **245**, 379-85.

60 J. L. Bos, ras Oncogenes in Human Cancer: A Review, *Cancer Res.*, 1989, **49**, 4682-4689.

61 Y. Reiss, J. L. Goldstein, M. C. Seabra, P. J. Casey and M. S. Brown, Inhibition of purified p21ras farnesyl:protein transferase by Cys-AAX tetrapeptides, *Cell*, 1990, **62**, 81-88.

62 E. C. Lerner, T.-T. Zhang, D. B. Knowles, Y. Qian, A. D. Hamilton and S. M. Sebti, Inhibition of the prenylation of K-Ras, but not H- or N-Ras, is highly resistant to CAAX peptidomimetics and requires both a farnesyltransferase and a geranylgeranyltransferase I inhibitor in human tumor cell lines, *Oncogene*, 1997, **15**, 1283-1288.

63 C. A. Rowell, J. J. Kowalczyk, M. D. Lewis and A. M. Garcia, Direct Demonstration of Geranylgeranylation and Farnesylation of Ki-Ras in Vivo, *J. Biol. Chem.*, 1997, **272**, 14093-14097.

64 J. Sun, Y. Qian, A. D. Hamilton and S. M. Sebti, Both farnesyltransferase and geranylgeranyltransferase I inhibitors are required for inhibition of oncogenic K-Ras prenylation but each alone is sufficient to suppress human tumor growth in nude mouse xenografts, *Oncogene*, 1998, **16**, 1467-1473.

65 D. B. Whyte, P. Kirschmeier, T. N. Hockenberry, I. Nunez-Oliva, L. James, J. J. Catino, W. R. Bishop and J.-K. Pai, K- and N-Ras Are Geranylgeranylated in Cells Treated with Farnesyl Protein Transferase Inhibitors, *J. Biol. Chem.*, 1997, **272**, 14459-14464.

66 N. E. Kohl, C. A. Omer, M. W. Conner, N. J. Anthony, J. P. Davide, S. J. deSolms, E. A. Giuliani, R. P. Gomez, S. L. Graham and a. et, Inhibition of farnesyltransferase induces regression of mammary and salivary carcinomas in ras transgenic mice, *Nat. Med.*, 1995, **1**, 792-7.

67 D. W. End, G. Smets, A. V. Todd, T. L. Applegate, C. J. Fuery, P. Angibaud, M. Venet, G. Sanz, H. Poignet, S. Skrzat, A. Devine, W. Wouters and C. Bowden, Characterization of the antitumor effects of the selective farnesyl protein transferase inhibitor R115777 in vivo and in vitro, *Cancer Res.*, 2001, **61**, 131-137.

68 W. R. Bishop, R. Bond, J. Petrin, L. Wang, R. Patton, R. Doll, G. Njoroge, J. Catino, J. Schwartz and a. et, Novel tricyclic inhibitors of farnesyl protein transferase. Biochemical characterization and inhibition of Ras modification in transfected Cos cells, *J. Biol. Chem.*, 1995, **270**, 30611-18.

69 C. A. Buser, C. J. Dinsmore, C. Fernandes, I. Greenberg, K. Hamilton, S. D. Mosser, E. S. Walsh, T. M. Williams and K. S. Koblan, High-performance liquid chromatography/mass spectrometry characterization of Ki4B-Ras in PSN-1 cells treated with the prenyltransferase inhibitor L-778,123, *Anal. Biochem.*, 2001, **290**, 126-137.

70 A. T. Baines, D. Xu and C. J. Der, Inhibition of Ras for cancer treatment: the search continues, *Future Med. Chem.*, 2011, **3**, 1787-1808.

71 Clinical trials using farnesyltransferase inhibitors. www.clinicaltrials.gov (accessed July 2012).

72 S. Reddy and L. Comai, Lamin A, farnesylation and aging, *Exp. Cell Res.*, 2012, **318**, 1-7.
73 R. C. M. Hennekam, Hutchinson–Gilford progeria syndrome: Review of the phenotype, *Am. J. Med. Genet. A*, 2006, **140A**, 2603-2624.
74 S.-G. A. De, R. Bernard, P. Cau, C. Navarro, J. Amiel, I. Boccaccio, S. Lyonnet, C. L. Stewart, A. Munnich, M. M. Le and N. Levy, Lamin A truncation in Hutchinson-Gilford progeria, *Science*, 2003, **300**, 2055.
75 M. Eriksson, W. T. Brown, L. B. Gordon, M. W. Glynn, J. Singer, L. Scott, M. R. Erdos, C. M. Robbins, T. Y. Moses, P. Berglund, A. Dutra, E. Pak, S. Durkin, A. B. Csoka, M. Boehnke, T. W. Glover and F. S. Collins, Recurrent de novo point mutations in lamin A cause Hutchinson-Gilford progeria syndrome, *Nature*, 2003, **423**, 293-298.
76 H. J. Worman, Prelamin A prenylation and the treatment of progeria, *J. Lipid Res.*, 2010, **51**, 223-225.
77 W. R. Bishop, R. Doll and P. Kirschmeier, *Farnesyl transferase inhibitors: from targeted cancer therapeutic to a potential treatment for progeria*. Enzymes: 2011; Vol. 29, p 275-303.
78 H. J. Worman, L. G. Fong, A. Muchir and S. G. Young, Laminopathies and the long strange trip from basic cell biology to therapy, *J. Clin. Invest.*, 2009, **119**, 1825-1836.
79 R. D. Goldman, D. K. Shumaker, M. R. Erdos, M. Eriksson, A. E. Goldman, L. B. Gordon, Y. Gruenbaum, S. Khuon, M. Mendez, R. Varga and F. S. Collins, Accumulation of mutant lamin A causes progressive changes in nuclear architecture in Hutchinson-Gilford progeria syndrome, *Proc. Natl. Acad. Sci.* , 2004, **101**, 8963-8968.
80 L. G. Fong, D. Frost, M. Meta, X. Qiao, S. H. Yang, C. Coffinier and S. G. Young, A Protein Farnesyltransferase Inhibitor Ameliorates Disease in a Mouse Model of Progeria, *Science*, 2006, **311**, 1621-1623.
81 S. H. Yang, M. O. Bergo, J. I. Toth, X. Qiao, Y. Hu, S. Sandoval, M. Meta, P. Bendale, M. H. Gelb, S. G. Young and L. G. Fong, Blocking protein farnesyltransferase improves nuclear blebbing in mouse fibroblasts with a targeted Hutchinson-Gilford progeria syndrome mutation, *Proc. Natl. Acad. Sci.* , 2005, **102**, 10291-10296.
82 S. H. Yang, M. Meta, X. Qiao, D. Frost, J. Bauch, C. Coffinier, S. Majumdar, M. O. Bergo, S. G. Young and L. G. Fong, A farnesyltransferase inhibitor improves disease phenotypes in mice with a Hutchinson-Gilford progeria syndrome mutation, *J. Clin. Invest.*, 2006, **116**, 2115-2121.
83 S. H. Yang, X. Qiao, L. G. Fong and S. G. Young, Treatment with a farnesyltransferase inhibitor improves survival in mice with a Hutchinson-Gilford progeria syndrome mutation, *Biochim. Biophys. Acta*, 2008, **1781**, 36-39.

84 S. H. Yang, S. Y. Chang, D. A. Andres, H. P. Spielmann, S. G. Young and L. G. Fong, Assessing the efficacy of protein farnesyltransferase inhibitors in mouse models of progeria, *J. Lipid Res.*, 2010, **51**, 400-405.

85 I. Varela, S. Pereira, A. P. Ugalde, C. L. Navarro, M. F. Suarez, P. Cau, J. Cadinanos, F. G. Osorio, N. Foray, J. Cobo, C. F. de, N. Levy, J. M. P. Freije and C. Lopez-Otin, Combined treatment with statins and aminobisphosphonates extends longevity in a mouse model of human premature aging, *Nat. Med.*, 2008, **14**, 767-772.

86 M. Gerhard-Herman, L. B. Smoot, N. Wake, M. W. Kieran, M. E. Kleinman, D. T. Miller, A. Schwartzman, A. Giobbie-Hurder, D. Neuberg and L. B. Gordon, Mechanisms of Premature Vascular Aging in Children With Hutchinson-Gilford Progeria Syndrome, *Hypertension*, 2012, **59**, 92-97.

87 M. A. Merideth, L. B. Gordon, S. Clauss, V. Sachdev, A. C. M. Smith, M. B. Perry, C. C. Brewer, C. Zalewski, H. J. Kim, B. Solomon, B. P. Brooks, L. H. Gerber, M. L. Turner, D. L. Domingo, T. C. Hart, J. Graf, J. C. Reynolds, A. Gropman, J. A. Yanovski, M. Gerhard-Herman, F. S. Collins, E. G. Nabel, R. O. Cannon, III, W. A. Gahl and W. J. Introne, Phenotype and course of Hutchinson-Gilford progeria syndrome, *N. Engl. J. Med.*, 2008, **358**, 592-604.

88 Phase II Trial of Lonafarnib (a Farnesyltransferase Inhibitor) for Progeria. www.clinicaltrials.gov (accessed July 2012).

89 Study of Zoledronic Acid, Pravastatin, and Lonafarnib for Patients With Progeria. www.clinicaltrials.gov (accessed July 2012).

90 V. M. Zhang, M. Chavchich and N. C. Waters, Targeting protein kinases in the malaria parasite: update of an antimalarial drug target, *Curr. Top. Med. Chem.*, 2012, **12**, 456-472.

91 J. M. Kraus, H. B. Tatipaka, S. A. McGuffin, N. K. Chennamaneni, M. Karimi, J. Arif, C. L. M. J. Verlinde, F. S. Buckner and M. H. Gelb, Second Generation Analogues of the Cancer Drug Clinical Candidate Tipifarnib for Anti-Chagas Disease Drug Discovery, *J. Med. Chem.*, 2010, **53**, 3887-3898.

92 F. S. Buckner, R. T. Eastman, J. L. Nepomuceno-Silva, E. C. Speelmon, P. J. Myler, V. W. C. Van and K. Yokoyama, Cloning, heterologous expression, and substrate specificities of protein farnesyltransferases from Trypanosoma cruzi and Leishmania major, *Mol. Biochem. Parasitol.*, 2002, **122**, 181-188.

93 H. Field, I. Blench, S. Croft and M. C. Field, Characterisation of protein isoprenylation in procyclic form Trypanosoma brucei, *Mol Biochem Parasitol*, 1996, **82**, 67-80.

94 M. Ibrahim, N. Azzouz, P. Gerold and R. T. Schwarz, Identification and characterisation of Toxoplasma gondii protein farnesyltransferase, *Int. J. Parasitol.*, 2001, **31**, 1489-1497.

95 M. Kumagai, A. Makioka, T. Takeuchi and T. Nozaki, Molecular Cloning and Characterization of a Protein Farnesyltransferase from the Enteric Protozoan Parasite Entamoeba histolytica, *J. Biol. Chem.*, 2004, **279**, 2316-2323.

96 H. D. Lujan, M. R. Mowatt, G.-Z. Chen and T. E. Nash, Isoprenylation of proteins in the protozoan Giardia lamblia, *Mol. Biochem. Parasitol.*, 1995, **72**, 121-7.

97 D. Carrico, J. Ohkanda, H. Kendrick, K. Yokoyama, M. A. Blaskovich, C. J. Bucher, F. S. Buckner, V. W. C. Van, D. Chakrabarti, S. L. Croft, M. H. Gelb, S. M. Sebti and A. D. Hamilton, In vitro and in vivo antimalarial activity of peptidomimetic protein farnesyltransferase inhibitors with improved membrane permeability, *Bioorg. Med. Chem.*, 2004, **12**, 6517-6526.

98 L. Nallan, K. D. Bauer, P. Bendale, K. Rivas, K. Yokoyama, C. P. Horney, P. P. Rao, D. Floyd, L. J. Lombardo, D. K. Williams, A. Hamilton, S. Sebti, W. T. Windsor, P. C. Weber, F. S. Buckner, D. Chakrabarti, M. H. Gelb and V. W. C. Van, Protein Farnesyltransferase Inhibitors Exhibit Potent Antimalarial Activity, *J. Med. Chem.*, 2005, **48**, 3704-3713.

99 J. Wiesner, K. Kettler, J. Sakowski, R. Ortmann, A. M. Katzin, E. A. Kimura, K. Silber, G. Klebe, H. Jomaa and M. Schlitzer, Farnesyltransferase inhibitors inhibit the growth of malaria parasites in vitro and in vivo, *Angew. Chem. Int. Ed.*, 2003, **43**, 251-254.

100 K. Yokoyama, P. Trobridge, F. S. Buckner, J. Scholten, K. D. Stuart, V. W. C. Van and M. H. Gelb, The effects of protein farnesyltransferase inhibitors on trypanosomatids: inhibition of protein farnesylation and cell growth, *Mol. Biochem. Parasitol.*, 1998, **94**, 87-97.

101 R. T. Eastman, F. S. Buckner, K. Yokoyama, M. H. Gelb and V. W. C. Van, Fighting parasitic disease by blocking protein farnesylation, *J. Lipid Res.*, 2006, **47**, 233-240.

102 V. J. Bulbule, K. Rivas, C. L. M. J. Verlinde, V. W. C. Van and M. H. Gelb, 2-Oxotetrahydroquinoline-Based Antimalarials with High Potency and Metabolic Stability, *J. Med. Chem.*, 2008, **51**, 384-387.

103 S. Olepu, P. K. Suryadevara, K. Rivas, K. Yokoyama, C. L. M. J. Verlinde, D. Chakrabarti, V. W. C. Van and M. H. Gelb, 2-Oxo-tetrahydro-1,8-naphthyridines as selective inhibitors of malarial protein farnesyltransferase and as anti-malarials, *Bioorg. Med. Chem. Lett.*, 2008, **18**, 494-497.

104 S. Fletcher, C. G. Cummings, K. Rivas, W. P. Katt, C. Horney, F. S. Buckner, D. Chakrabarti, S. M. Sebti, M. H. Gelb, V. W. C. Van and A. D. Hamilton, Potent, Plasmodium-Selective Farnesyltransferase Inhibitors That Arrest the Growth of Malaria Parasites: Structure-Activity Relationships of Ethylenediamine-Analogue Scaffolds and Homology Model Validation, *J. Med. Chem.*, 2008, **51**, 5176-5197.

105 S. Duez, L. Coudray, E. Mouray, P. Grellier and J. Dubois, Towards the synthesis of bisubstrate inhibitors of protein farnesyltransferase: Synthesis and biological evaluation of new farnesylpyrophosphate analogues, *Bioorg. Med. Chem.*, 2010, **18**, 543-556.
106 E. Wong, V. Okhonin, M. V. Berezovski, T. Nozaki, H. Waldmann, K. Alexandrov and S. N. Krylov, "Inject-Mix-React-Separate-and-Quantitate" (IMReSQ) Method for Screening Enzyme Inhibitors, *J. Am. Chem. Soc.*, 2008, **130**, 11862-11863.
107 G. Gupta, H. Qin and J. Song, Intrinsically unstructured domain 3 of hepatitis C virus NS5A forms a "fuzzy complex" with VAPB-MSP domain which carries ALS-causing mutations, *PLoS One*, 2012, **7**, e39261.
108 V. Lohmann, F. Korner, J.-O. Koch, U. Herian, L. Theilmann and R. Bartenschlager, Replication of Subgenomic Hepatitis C Virus RNAs in a Hepatoma Cell Line, *Science*, 1999, **285**, 110-113.
109 J. Ye, C. Wang, R. Sumpter, M. S. Brown, J. L. Goldstein and M. Gale, Disruption of hepatitis C virus RNA replication through inhibition of host protein geranylgeranylation, *Proc. Natl. Acad. Sci.*, 2003, **100**, 15865-15870.
110 A. Ciancio and M. Rizzetto, Hepatitis: PEG-IFN for the treatment of hepatitis D, *Nat. Rev. Gastroenterol. Hepatol.*, 2011, **8**, 304-306.
111 J. C. Otto and P. J. Casey, The Hepatitis Delta Virus Large Antigen Is Farnesylated Both in Vitro and in Animal Cells, *J. Biol. Chem.*, 1996, **271**, 4569-4572.
112 B. B. Bordier, P. L. Marion, K. Ohashi, M. A. Kay, H. B. Greenberg, J. L. Casey and J. S. Glenn, A Prenylation Inhibitor Prevents Production of Infectious Hepatitis Delta Virus Particles, *J. Virol.*, 2002, **76**, 10465-10472.
113 J. S. Glenn, J. C. Marsters, Jr. and H. B. Greenberg, Use of a prenylation inhibitor as a novel antiviral agent, *J. Virol.*, 1998, **72**, 9303-9306.
114 C. E. Walters, G. Pryce, D. J. R. Hankey, S. M. Sebti, A. D. Hamilton, D. Baker, J. Greenwood and P. Adamson, Inhibition of Rho GTPases with Protein Prenyltransferase Inhibitors Prevents Leukocyte Recruitment to the Central Nervous System and Attenuates Clinical Signs of Disease in an Animal Model of Multiple Sclerosis, *J. Immunol.*, 2002, **168**, 4087-4094.
115 F. P. Coxon, M. H. Helfrich, H. R. Van't, S. Sebti, S. H. Ralston, A. Hamilton and M. J. Rogers, Protein geranylgeranylation is required for osteoclast formation, function, and survival: Inhibition by bisphosphonates and GGTI-298, *J. Bone Miner. Res.*, 2000, **15**, 1467-1476.
116 M. A. Hast, C. B. Nichols, S. M. Armstrong, S. M. Kelly, H. W. Hellinga, J. A. Alspaugh and L. S. Beese, Structures of Cryptococcus neoformans Protein Farnesyltransferase Reveal Strategies for Developing Inhibitors That Target Fungal Pathogens, *J. Biol. Chem.*, 2011, **286**, 35149-35162.

117 M. A. Vallim, L. Fernandes and J. A. Alspaugh, The RAM1 gene encoding a protein-farnesyltransferase α-subunit homologue is essential in Cryptococcus neoformans, *Microbiology*, 2004, **150**, 1925-1935.
118 L. M. Work, A. R. McPhaden, N. J. Pyne, S. Pyne, R. M. Wadsworth and C. L. Wainwright, Short-Term Local Delivery of an Inhibitor of Ras Farnesyltransferase Prevents Neointima Formation In Vivo After Porcine Coronary Balloon Angioplasty, *Circulation*, 2001, **104**, 1538-1543.
119 G. C. Prendergast, Actin' up: RhoB in cancer and apoptosis, *Nat. Rev. Cancer*, 2001, **1**, 162-168.
120 S. M. Sebti and C. J. Der, Searching for the elusive targets of farnesyltransferase inhibitors, *Nat Rev Cancer*, 2003, **3**, 945-951.
121 S. Maurer-Stroh, M. Koranda, W. Benetka, G. Schneider, F. L. Sirota and F. Eisenhaber, Towards Complete Sets of Farnesylated and Geranylgeranylated Proteins, *PLoS Comput Biol*, 2007, **3**, e66.
122 S. Ø. M. Sebti, Protein farnesylation: Implications for normal physiology, malignant transformation, and cancer therapy, *Cancer Cell*, 2005, **7**, 297-300.
123 A. Hosokawa, J. W. Wollack, Z. Zhang, L. Chen, G. Barany and M. D. Distefano, Evaluation of an alkyne-containing analogue of farnesyl diphosphate as a dual substrate for protein-prenyltransferases, *Int. J. Pept. Res. Ther.*, 2007, **13**, 345-354.
124 B. P. Duckworth, Z. Zhang, A. Hosokawa and M. D. Distefano, Selective labeling of proteins by using protein farnesyltransferase, *Chembiochem*, 2007, **8**, 98-105.
125 F. O. Onono, M. A. Morgan, H. P. Spielmann, D. A. Andres, T. Subramanian, A. Ganser and C. W. M. Reuter, A Tagging-via-substrate Approach to Detect the Farnesylated Proteome Using Two-dimensional Electrophoresis Coupled with Western Blotting, *Mol. Cell. Proteomics*, 2010, **9**, 742-751.
126 J. D. Andersen, K. L. M. Boylan, F. S. Xue, L. B. Anderson, B. A. Witthuhn, T. W. Markowski, L. Higgins and A. P. N. Skubitz, Identification of candidate biomarkers in ovarian cancer serum by depletion of highly abundant proteins and differential in-gel electrophoresis, *Electrophoresis*, 2010, **31**, 599-610.
127 A. Shevchenko, M. Wilm, O. Vorm and M. Mann, Mass Spectrometric Sequencing of Proteins from Silver-Stained Polyacrylamide Gels, *Anal. Chem.*, 1996, **68**, 850-858.
128 A. Keller, A. I. Nesvizhskii, E. Kolker and R. Aebersold, Empirical Statistical Model To Estimate the Accuracy of Peptide Identifications Made by MS/MS and Database Search, *Anal. Chem.*, 2002, **74**, 5383-5392.
129 A. I. Nesvizhskii, A. Keller, E. Kolker and R. Aebersold, A Statistical Model for Identifying Proteins by Tandem Mass Spectrometry, *Anal. Chem.*, 2003, **75**, 4646-4658.

130 C. R. Bertozzi, A Decade of Bioorthogonal Chemistry, *Accounts Chem. Res.*, 2011, **44**, 651-653.
131 M. Boyce and C. R. Bertozzi, Bringing chemistry to life, *Nat. Meth.*, 2011, **8**, 638-642.
132 H. C. Hang and M. E. Linder, Exploring Protein Lipidation with Chemical Biology, *Chem. Rev.*, 2011, **111**, 6341-6358.
133 R. N. Hannoush and J. Sun, The chemical toolbox for monitoring protein fatty acylation and prenylation, *Nat. Chem. Biol.*, 2010, **6**, 498-506.
134 N. J. Agard, Chemical Approaches to Glycobiology. In *Chem. Glycobiol.*, 2008; Vol. 990, pp 251-271.
135 S. R. Hanson, T.-L. Hsu, E. Weerapana, K. Kishikawa, G. M. Simon, B. F. Cravatt and C.-H. Wong, Tailored Glycoproteomics and Glycan Site Mapping Using Saccharide-Selective Bioorthogonal Probes, *J. Am. Chem. Soc.*, 2007, **129**, 7266-7267.
136 C.-Y. Wu and C.-H. Wong, Chemistry and glycobiology, *Chem. Comm.*, 2011, **47**, 6201-6207.
137 M. A. Kostiuk, B. O. Keller and L. G. Berthiaume, Non-radioactive detection of palmitoylated mitochondrial proteins using an azido-palmitate analogue, *Methods Enzymol.*, 2009, **457**, 149-165.
138 B. R. Martin and B. F. Cravatt, Large-scale profiling of protein palmitoylation in mammalian cells, *Nat. Meth.*, 2009, **6**, 135-138.
139 J. S. Yount, G. Charron and H. C. Hang, Bioorthogonal proteomics of 15-hexadecynyloxyacetic acid chemical reporter reveals preferential targeting of fatty acid modified proteins and biosynthetic enzymes, *Bioorgan. Med. Chem.* , 2012, **20**, 650-654.
140 R. N. Hannoush, Profiling cellular myristoylation and palmitoylation using ω-alkynyl fatty acids, *Meth. Mol. Biol.*, 2012, **800**, 85-94.
141 R. N. Hannoush and N. Arenas-Ramirez, Imaging the Lipidome: ω-Alkynyl Fatty Acids for Detection and Cellular Visualization of Lipid-Modified Proteins, *ACS Chem. Biol.*, 2009, **4**, 581-587.
142 A. F. H. Berry, W. P. Heal, A. K. Tarafder, T. Tolmachova, R. A. Baron, M. C. Seabra and E. W. Tate, Rapid Multilabel Detection of Geranylgeranylated Proteins by Using Bioorthogonal Ligation Chemistry, *ChemBioChem*, 2010, **11**, 771-773.
143 G. Charron, L. K. Tsou, W. Maguire, J. S. Yount and H. C. Hang, Alkynyl-farnesol reporters for detection of protein S-prenylation in cells, *Mol. Biosys.*, 2011, **7**, 67-73.
144 A. J. DeGraw, C. Palsuledesai, J. D. Ochocki, J. K. Dozier, S. Lenevich, M. Rashidian and M. D. Distefano, Evaluation of alkyne-modified isoprenoids as chemical reporters of protein prenylation, *Chem. Biol. Drug Des.*, 2010, **76**, 460-471.

145 P. V. Chang, J. A. Prescher, E. M. Sletten, J. M. Baskin, I. A. Miller, N. J. Agard, A. Lo and C. R. Bertozzi, Copper-free click chemistry in living animals, *Proc. Natl. Acad. Sci.*, 2010, **107**, 1821-1826.
146 K. W. Dehnert, J. M. Baskin, S. T. Laughlin, B. J. Beahm, N. N. Naidu, S. L. Amacher and C. R. Bertozzi, Imaging the Sialome during Zebrafish Development with Copper-Free Click Chemistry, *ChemBioChem*, 2012, n/a-n/a.
147 K. W. Dehnert, B. J. Beahm, T. T. Huynh, J. M. Baskin, S. T. Laughlin, W. Wang, P. Wu, S. L. Amacher and C. R. Bertozzi, Metabolic Labeling of Fucosylated Glycans in Developing Zebrafish, *ACS Chem. Biol.*, 2011, **6**, 547-552.
148 E. M. Sletten and C. R. Bertozzi, From Mechanism to Mouse: A Tale of Two Bioorthogonal Reactions, *Accounts Chem. Res.*, 2011, **44**, 666-676.
149 W. Benetka, M. Koranda, S. Maurer-Stroh, F. Pittner and F. Eisenhaber, Farnesylation or geranylgeranylation? Efficient assays for testing protein prenylation in vitro and in vivo, *BMC Biochemistry*, 2006, **7**, 6.
150 N. Berndt and S. M. Sebti, Measurement of protein farnesylation and geranylgeranylation in vitro, in cultured cells and in biopsies, and the effects of prenyl transferase inhibitors, *Nat. Protocols*, 2011, **6**, 1775-1791.
151 L. N. Chan, C. Hart, L. Guo, T. Nyberg, B. S. J. Davies, L. G. Fong, S. G. Young, B. J. Agnew and F. Tamanoi, A novel approach to tag and identify geranylgeranylated proteins, *Electrophoresis*, 2009, **30**, 3598-3606.
152 V. V. Rostovtsev, L. G. Green, V. V. Fokin and K. B. Sharpless, A Stepwise Huisgen Cycloaddition Process: Copper(I)-Catalyzed Regioselective "Ligation" of Azides and Terminal Alkynes, *Angew. Chem. Int. Ed.*, 2002, **41**, 2596-2599.
153 Y. Kho, S. C. Kim, C. Jiang, D. Barma, S. W. Kwon, J. Cheng, J. Jaunbergs, C. Weinbaum, F. Tamanoi, J. Falck and Y. Zhao, A tagging-via-substrate technology for detection and proteomics of farnesylated proteins, *Proc. Natl. Acad. Sci. U. S. A.*, 2004, **101**, 12479-12484.
154 J. D. Ochocki, D. G. Mullen, E. V. Wattenberg and M. D. Distefano, Evaluation of a cell penetrating prenylated peptide lacking an intrinsic fluorophore via in situ click reaction, *Bioorg. Med. Chem. Lett.*, 2011, **21**, 4998-5001.
155 L. P. Wright and M. R. Philips, Thematic review series: lipid posttranslational modifications. CAAX modification and membrane targeting of Ras, *J. Lipid Res.*, 2006, **47**, 883-91.
156 M. Hara, K. Akasaka, S. Akinaga, M. Okabe, H. Nakano, R. Gomez, D. Wood, M. Uh and F. Tamanoi, Identification of Ras farnesyltransferase inhibitors by microbial screening, *Proc. Natl. Acad. Sci.*, 1993, **90**, 2281-5.
157 J. B. Gibbs, D. L. Pompliano, S. D. Mosser, E. Rands, R. B. Lingham, S. B. Singh, E. M. Scolnick, N. E. Kohl and A. Oliff, Selective inhibition of

farnesyl-protein transferase blocks Ras processing in vivo, *J. Biol. Chem.*, 1993, **268**, 7617-20.

158 G. Juhasz, B. Erdi, M. Sass and T. P. Neufeld, Atg7-dependent autophagy promotes neuronal health, stress tolerance, and longevity but is dispensable for metamorphosis in Drosophila, *Gene. Dev.*, 2007, **21**, 3061-3066.

159 B. Levine and G. Kroemer, Autophagy in the Pathogenesis of Disease, *Cell*, 2008, **132**, 27-42.

160 N. Mizushima and B. Levine, Autophagy in mammalian development and differentiation, *Nat Cell Biol*, 2010, **12**, 823-830.

161 N. Raimundo and G. S. Shadel, A "radical" mitochondrial view of autophagy-related pathology, *Aging*, 2009, **1**, 354-356.

162 K. C. Walls, A. P. Ghosh, A. V. Franklin, B. J. Klocke, M. E. Ballestas, J. J. Shacka, J. Zhang and K. A. Roth, Lysosome dysfunction triggers Atg7-dependent neural apoptosis, *J. Biol. Chem.*, 2010.

163 G. P. Hooff, I. Peters, W. G. Wood, W. E. Muller and G. P. Eckert, Modulation of cholesterol, farnesylpyrophosphate, and geranylgeranylpyrophosphate in neuroblastoma SH-SY5Y-APP695 cells: impact on amyloid beta-protein production, *Mol. Neurobiol.*, 2010, **41**, 341-50.

164 S. L. Cole and R. Vassar, Isoprenoids and Alzheimer's disease: A complex relationship, *Neurobiol. Dis.*, 2006, **22**, 209-222.

165 S. Pedrini, T. L. Carter, G. Prendergast, S. Petanceska, M. E. Ehrlich and S. Gandy, Modulation of Statin-Activated Shedding of Alzheimer APP Ectodomain by ROCK, *PLoS Med*, 2005, **2**, e18.

166 A. C. R. G. Fonseca, R. Resende, C. R. Oliveira and C. M. F. Pereira, Cholesterol and statins in Alzheimer's disease: current controversies, *Exp. Neurol.*, 2010, **223**, 282-293.

167 M. O. W. Grimm, H. S. Grimm and T. Hartmann, Amyloid beta as a regulator of lipid homeostasis, *Trends Mol. Med.*, 2007, **13**, 337-344.

168 W. T. Hunt, P. B. Salins, C. M. Anderson and F. M. Amara, Neuroprotective role of statins in Alzheimer's disease: anti-apoptotic signaling, *Open Neurosci. J.*, 2010, **4**, 13-22.

169 M. M. Fernandez, F. J. Castro, d. L. H. S. Perez, L. A. Mandaluniz, M. M. Gordejuela and I. J. J. Zarranz, Risk factors for dementia in the epidemiological study of Munguialde County (Basque Country-Spain), *BMC Neurol*, 2008, **8**, 39.

170 M. A. Pappolla, T. K. Bryant-Thomas, D. Herbert, J. Pacheco, G. M. Fabra, M. Manjon, X. Girones, T. L. Henry, E. Matsubara, D. Zambon, B. Wolozin, M. Sano, F. F. Cruz-Sanchez, L. J. Thal, S. S. Petanceska and L. M. Refolo, Mild hypercholesterolemia is an early risk factor for the development of Alzheimer amyloid pathology, *Neurology*, 2003, **61**, 199-205.

171 M. A. Lindorfer, N. E. Sherman, K. A. Woodfork, J. E. Fletcher, D. F. Hunt and J. C. Garrison, G protein gamma subunits with altered prenylation sequences are properly modified when expressed in Sf9 cells, *J. Biol. Chem.* , 1996, **271**, 18582-18587.

172 J. W. Fenton, II, W. P. Jeske, J. L. Catalfamo, D. V. Brezniak, D. G. Moon and G. X. Shen, Statin drugs and dietary isoprenoids downregulate protein prenylation in signal transduction and are antithrombotic and prothrombolytic agents, *Biochemistry* 2002, **67**, 85-91.

173 P. Workman, *Farnesyltransferase Inhibitors in Cancer Therapy* Humana Press Inc.: 2001; p 1-20.

174 M.-O. Roy, R. Leventis and J. R. Silvius, Mutational and Biochemical Analysis of Plasma Membrane Targeting Mediated by the Farnesylated, Polybasic Carboxy Terminus of K-ras4B, *Biochemistry*, 2000, **39**, 8298-8307.

175 H. Waldmann, M. Schelhaas, E. Nagele, J. Kuhlmann, A. Wittinghofer, H. Schroeder and J. R. Silvius, Chemoenzymic synthesis of fluorescent N-Ras lipopeptides and their use in membrane localization studies in vivo, *Angew. Chem., Int. Ed. Engl.*, 1997, **36**, 2238-2241.

176 J. W. Wollack, N. A. Zeliadt, D. G. Mullen, G. Amundson, S. Geier, S. Falkum, E. V. Wattenberg, G. Barany and M. D. Distefano, Multifunctional Prenylated Peptides for Live Cell Analysis, *J. Am. Chem. Soc.*, 2009, **131**, 7293-7303.

177 L. A. Greene and A. S. Tischler, Establishment of a noradrenergic clonal line of rat adrenal pheochromocytoma cells which respond to nerve growth factor, *Proc. Natl. Acad. Sci.*, 1976, **73**, 2424-2428.

178 D. S. King, C. G. Fields and G. B. Fields, A cleavage method which minimizes side reactions following Fmoc solid phase peptide synthesis, *Int. J. Pept. Protein Res.* , 1990, **36**, 255-66.

179 C. B. Xue, J. M. Becker and F. Naider, Efficient regioselective isoprenylation of peptides in acidic aqueous solution using zinc acetate as catalyst, *Tetrahedron Lett.* , 1992, **33**, 1435-8.

180 S. L. Moores, M. D. Schaber, S. D. Mosser, E. Rands, M. B. O'Hara, V. M. Garsky, M. S. Marshall, D. L. Pompliano and J. B. Gibbs, Sequence dependence of protein isoprenylation, *J. Biol. Chem.*, 1991, **266**, 14603-10.

181 J. P. Richard, K. Melikov, E. Vives, C. Ramos, B. Verbeure, M. J. Gait, L. V. Chernomordik and B. Lebleu, Cell-penetrating peptides. A reevaluation of the mechanism of cellular uptake, *J Biol Chem*, 2003, **278**, 585-90.

182 J. W. Wollack, N. A. Zeliadt, J. D. Ochocki, D. G. Mullen, G. Barany, E. V. Wattenberg and M. D. Distefano, Investigation of the sequence and length dependence for cell-penetrating prenylated peptides, *Bioorg. Med. Chem. Lett.* , 2010, **20**, 161-163.

183 R. L. Levine, J. Moskovitz and E. R. Stadtman, Oxidation of methionine in proteins: roles in antioxidant defense and cellular regulation, *IUBMB Life*, 2000, **50**, 301-7.
184 W. Du, Z. Cui, Z. C. Tsui, Q. Chen and M. C. Willingham, In situ immunocytochemical detection of altered membrane composition induced by cell-cell contact in cultured mammalian cells, *Microsc Res Tech*, 2008, **71**, 749-59.
185 I. Massodi, G. L. Bidwell, 3rd and D. Raucher, Evaluation of cell penetrating peptides fused to elastin-like polypeptide for drug delivery, *J. Control Release*, 2005, **108**, 396-408.
186 E. J. Stewart, F. Aslund and J. Beckwith, Disulfide bond formation in the Escherichia coli cytoplasm: an in vivo role reversal for the thioredoxins, *EMBO J.*, 1998, **17**, 5543-50.
187 S. N. Arkhipov, M. Berezovski, J. Jitkova and S. N. Krylov, Chemical cytometry for monitoring metabolism of a Ras-mimicking substrate in single cells, *Cytometry, Part A* 2005, **63A**, 41-47.
188 M. Berezovski, W.-P. Li, C. D. Poulter and S. N. Krylov, Measuring the activity of farnesyltransferase by capillary electrophoresis with laser-induced fluorescence detection, *Electrophoresis* 2002, **23**, 3398-3403.
189 J. Jitkova, C. N. Carrigan, C. D. Poulter and S. N. Krylov, Monitoring the three enzymatic activities involved in posttranslational modifications of Ras proteins, *Anal. Chim. Acta* 2004, **521**, 1-7.
190 A. B. Meriin, J. A. Yaglom, V. L. Gabai, L. Zon, S. Ganiatsas, D. D. Mosser, L. Zon and M. Y. Sherman, Protein-damaging stresses activate c-Jun N-terminal kinase via inhibition of its dephosphorylation: a novel pathway controlled by HSP72, *Mol. Cell. Biol.* , 1999, **19**, 2547-55.
191 D. Mazia, G. Schatten and W. Sale, Adhesion of cells to surfaces coated with polylysine. Applications to electron microscopy, *J. Cell Biol.*, 1975, **66**, 198-200.
192 L. F. Yousif, K. M. Stewart, K. L. Horton and S. O. Kelley, Mitochondria-penetrating peptides: sequence effects and model cargo transport, *Chembiochem*, 2009, **10**, 2081-8.
193 J. Adler and I. Parmryd, Quantifying colocalization by correlation: the Pearson correlation coefficient is superior to the Mander's overlap coefficient, *Cytometry A*, 2010, **77**, 733-42.
194 K. Bracha-Drori, K. Shichrur, T. C. Lubetzky and S. Yalovsky, Functional analysis of Arabidopsis postprenylation CaaX processing enzymes and their function in subcellular protein targeting, *Plant Physiol.*, 2008, **148**, 119-131.
195 I. L. Medintz, T. Pons, J. B. Delehanty, K. Susumu, F. M. Brunel, P. E. Dawson and H. Mattoussi, Intracellular Delivery of Quantum Dot-Protein Cargos Mediated by Cell Penetrating Peptides, *Bioconjugate Chem.*, 2008, **19**, 1785-1795.

Appendix A. Cell Penetrating Prenylated Peptides to Study Protein Prenylation *in vivo*.

A.1 Introduction

In chapters 5 and 6 I discussed the use of cell penetrating prenylated peptides that could be used for *in vivo* analysis. This work served to lay the foundation for future studies by designing peptides and optimizing them for cellular uptake. Since these peptides were initially developed, we have been focused on applying them in cellular systems to study the enzymology and kinetics of the protein prenyltransferases.

Because the amount of peptide that gets inside of a cell and gets modified is very small (likely sub-micromolar), one needs an incredibly sensitive method for detecting such small amounts of peptide. One such method is to use capillary electrophoresis with laser induced fluorescence detection (CE-LIF). CE-LIF has been shown to be able to detect attomoles of material, uses small sample volumes (can be sub-microliter), and is a rapid analysis technique. In CE-LIF, a narrow capillary (typically 10-100 um in diameter), lined with silica, is used to separate species based on charge, as a current is applied from one end of the capillary to the other. With laser induced fluorescence detection, the species of interest are detected via fluorescence of an attached fluorophore. Because the species we want to separate largely have the same charge, but different hydrophobicity (i.e. separating a non-prenylated from a prenylated peptide), we

will use a modification of CE-LIF, termed micellar electrokinetic chromatography (MEKC). In MEKC, the buffer that is used in the capillary contains micelles, usually through the addition of detergents such as sodium dodecyl sulfate (SDS) above their respective critical micelle concentration (CMC). Hydrophobic species interact with the micelles and are retained in the capillary longer than species that are not hydrophobic and that do not interact with the micelles, thus changing the main property of separation to hydrophobicity, instead of charge.

A.2 Research Objectives

The goal of this research is to use the disulfide linked peptides **5a** and **5b** from chapter 5 (see Figure A.1 for an example) to study the enzymology of protein prenyltransferases *in vivo* using a combination of cell culture techniques and CE-LIF.

A.3 Results and Discussion

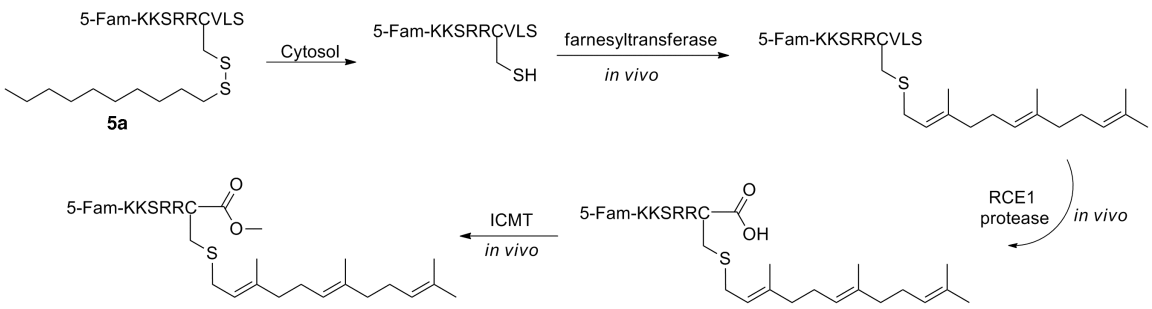

Figure A.1. Schematic representation of the fate of peptide 5a after being given to live cells. Once the peptide penetrates the cellular membrane, it enters the cytosol, which is a reducing environment, reducing the peptide disulfide to the free thiol. This peptide is a substrate for the prenyltransferase enzyme and should be converted by the cell to a prenylated form, which is later detected by CE-LIF.

A.3.1 Detection limit of CE-LIF

We have already shown that peptides **5a** and **5b** are able to freely penetrate cells (see chapter 5, figure 5.3), and with this information the next step is to see if we can detect low levels of these peptides using CE-LIF. The amount of peptide that is given to cells is generally in the low micromolar range, the amount that penetrates cells is much less than that, and that amount that actually gets modified by the cellular machinery is likely to be significantly lower, perhaps in the low nanomolar range. Thus, to see if MEKC CE-LIF is a viable technique, the detection limit for these peptides must first be determined. To answer this question, we first injected 5-carboxyfluorescein (5-Fam) at various concentrations into the capillary and monitored the separation using laser induced fluorescence (LIF) of the 5-Fam group, as this is the same fluorophore attached to our peptides (Figure A.1). The data demonstrate that the 5-Fam group is resolved well as a single peak with a t_R of approximately 8.5 minutes. In addition, the 5-Fam can be detected at 10 nM and could be detected lower, as the signal to noise ratio is still quite large. It is important to note that the inherent drawback of CE is that often there is considerable variation in the t_R of species over repeat injections. It's not uncommon to see variation of 5% or more between injections, and thus an internal standard is often used to correct this (although our initial work has not used internal standards as of yet).

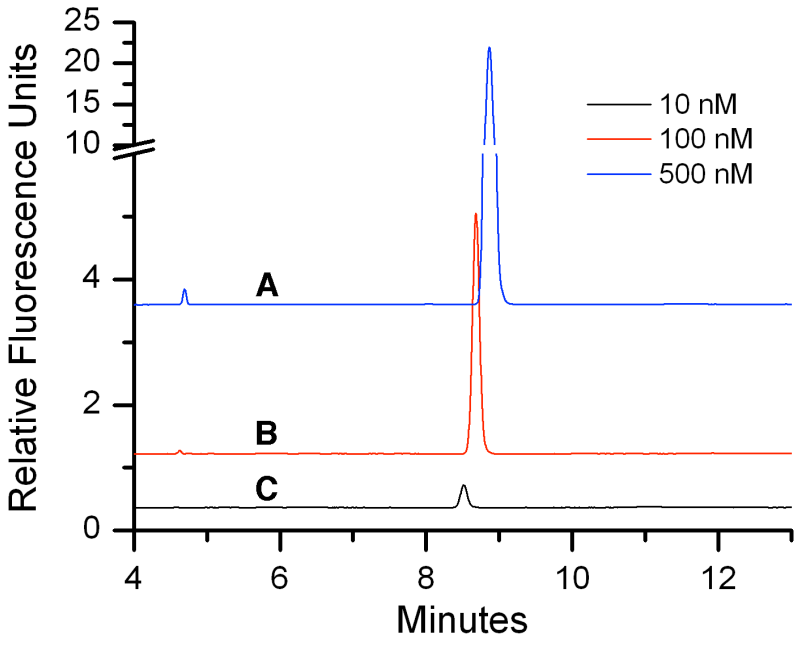

Figure A.2. MEKC CE-LIF chromatograms of 5-Fam injections to determine the limit of detection. In (A), 500 nM 5-Fam was injected, in (B), 100 nM was injected, and in (C) 10 nM was injected. This data demonstrates that species lower than 10 nM can be detected with this technique.

A.3.2 Incubating HeLa with Disulfide Linked Peptides

Having established that we can detect low levels of the fluorophore attached to our peptides, we chose to incubate the disulfide linked peptide **5b** with HeLa cells. The sequence of this peptide, 5-Fam-KKSRRC(S-decyl)VLS, has been shown to enter HeLa cells well and avoids the problems of methionine oxidation that could happen with peptide **5a** (CVIM CAAX box). Upon incubation of HeLa cells with **5b** at 1 μM for 2 hours, the cells were rinsed and placed back in the incubator for either 4 or 24 hours to let the peptide be processed by the cells. Following this incubation, the cells were rinsed and trypsinized for 15 minutes to remove any surface-bound peptide and then were lysed. The lysate was diluted 1 to 10 in CE run buffer, then injected into the capillary for separation (Figure A.2). In Figure A.2, chromatogram C, the peptide 5-Fam-KKSRRCVLS, the free thiol peptide, was injected by itself as a standard for comparison at a concentration of 2.5 nM. Chromatograms (A) and (B) in Figure A.2 are after the 2 h peptide incubation with HeLa cells; in (A), an additional 24 h incubation was used and in (B), a 4 h incubation was used. Firstly, the peak at approximately 3 minutes represents the free thiol peptide, and this peak can be detected in the HeLa lysates in (A) and (B), providing evidence that the disulfide linked peptide is reduced once it enters the cytosol of HeLa cells. Furthermore, a new peak at approximately 8 minutes appears and represents the farnesylated peptide, 5-Fam-KKSRRC(far)VLS. After a 4 h rest period in Figure A.2B, the peak is quite

small in area as only minimal farnesylation has occurred. After the 24 h rest (Figure A.2A), the peak grows in area as significantly more farnesylation has occurred (note the break in the scale of the y-axis). These data demonstrate that MEKC CE-LIF can be used to detect peptide processing after incubation with mammalian cells.

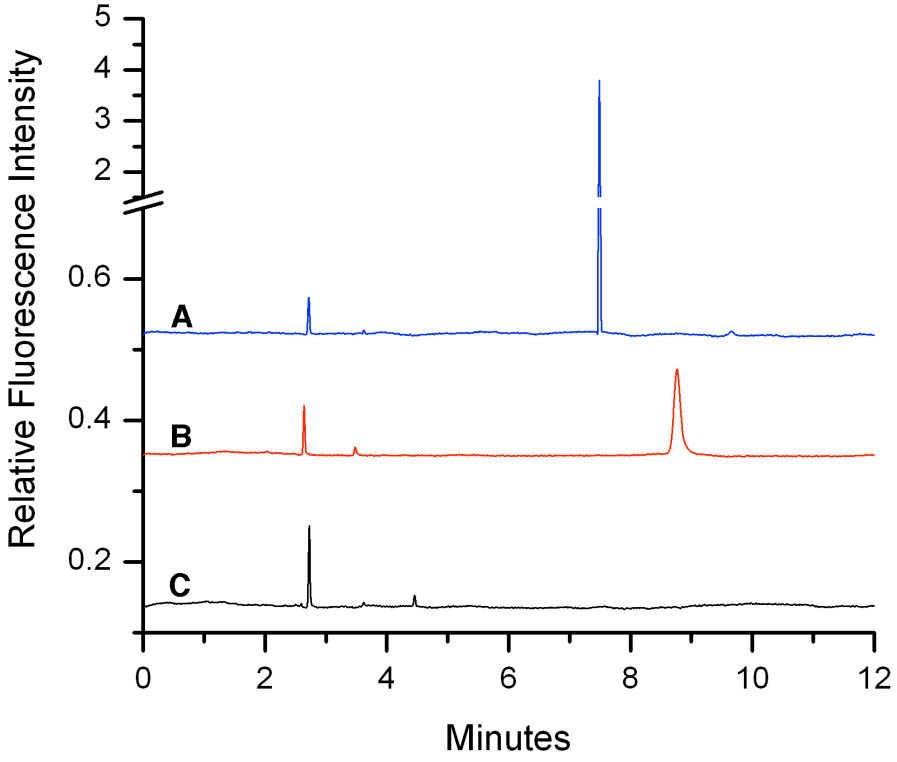

Figure A.3. MEKC CE-LIF chromatograms of a HeLa lysate after treatment with peptide 5b. In each chromatogram, 5b was incubated with HeLa cells at 1 μM for 2 h. In (A), the cells were incubated an additional 24 h to allow processing while in (B) they were incubated for 4 h. Chromatogram (C) is an injection standard of peptide 5-Fam-KKSRRCVLS free thiol for t_R comparison. The free thiol peptide can be seen in both (A) and (B), demonstrating the disulfide is reduced upon cellular incubation. Additionally, a new peak at approximately 8 minutes represents the farnesylated peptide (5-Fam-KKSRRC(far)VLS). This peak is small after 4 h because only minimal processing has occurred, but after 24 h the peak grew in area as more peptide was processed (note the break in the y-axis scale).

A.3.3 Treating HeLa with Disulfide and FTI

One method to verify the results we observed in Figure A.2 is to use an FTI to inhibit the farnesyltransferase enzyme. If this enzyme is inhibited the peptide can no longer be processed inside of cells and thus the peak at 8 minutes should reduce in area. In this experiment, the cells were first incubated with FTI for 24 hours to shut down the farnesyltransferase activity. Next, peptide **5b** was incubated with the cells for 2 hours at 1 μM. The cells were then rinsed and placed back in the incubator for 24h (FTI was also re-added to the cells to keep the enzyme inactive). Following the additional incubation, the cells were lysed, diluted 1 to 10 in CE run buffer, and injected into the capillary and separated (Figure A.3). In contrast to Figure A.2, this experiment shows a reduction in the size of the peak at 8 minutes (the farnesylated peptide) and a concomitant increase in the peak of the free thiol peptide at 3 minutes (Figure A.3A). This indicates that the farnesyltransferase enzyme has been inhibited by the FTI and prevents most of the peptide from becoming farnesylated, which leads to an accumulation of the free thiol precursor. Together, this data demonstrates that MEKC CE-LIF can be used to monitor the processing of a precursor peptide that has been incubated with HeLa cells. This lays the foundation to allow for kinetic measurements to be obtained from *in vivo* information.

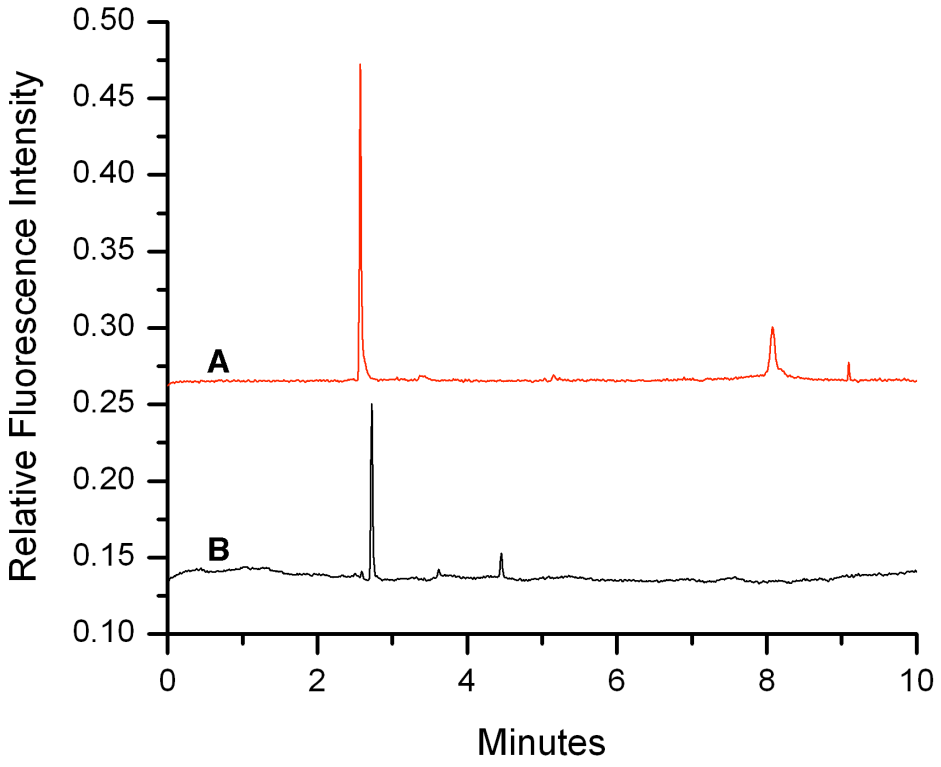

Figure A.4. MEKC CE-LIF chromatogram of a HeLa lysate after treatment with peptide 5b as well as an FTI (A). In (B), the 5-Fam-KKSRRCVLS free thiol peptide was injected as a standard for comparison. Chromatogram (A) shows that, in comparison to Figure A.2, the peak at 8 minutes is significantly reduced with FTI treatment. Furthermore, there is a concomitant increase in the amount of free thiol peptide (peak at 3 minutes). This indicates that the FTI has prevented most of the peptide from being processed and results in the accumulation of the free thiol peptide.

A.4 Conclusions and Future Outlook

In this chapter I have described our work to develop a method to monitor the activity of the farnesyltransferase enzyme in living systems. Our data demonstrate that this may be possible, as processing of a prototypic fluorescently labeled peptide sequence is successful, and that using an FTI inhibits the detection of the farnesylated peptide. This introductory work serves to lay the foundation for kinetic analysis of the farnesyltransferase enzyme in living systems. To perform these analyses, MEKC CE-LIF can be used at varying time points of peptide incubation to monitor the formation of farnesylated products. Using an internal standard such as fluorescein, which does not interfere with the peaks in our current chromatograms (data not shown), we can quantify the amount of peptide in each peak and thus get conversion information in meaningful units, e.g. μmoles/min. Experiments to utilize this method for kinetics applications are currently underway.

Appendix B. Copyright Permissions

Chapter 3:

JOHN WILEY AND SONS LICENSE
TERMS AND CONDITIONS

Aug 28, 2012

This is a License Agreement between Joshua Ochocki ("You") and John Wiley and Sons ("John Wiley and Sons") provided by Copyright Clearance Center ("CCC"). The license consists of your order details, the terms and conditions provided by John Wiley and Sons, and the payment terms and conditions.
All payments must be made in full to CCC. For payment instructions, please see information listed at the bottom of this form.

License Number
2955070721473

License date
Jul 23, 2012

Licensed content publisher
John Wiley and Sons

Licensed content publication
Chemical Biology & Drug Design

Licensed content title
Evaluation of Alkyne-Modified Isoprenoids as Chemical Reporters of Protein Prenylation

Licensed content author
Amanda J. DeGraw,Charuta Palsuledesai,Joshua D. Ochocki,Jonathan K. Dozier,Stepan Lenevich,Mohammad Rashidian,Mark D. Distefano

Licensed content date
Oct 11, 2010

Start page
460

End page
471

Type of use
Dissertation/Thesis

Requestor type
Author of this Wiley article

Format
Print and electronic

Portion
Text extract

Will you be translating?
No

Order reference number
Total
0.00 USD

Terms and Conditions
TERMS AND CONDITIONS

Terms and Conditions
1. The materials you have requested permission to reproduce (the "Materials") are protected by copyright.
2. You are hereby granted a personal, non-exclusive, non-sublicensable, non-transferable, worldwide, limited license to reproduce the Materials for the purpose specified in the licensing process. This license is for a one-time use only with a maximum distribution equal to the number that you identified in the licensing process. Any form of republication granted by this licence must be

completed within two years of the date of the grant of this licence (although copies prepared before may be distributed thereafter). The Materials shall not be used in any other manner or for any other purpose. Permission is granted subject to an appropriate acknowledgement given to the author, title of the material/book/journal and the publisher. You shall also duplicate the copyright notice that appears in the Wiley publication in your use of the Material. Permission is also granted on the understanding that nowhere in the text is a previously published source acknowledged for all or part of this Material. Any third party material is expressly excluded from this permission.

3. With respect to the Materials, all rights are reserved. Except as expressly granted by the terms of the license, no part of the Materials may be copied, modified, adapted (except for minor reformatting required by the new Publication), translated, reproduced, transferred or distributed, in any form or by any means, and no derivative works may be made based on the Materials without the prior permission of the respective copyright owner. You may not alter, remove or suppress in any manner any copyright, trademark or other notices displayed by the Materials. You may not license, rent, sell, loan, lease, pledge, offer as security, transfer or assign the Materials, or any of the rights granted to you hereunder to any other person.

4. The Materials and all of the intellectual property rights therein shall at all times remain the exclusive property of John Wiley & Sons Inc or one of its related companies (WILEY) or their respective licensors, and your interest therein is only that of having possession of and the right to reproduce the Materials pursuant to Section 2 herein during the continuance of this Agreement. You agree that you own no right, title or interest in or to the Materials or any of the intellectual property rights therein. You shall have no rights hereunder other than the license as provided for above in Section 2. No right, license or interest to any trademark, trade name, service mark or other branding ("Marks") of WILEY or its licensors is granted hereunder, and you agree that you shall not assert any such right, license or interest with respect thereto.

5. NEITHER WILEY NOR ITS LICENSORS MAKES ANY WARRANTY OR REPRESENTATION OF ANY KIND TO YOU OR ANY THIRD PARTY, EXPRESS, IMPLIED OR STATUTORY, WITH RESPECT TO THE MATERIALS OR THE ACCURACY OF ANY INFORMATION CONTAINED IN THE MATERIALS, INCLUDING, WITHOUT LIMITATION, ANY IMPLIED WARRANTY OF MERCHANTABILITY, ACCURACY, SATISFACTORY QUALITY, FITNESS FOR A PARTICULAR PURPOSE, USABILITY, INTEGRATION OR NON-INFRINGEMENT AND ALL SUCH WARRANTIES ARE HEREBY EXCLUDED BY WILEY AND ITS LICENSORS AND WAIVED BY YOU.

6. WILEY shall have the right to terminate this Agreement immediately upon breach of this Agreement by you.

7. You shall indemnify, defend and hold harmless WILEY, its Licensors and their respective directors, officers, agents and employees, from and against any

actual or threatened claims, demands, causes of action or proceedings arising from any breach of this Agreement by you.

8. IN NO EVENT SHALL WILEY OR ITS LICENSORS BE LIABLE TO YOU OR ANY OTHER PARTY OR ANY OTHER PERSON OR ENTITY FOR ANY SPECIAL, CONSEQUENTIAL, INCIDENTAL, INDIRECT, EXEMPLARY OR PUNITIVE DAMAGES, HOWEVER CAUSED, ARISING OUT OF OR IN CONNECTION WITH THE DOWNLOADING, PROVISIONING, VIEWING OR USE OF THE MATERIALS REGARDLESS OF THE FORM OF ACTION, WHETHER FOR BREACH OF CONTRACT, BREACH OF WARRANTY, TORT, NEGLIGENCE, INFRINGEMENT OR OTHERWISE (INCLUDING, WITHOUT LIMITATION, DAMAGES BASED ON LOSS OF PROFITS, DATA, FILES, USE, BUSINESS OPPORTUNITY OR CLAIMS OF THIRD PARTIES), AND WHETHER OR NOT THE PARTY HAS BEEN ADVISED OF THE POSSIBILITY OF SUCH DAMAGES. THIS LIMITATION SHALL APPLY NOTWITHSTANDING ANY FAILURE OF ESSENTIAL PURPOSE OF ANY LIMITED REMEDY PROVIDED HEREIN.

9. Should any provision of this Agreement be held by a court of competent jurisdiction to be illegal, invalid, or unenforceable, that provision shall be deemed amended to achieve as nearly as possible the same economic effect as the original provision, and the legality, validity and enforceability of the remaining provisions of this Agreement shall not be affected or impaired thereby.

10. The failure of either party to enforce any term or condition of this Agreement shall not constitute a waiver of either party's right to enforce each and every term and condition of this Agreement. No breach under this agreement shall be deemed waived or excused by either party unless such waiver or consent is in writing signed by the party granting such waiver or consent. The waiver by or consent of a party to a breach of any provision of this Agreement shall not operate or be construed as a waiver of or consent to any other or subsequent breach by such other party.

11. This Agreement may not be assigned (including by operation of law or otherwise) by you without WILEY's prior written consent.

12. Any fee required for this permission shall be non-refundable after thirty (30) days from receipt.

13. These terms and conditions together with CCC’s Billing and Payment terms and conditions (which are incorporated herein) form the entire agreement between you and WILEY concerning this licensing transaction and (in the absence of fraud) supersedes all prior agreements and representations of the parties, oral or written. This Agreement may not be amended except in writing signed by both parties. This Agreement shall be binding upon and inure to the benefit of the parties' successors, legal representatives, and authorized assigns.

14. In the event of any conflict between your obligations established by these terms and conditions and those established by CCC’s Billing and Payment terms and conditions, these terms and conditions shall prevail.

15. WILEY expressly reserves all rights not specifically granted in the combination of (i) the license details provided by you and accepted in the course of this licensing transaction, (ii) these terms and conditions and (iii) CCC's Billing and Payment terms and conditions.
16. This Agreement will be void if the Type of Use, Format, Circulation, or Requestor Type was misrepresented during the licensing process.
17. This Agreement shall be governed by and construed in accordance with the laws of the State of New York, USA, without regards to such state's conflict of law rules. Any legal action, suit or proceeding arising out of or relating to these Terms and Conditions or the breach thereof shall be instituted in a court of competent jurisdiction in New York County in the State of New York in the United States of America and each party hereby consents and submits to the personal jurisdiction of such court, waives any objection to venue in such court and consents to service of process by registered or certified mail, return receipt requested, at the last known address of such party.

Wiley Open Access Terms and Conditions

All research articles published in Wiley Open Access journals are fully open access: immediately freely available to read, download and share. Articles are published under the terms of the Creative Commons Attribution Non Commercial License. which permits use, distribution and reproduction in any medium, provided the original work is properly cited and is not used for commercial purposes. The license is subject to the Wiley Open Access terms and conditions:
Wiley Open Access articles are protected by copyright and are posted to repositories and websites in accordance with the terms of the Creative Commons Attribution Non Commercial License. At the time of deposit, Wiley Open Access articles include all changes made during peer review, copyediting, and publishing. Repositories and websites that host the article are responsible for incorporating any publisher-supplied amendments or retractions issued subsequently.
Wiley Open Access articles are also available without charge on Wiley's publishing platform, Wiley Online Library or any successor sites.

Use by non-commercial users

For non-commercial and non-promotional purposes individual users may access, download, copy, display and redistribute to colleagues Wiley Open Access articles, as well as adapt, translate, text- and data-mine the content subject to the following conditions:
The authors' moral rights are not compromised. These rights include the right of "paternity" (also known as "attribution" - the right for the author to be identified as

AGREEMENT WITH AND ARE WILLING TO ACCEPT ALL OF YOUR OBLIGATIONS AS SET FORTH IN THIS AGREEMENT.

v1.7
If you would like to pay for this license now, please remit this license along with your payment made payable to "COPYRIGHT CLEARANCE CENTER" otherwise you will be invoiced within 48 hours of the license date. Payment should be in the form of a check or money order referencing your account number and this invoice number RLNK500823983.
Once you receive your invoice for this order, you may pay your invoice by credit card. Please follow instructions provided at that time.

Make Payment To:
Copyright Clearance Center
Dept 001
P.O. Box 843006
Boston, MA 02284-3006

For suggestions or comments regarding this order, contact RightsLink Customer Support: customercare@copyright.com or +1-877-622-5543 (toll free in the US) or +1-978-646-2777.

Gratis licenses (referencing $0 in the Total field) are free. Please retain this printable license for your reference. No payment is required.

Chapter 5:

JOHN WILEY AND SONS LICENSE
TERMS AND CONDITIONS

Aug 28, 2012

This is a License Agreement between Joshua Ochocki ("You") and John Wiley and Sons ("John Wiley and Sons") provided by Copyright Clearance Center ("CCC"). The license consists of your order details, the terms and conditions provided by John Wiley and Sons, and the payment terms and conditions.
All payments must be made in full to CCC. For payment instructions, please see information listed at the bottom of this form.

License Number
2955070786256

License date
Jul 23, 2012

Licensed content publisher
John Wiley and Sons

Licensed content publication
Chemical Biology & Drug Design

Licensed content title
Enlarging the Scope of Cell-Penetrating Prenylated Peptides to Include Farnesylated ‘CAAX’ Box Sequences and Diverse Cell Types

Licensed content author
Joshua D. Ochocki,Urule Igbavboa,W. Gibson Wood,Elizabeth V. Wattenberg,Mark D. Distefano

Licensed content date
Jun 23, 2010

Start page
107

End page
115

Type of use
Dissertation/Thesis

Requestor type
Author of this Wiley article

Format
Print and electronic

Portion
Full article

Will you be translating?
No

Order reference number
Total
0.00 USD

Terms and Conditions
TERMS AND CONDITIONS
This copyrighted material is owned by or exclusively licensed to John Wiley & Sons, Inc. or one of its group companies (each a "Wiley Company") or a society for whom a Wiley Company has exclusive publishing rights in relation to a particular journal (collectively WILEY"). By clicking "accept" in connection with completing this licensing transaction, you agree that the following terms and conditions apply to this transaction (along with the billing and payment terms and conditions established by the Copyright Clearance Center Inc., ("CCC's Billing and Payment terms and conditions"), at the time that you opened your Rightslink account (these are available at any time at http://myaccount.copyright.com)

Terms and Conditions

1. The materials you have requested permission to reproduce (the "Materials") are protected by copyright.
2. You are hereby granted a personal, non-exclusive, non-sublicensable, non-transferable, worldwide, limited license to reproduce the Materials for the purpose specified in the licensing process. This license is for a one-time use only with a maximum distribution equal to the number that you identified in the licensing process. Any form of republication granted by this licence must be completed within two years of the date of the grant of this licence (although copies prepared before may be distributed thereafter). The Materials shall not be used in any other manner or for any other purpose. Permission is granted subject

to an appropriate acknowledgement given to the author, title of the material/book/journal and the publisher. You shall also duplicate the copyright notice that appears in the Wiley publication in your use of the Material. Permission is also granted on the understanding that nowhere in the text is a previously published source acknowledged for all or part of this Material. Any third party material is expressly excluded from this permission.

3. With respect to the Materials, all rights are reserved. Except as expressly granted by the terms of the license, no part of the Materials may be copied, modified, adapted (except for minor reformatting required by the new Publication), translated, reproduced, transferred or distributed, in any form or by any means, and no derivative works may be made based on the Materials without the prior permission of the respective copyright owner. You may not alter, remove or suppress in any manner any copyright, trademark or other notices displayed by the Materials. You may not license, rent, sell, loan, lease, pledge, offer as security, transfer or assign the Materials, or any of the rights granted to you hereunder to any other person.

4. The Materials and all of the intellectual property rights therein shall at all times remain the exclusive property of John Wiley & Sons Inc or one of its related companies (WILEY) or their respective licensors, and your interest therein is only that of having possession of and the right to reproduce the Materials pursuant to Section 2 herein during the continuance of this Agreement. You agree that you own no right, title or interest in or to the Materials or any of the intellectual property rights therein. You shall have no rights hereunder other than the license as provided for above in Section 2. No right, license or interest to any trademark, trade name, service mark or other branding ("Marks") of WILEY or its licensors is granted hereunder, and you agree that you shall not assert any such right, license or interest with respect thereto.

5. NEITHER WILEY NOR ITS LICENSORS MAKES ANY WARRANTY OR REPRESENTATION OF ANY KIND TO YOU OR ANY THIRD PARTY, EXPRESS, IMPLIED OR STATUTORY, WITH RESPECT TO THE MATERIALS OR THE ACCURACY OF ANY INFORMATION CONTAINED IN THE MATERIALS, INCLUDING, WITHOUT LIMITATION, ANY IMPLIED WARRANTY OF MERCHANTABILITY, ACCURACY, SATISFACTORY QUALITY, FITNESS FOR A PARTICULAR PURPOSE, USABILITY, INTEGRATION OR NON-INFRINGEMENT AND ALL SUCH WARRANTIES ARE HEREBY EXCLUDED BY WILEY AND ITS LICENSORS AND WAIVED BY YOU.

6. WILEY shall have the right to terminate this Agreement immediately upon breach of this Agreement by you.

7. You shall indemnify, defend and hold harmless WILEY, its Licensors and their respective directors, officers, agents and employees, from and against any actual or threatened claims, demands, causes of action or proceedings arising from any breach of this Agreement by you.

8. IN NO EVENT SHALL WILEY OR ITS LICENSORS BE LIABLE TO YOU OR ANY OTHER PARTY OR ANY OTHER PERSON OR ENTITY FOR ANY SPECIAL, CONSEQUENTIAL, INCIDENTAL, INDIRECT, EXEMPLARY OR PUNITIVE DAMAGES, HOWEVER CAUSED, ARISING OUT OF OR IN CONNECTION WITH THE DOWNLOADING, PROVISIONING, VIEWING OR USE OF THE MATERIALS REGARDLESS OF THE FORM OF ACTION, WHETHER FOR BREACH OF CONTRACT, BREACH OF WARRANTY, TORT, NEGLIGENCE, INFRINGEMENT OR OTHERWISE (INCLUDING, WITHOUT LIMITATION, DAMAGES BASED ON LOSS OF PROFITS, DATA, FILES, USE, BUSINESS OPPORTUNITY OR CLAIMS OF THIRD PARTIES), AND WHETHER OR NOT THE PARTY HAS BEEN ADVISED OF THE POSSIBILITY OF SUCH DAMAGES. THIS LIMITATION SHALL APPLY NOTWITHSTANDING ANY FAILURE OF ESSENTIAL PURPOSE OF ANY LIMITED REMEDY PROVIDED HEREIN.

9. Should any provision of this Agreement be held by a court of competent jurisdiction to be illegal, invalid, or unenforceable, that provision shall be deemed amended to achieve as nearly as possible the same economic effect as the original provision, and the legality, validity and enforceability of the remaining provisions of this Agreement shall not be affected or impaired thereby.

10. The failure of either party to enforce any term or condition of this Agreement shall not constitute a waiver of either party's right to enforce each and every term and condition of this Agreement. No breach under this agreement shall be deemed waived or excused by either party unless such waiver or consent is in writing signed by the party granting such waiver or consent. The waiver by or consent of a party to a breach of any provision of this Agreement shall not operate or be construed as a waiver of or consent to any other or subsequent breach by such other party.

11. This Agreement may not be assigned (including by operation of law or otherwise) by you without WILEY's prior written consent.

12. Any fee required for this permission shall be non-refundable after thirty (30) days from receipt.

13. These terms and conditions together with CCC’s Billing and Payment terms and conditions (which are incorporated herein) form the entire agreement between you and WILEY concerning this licensing transaction and (in the absence of fraud) supersedes all prior agreements and representations of the parties, oral or written. This Agreement may not be amended except in writing signed by both parties. This Agreement shall be binding upon and inure to the benefit of the parties' successors, legal representatives, and authorized assigns.

14. In the event of any conflict between your obligations established by these terms and conditions and those established by CCC’s Billing and Payment terms and conditions, these terms and conditions shall prevail.

15. WILEY expressly reserves all rights not specifically granted in the combination of (i) the license details provided by you and accepted in the course

of this licensing transaction, (ii) these terms and conditions and (iii) CCC's Billing and Payment terms and conditions.
16. This Agreement will be void if the Type of Use, Format, Circulation, or Requestor Type was misrepresented during the licensing process.
17. This Agreement shall be governed by and construed in accordance with the laws of the State of New York, USA, without regards to such state's conflict of law rules. Any legal action, suit or proceeding arising out of or relating to these Terms and Conditions or the breach thereof shall be instituted in a court of competent jurisdiction in New York County in the State of New York in the United States of America and each party hereby consents and submits to the personal jurisdiction of such court, waives any objection to venue in such court and consents to service of process by registered or certified mail, return receipt requested, at the last known address of such party.

Wiley Open Access Terms and Conditions

All research articles published in Wiley Open Access journals are fully open access: immediately freely available to read, download and share. Articles are published under the terms of the Creative Commons Attribution Non Commercial License. which permits use, distribution and reproduction in any medium, provided the original work is properly cited and is not used for commercial purposes. The license is subject to the Wiley Open Access terms and conditions:
Wiley Open Access articles are protected by copyright and are posted to repositories and websites in accordance with the terms of the Creative Commons Attribution Non Commercial License. At the time of deposit, Wiley Open Access articles include all changes made during peer review, copyediting, and publishing. Repositories and websites that host the article are responsible for incorporating any publisher-supplied amendments or retractions issued subsequently.
Wiley Open Access articles are also available without charge on Wiley's publishing platform, Wiley Online Library or any successor sites.

Use by non-commercial users

For non-commercial and non-promotional purposes individual users may access, download, copy, display and redistribute to colleagues Wiley Open Access articles, as well as adapt, translate, text- and data-mine the content subject to the following conditions:

The authors' moral rights are not compromised. These rights include the right of "paternity" (also known as "attribution" - the right for the author to be identified as such) and "integrity" (the right for the author not to have the work altered in such a way that the author's reputation or integrity may be impugned).

v1.7
If you would like to pay for this license now, please remit this license along with your payment made payable to "COPYRIGHT CLEARANCE CENTER" otherwise you will be invoiced within 48 hours of the license date. Payment should be in the form of a check or money order referencing your account number and this invoice number RLNK500823984.
Once you receive your invoice for this order, you may pay your invoice by credit card. Please follow instructions provided at that time.

Make Payment To:
Copyright Clearance Center
Dept 001
P.O. Box 843006
Boston, MA 02284-3006

For suggestions or comments regarding this order, contact RightsLink Customer Support: customercare@copyright.com or +1-877-622-5543 (toll free in the US) or +1-978-646-2777.

Gratis licenses (referencing $0 in the Total field) are free. Please retain this printable license for your reference. No payment is required.

Chapter 6:

ELSEVIER LICENSE
TERMS AND CONDITIONS

Aug 28, 2012

This is a License Agreement between Joshua Ochocki ("You") and Elsevier ("Elsevier") provided by Copyright Clearance Center ("CCC"). The license consists of your order details, the terms and conditions provided by Elsevier, and the payment terms and conditions.
All payments must be made in full to CCC. For payment instructions, please see information listed at the bottom of this form.

Supplier
Elsevier Limited
The Boulevard,Langford Lane
Kidlington,Oxford,OX5 1GB,UK

Registered Company Number
1982084

Customer name
Joshua Ochocki

Customer address
207 Pleasant St SE
Minneapolis, MN 55455

License number
2955070891884

License date
Jul 23, 2012

Licensed content publisher
Elsevier

Licensed content publication
Bioorganic & Medicinal Chemistry Letters

Licensed content title

Evaluation of a cell penetrating prenylated peptide lacking an intrinsic fluorophore via in situ click reaction

Licensed content author
Joshua D. Ochocki,Daniel G. Mullen,Elizabeth V. Wattenberg,Mark D. Distefano

Licensed content date
1 September 2011

Licensed content volume number
21

Licensed content issue number
17

Number of pages
4

Start Page
4998

End Page
5001

Type of Use
reuse in a thesis/dissertation

Intended publisher of new work
other

Portion
full article

Format
both print and electronic

Are you the author of this Elsevier article?
Yes

Will you be translating?
No

Order reference number

Title of your thesis/dissertation

STUDIES OF PROTEIN PRENYLATION IN LIVING SYSTEMS: IMPLICATIONS TOWARD THE BETTER UNDERSTANDING OF DISEASES

Expected completion date
Sep 2012

Estimated size (number of pages)
200

Elsevier VAT number
GB 494 6272 12

Permissions price
0.00 USD
VAT/Local Sales Tax
0.0 USD / 0.0 GBP

Total
0.00 USD

Terms and Conditions

INTRODUCTION

1. The publisher for this copyrighted material is Elsevier. By clicking "accept" in connection with completing this licensing transaction, you agree that the following terms and conditions apply to this transaction (along with the Billing and Payment terms and conditions established by Copyright Clearance Center, Inc. ("CCC"), at the time that you opened your Rightslink account and that are available at any time at http://myaccount.copyright.com).

GENERAL TERMS

2. Elsevier hereby grants you permission to reproduce the aforementioned material subject to the terms and conditions indicated.
3. Acknowledgement: If any part of the material to be used (for example, figures) has appeared in our publication with credit or acknowledgement to another source, permission must also be sought from that source. If such permission is not obtained then that material may not be included in your publication/copies.

Suitable acknowledgement to the source must be made, either as a footnote or in a reference list at the end of your publication, as follows:
“Reprinted from Publication title, Vol /edition number, Author(s), Title of article / title of chapter, Pages No., Copyright (Year), with permission from Elsevier [OR APPLICABLE SOCIETY COPYRIGHT OWNER].” Also Lancet special credit - “Reprinted from The Lancet, Vol. number, Author(s), Title of article, Pages No., Copyright (Year), with permission from Elsevier.”
4. Reproduction of this material is confined to the purpose and/or media for which permission is hereby given.
5. Altering/Modifying Material: Not Permitted. However figures and illustrations may be altered/adapted minimally to serve your work. Any other abbreviations, additions, deletions and/or any other alterations shall be made only with prior written authorization of Elsevier Ltd. (Please contact Elsevier at permissions@elsevier.com)
6. If the permission fee for the requested use of our material is waived in this instance, please be advised that your future requests for Elsevier materials may attract a fee.
7. Reservation of Rights: Publisher reserves all rights not specifically granted in the combination of (i) the license details provided by you and accepted in the course of this licensing transaction, (ii) these terms and conditions and (iii) CCC's Billing and Payment terms and conditions.
8. License Contingent Upon Payment: While you may exercise the rights licensed immediately upon issuance of the license at the end of the licensing process for the transaction, provided that you have disclosed complete and accurate details of your proposed use, no license is finally effective unless and until full payment is received from you (either by publisher or by CCC) as provided in CCC's Billing and Payment terms and conditions. If full payment is not received on a timely basis, then any license preliminarily granted shall be deemed automatically revoked and shall be void as if never granted. Further, in the event that you breach any of these terms and conditions or any of CCC's Billing and Payment terms and conditions, the license is automatically revoked and shall be void as if never granted. Use of materials as described in a revoked license, as well as any use of the materials beyond the scope of an unrevoked license, may constitute copyright infringement and publisher reserves the right to take any and all action to protect its copyright in the materials.
9. Warranties: Publisher makes no representations or warranties with respect to the licensed material.
10. Indemnity: You hereby indemnify and agree to hold harmless publisher and CCC, and their respective officers, directors, employees and agents, from and against any and all claims arising out of your use of the licensed material other than as specifically authorized pursuant to this license.

11. No Transfer of License: This license is personal to you and may not be sublicensed, assigned, or transferred by you to any other person without publisher's written permission.
12. No Amendment Except in Writing: This license may not be amended except in a writing signed by both parties (or, in the case of publisher, by CCC on publisher's behalf).
13. Objection to Contrary Terms: Publisher hereby objects to any terms contained in any purchase order, acknowledgment, check endorsement or other writing prepared by you, which terms are inconsistent with these terms and conditions or CCC's Billing and Payment terms and conditions. These terms and conditions, together with CCC's Billing and Payment terms and conditions (which are incorporated herein), comprise the entire agreement between you and publisher (and CCC) concerning this licensing transaction. In the event of any conflict between your obligations established by these terms and conditions and those established by CCC's Billing and Payment terms and conditions, these terms and conditions shall control.
14. Revocation: Elsevier or Copyright Clearance Center may deny the permissions described in this License at their sole discretion, for any reason or no reason, with a full refund payable to you. Notice of such denial will be made using the contact information provided by you. Failure to receive such notice will not alter or invalidate the denial. In no event will Elsevier or Copyright Clearance Center be responsible or liable for any costs, expenses or damage incurred by you as a result of a denial of your permission request, other than a refund of the amount(s) paid by you to Elsevier and/or Copyright Clearance Center for denied permissions.

LIMITED LICENSE

The following terms and conditions apply only to specific license types:

15. Translation: This permission is granted for non-exclusive world English rights only unless your license was granted for translation rights. If you licensed translation rights you may only translate this content into the languages you requested. A professional translator must perform all translations and reproduce the content word for word preserving the integrity of the article. If this license is to re-use 1 or 2 figures then permission is granted for non-exclusive world rights in all languages.
16. Website: The following terms and conditions apply to electronic reserve and author websites:
Electronic reserve: If licensed material is to be posted to website, the web site is to be password-protected and made available only to bona fide students registered on a relevant course if:
This license was made in connection with a course,

This permission is granted for 1 year only. You may obtain a license for future website posting,
All content posted to the web site must maintain the copyright information line on the bottom of each image,
A hyper-text must be included to the Homepage of the journal from which you are licensing at http://www.sciencedirect.com/science/journal/xxxxx or the Elsevier homepage for books at http://www.elsevier.com , and
Central Storage: This license does not include permission for a scanned version of the material to be stored in a central repository such as that provided by Heron/XanEdu.
17. Author website for journals with the following additional clauses:
All content posted to the web site must maintain the copyright information line on the bottom of each image, and the permission granted is limited to the personal version of your paper. You are not allowed to download and post the published electronic version of your article (whether PDF or HTML, proof or final version), nor may you scan the printed edition to create an electronic version. A hyper-text must be included to the Homepage of the journal from which you are licensing at http://www.sciencedirect.com/science/journal/xxxxx . As part of our normal production process, you will receive an e-mail notice when your article appears on Elsevier's online service ScienceDirect (www.sciencedirect.com). That e-mail will include the article's Digital Object Identifier (DOI). This number provides the electronic link to the published article and should be included in the posting of your personal version. We ask that you wait until you receive this e-mail and have the DOI to do any posting.
Central Storage: This license does not include permission for a scanned version of the material to be stored in a central repository such as that provided by Heron/XanEdu.
18. Author website for books with the following additional clauses:
Authors are permitted to place a brief summary of their work online only.
A hyper-text must be included to the Elsevier homepage at http://www.elsevier.com . All content posted to the web site must maintain the copyright information line on the bottom of each image. You are not allowed to download and post the published electronic version of your chapter, nor may you scan the printed edition to create an electronic version.
Central Storage: This license does not include permission for a scanned version of the material to be stored in a central repository such as that provided by Heron/XanEdu.
19. Website (regular and for author): A hyper-text must be included to the Homepage of the journal from which you are licensing at http://www.sciencedirect.com/science/journal/xxxxx. or for books to the Elsevier homepage at http://www.elsevier.com
20. Thesis/Dissertation: If your license is for use in a thesis/dissertation your thesis may be submitted to your institution in either print or electronic form.

Should your thesis be published commercially, please reapply for permission. These requirements include permission for the Library and Archives of Canada to supply single copies, on demand, of the complete thesis and include permission for UMI to supply single copies, on demand, of the complete thesis. Should your thesis be published commercially, please reapply for permission.
21. Other Conditions:
v1.6
If you would like to pay for this license now, please remit this license along with your payment made payable to "COPYRIGHT CLEARANCE CENTER" otherwise you will be invoiced within 48 hours of the license date. Payment should be in the form of a check or money order referencing your account number and this invoice number RLNK500823986.
Once you receive your invoice for this order, you may pay your invoice by credit card. Please follow instructions provided at that time.
Make Payment To:
Copyright Clearance Center
Dept 001
P.O. Box 843006
Boston, MA 02284-3006

For suggestions or comments regarding this order, contact RightsLink Customer Support: customercare@copyright.com or +1-877-622-5543 (toll free in the US) or +1-978-646-2777.

Gratis licenses (referencing $0 in the Total field) are free. Please retain this printable license for your reference. No payment is required.